



POLITECNICO DI TORINO

Master of Science in Civil Engineering

Master's Degree Thesis

**Digital Twin of Metro Infrastructure through BIM and IoT Sensor
Integration:
The Case of Certosa Metro Station, Turin**

REVIEWERS:

Prof. Anna Osello
Prof. Matteo Del Giudice

AUTHOR:

Nur Sena Bayindir

Acknowledgements

First and foremost, I would like to express my deepest gratitude to Professor Anna Osello and Professor Matteo Del Guidice for offering me the opportunity to develop this thesis under their supervision. Their guidance, expertise, and trust provided me with the freedom to explore ideas while ensuring a rigorous academic framework. I am also profoundly grateful to Daniel Rodriguez Polania, whose continuous support and dedication went far beyond expectations. Despite not being physically present in Turin for much of this journey, his commitment through countless online meetings and thoughtful feedback was invaluable. His patience, encouragement, and technical guidance not only helped me overcome challenges but also played a decisive role in shaping this thesis into its final form.

My time at Politecnico di Torino has been an extraordinary journey that broadened my academic horizons, strengthened my technical skills, and deepened my understanding of civil engineering. Completing this Master's degree is not only a personal milestone but also a source of immense pride and joy. The multicultural environment, demanding coursework, and collaborative projects have shaped me into a more capable engineer and a more open-minded individual.

I owe my greatest thanks to my family, who have been the foundation of all my achievements. To my father, Adil Bayindir, my professional role model and the person who first ignited my passion for civil engineering he showed me, through his own dedication, the beauty and responsibility of this profession. To my mother, Kadriye Bayindir, whose unconditional love and constant encouragement bridged every distance between us, you have always been my safe harbor. And to my sister, Neslisah Bayindir, my closest friend and confidant, your steady presence and belief in me have carried me through difficult days. This accomplishment belongs as much to you as it does to me.

I am also profoundly grateful to my partner, Idris Guven, whose love, understanding, and steady support have made life in Turin not only manageable but truly meaningful. Your presence has turned challenges into shared victories and has filled this journey with joy. Thank you for standing beside me through every late night, doubt, and triumph. I would also like to extend my heartfelt thanks to Idris's family, whose kindness and care touched me deeply. His mother's emotional support and their encouragement during my hardest moments are memories I will cherish forever.

I would also like to extend my heartfelt thanks to Murat Lacin, a dear friend whose kindness, humor, and practical support made my years in Turin brighter and less daunting. Your companionship has been invaluable, and I am grateful for every moment of shared laughter and guidance.

Finally, I wish to dedicate this work to the enduring love I hold for civil engineering itself. This discipline has taught me to see structures not only as concrete and steel but as living connections between people, places, and possibilities. It is a field where science meets creativity and responsibility meets innovation. I am excited to carry forward the knowledge, values, and passion that this Master's journey and this thesis have instilled in me, as I continue to contribute to the profession I cherish.

Thank you all,

Nur Sena Bayindir

Abstract

This thesis explores the integration of Building Information Modeling (BIM) technologies with Structural Health Monitoring (SHM) strategies for the development of a digital twin of the Certosa Metro Station project in Turin, carried out in collaboration with Infra.To. The work addresses the current gap between traditional structural monitoring practices and next generation digital platforms, with the goal of enabling real time visualization, analysis, and decision making within urban infrastructure.

The research begins with the creation of a georeferenced 3D environment derived from QGIS and CAD data, later refined in Revit and InfraWorks to obtain a realistic representation of the project site and its surrounding built environment. A BIM-based model of the metro station was prepared, maintaining the correct structural alignment and underground levels. This model was then extended to host IoT-based virtual sensors, including accelerometers, tiltmeters, and inclinometer chains, strategically positioned on both the structure and the surrounding soil.

In particular, two nearby buildings were modeled with accelerometers and tiltmeters to evaluate vibration and inclination responses, while an inclinometer chain was placed beneath the railway alignment to capture ground settlements and shear deformations. Sensor parameters and metadata were defined in Revit through shared and project parameters, ensuring consistency with Tandem requirements.

Subsequently, data integration workflows were implemented: synthetic datasets were generated in Excel/Python and processed in Jupyter Notebook to automate their conversion into JSON streams. These datasets were uploaded and connected to Autodesk Tandem, where each sensor was mapped to its respective digital counterpart. The workflows were tested to ensure that sensor connections could be visualized in real time, laying the groundwork for vibration and settlement simulations.

The preliminary results demonstrate the feasibility of combining BIM environments with SHM data streams to build a functioning digital twin for metro infrastructure. The study highlights both the technical potential and the practical challenges of such integration, particularly in terms of data formatting, parameter mapping, and interoperability across software platforms.

Overall, the thesis provides a structured methodology for bridging BIM and SHM through digital twins, offering a replicable framework that can be applied to similar infrastructure projects beyond Turin.

TABLE OF CONTENTS

Abstract.....	5
1. Introduction.....	12
2. Literature Review	15
2.1 Building Information Modeling (BIM).....	15
2.1.1 Definition	15
2.1.2 Context in Infrastructure and Monitoring.....	17
2.1.3 Previous Approaches and Relevance to This Study	17
2.2 Structural Health Monitoring (SHM).....	18
2.2.1 Definition and Principles.....	19
2.2.2 Context in Infrastructure and Urban Projects	20
2.2.3 Previous Approaches and Relevance to This Study	21
2.3 Digital Twin and Autodesk Tandem	22
2.4 IoT Sensors for Structural Health Monitoring	29
2.4.1 Accelerometers	33
2.4.2 Tiltmeters.....	35
2.4.3 Inclinator Chains	36
2.4.3.1 Theoretical Basis of Inclinator Chains.....	37
2.4.3.2 Theoretical Principle	38
2.4.4 Topographic Benchmarks.....	40
3. Methodology	42
3.1 Case Study Definition	45
3.2 Modeling Workflow	50
3.3 Sensor Integration in BIM	53
3.3.1 Creation of Sensor Families.....	53
3.3.2 Definition of Parameters	54
3.3.3 Placement of Sensors	54
3.3.4 Interoperability Considerations.....	61
3.4 Data Workflow and IoT Simulation.....	62
3.5.1 Accelerometer Data Interpretation and Risk Assessment.....	84
3.5.2 Tiltmeter Data Interpretation and Risk Assessment.....	89
3.5.3 Inclinator Chain Analysis and Interpretation	93
3.5.3.1 Az (Acceleration) Measurements.....	94
3.5.3.2 Settlement (Si) Measurements	98
3.5.3.3 Risk Assessment	101
3.5.4 Topographic Benchmark Analysis.....	103

5. Recommendations and Future Work.....	110
6. Conclusion.....	114
<i>References</i>.....	116

LIST OF FIGURES

Figure 1 - Building Information Modelling (BIM)	15
Figure 2 - BIM Example Building.....	16
Figure 3 - Structural Health Monitoring (SHM)	18
Figure 4 - Structural Health Monitoring (SHM) Workflow	19
Figure 5 - Digital Twin Workflow	22
Figure 6 - Digital Twin Environment	23
Figure 7 - Digital Thread Workflow	24
Figure 8 - Autodesk Tandem Example	25
Figure 9 - Autodesk Tandem work of Certosa Metro Station Area	26
Figure 10 - Communication architecture for IoT-based Structural Health Monitoring systems	27
Figure 11 - IoT sensors workflow.....	29
Figure 12 - Certosa Metro Area Sensors Placement Scheme.....	32
Figure 13 - Accelerometers.....	33
Figure 14 - Accelerometers Workflow.....	34
Figure 15 - Tiltmeter SISGEO.....	35
Figure 16 - Inclinator Chain.....	36
Figure 17 - Modular Underground Monitoring System (MUMS).....	37
Figure 18 - Topographic Benchmark.....	40
Figure 19 - Benchmark TOPO Map Example	41
Figure 20 - Workflow of Project	42
Figure 21 - The Region Around the Certosa Metro Area Studied	45
Figure 22 - Downloaded region in CADmapper	46
Figure 23 - The BIM model of the station provided by Infra.To.....	46
Figure 24 - Certosa Metro Area Plan.....	48
Figure 25 - QGIS topographic data of the Certosa area	50
Figure 26 - Certosa region BIM model designed in Revit	51
Figure 27 - Region of Certosa created in InfraWorks	52
Figure 28 - Gruppo CIDIU Building (B1) Revit Model Front View Sensors Placement.....	55
Figure 29 - Gruppo CIDIU Building (B1) Revit Model Back View Sensors Placement.....	55
Figure 30 - Abandoned Building (B2) Side View of Sensors Placement.....	56
Figure 31 - Abandoned Building (B2) Top View of Sensors Placement	57
Figure 32 - Inclinator Chains Placement in Railway Alignment	57
Figure 33 - Inclinator Chain 1 underground view of nodes	58
Figure 34 - Inclinator Chain 2 underground view of nodes	59
Figure 35 - Topographic Benchmark Placement in Park Area.....	60
Figure 36 - Shared Parameters in Revit.....	61
Figure 37 - Workflow of sending data to Tandem	62
Figure 38 - Autodesk Tandem Parameters	77
Figure 39 - Tandem Charts.....	78
Figure 40 - Parameters.....	79
Figure 41 - Tandem Overview.....	79

Figure 42 - Thresholds.....	80
Figure 43 - Tandem Connections	82
Figure 44 - Connection of Sensors in Certosa Area	83
Figure 45 - B1_Accelerometer1 Chart	84
Figure 46 - B1_Accelerometer 2 Chart	84
Figure 47 - B2_Accelerometer1 Chart	85
Figure 48 - B2_Accelerometer2 Chart	86
Figure 49 - Combined Chart of Accelerometers.....	87
Figure 50 - B1_Tiltmeter1 Chart.....	89
Figure 51 - B1_Tiltmeter2 Chart.....	89
Figure 52 - B2_Tiltmeter1 Chart.....	90
Figure 53 - B2_Tiltmeter2 Chart.....	91
Figure 54 - Combined Chart of Tiltmeters	91
Figure 55 - Inclinator Chains Aligned in Railway.....	94
Figure 56 - Inclinator Chain1 nodes	95
Figure 57 - Inclinator Chain1 node-5 Az Chart	95
Figure 58 - Inclinator Chain 2 node-5 Az Chart	96
Figure 59 - Inclinator Chain 1 Node-1 Az Chart	96
Figure 60 - Inclinator Chain 2 Node-1 Az Chart	97
Figure 61 - Combined Chart of Inclinator Chains Az Data.....	97
Figure 62 - Inclinator Chain 1 Node-5 Si Chart	98
Figure 63 - Inclinator Chain 2 Node-5 Si Chart	99
Figure 64 - Inclinator Chain 1 Node-1 Si Chart	99
Figure 65 - Inclinator Chain 2 Node-1 Si Chart	100
Figure 66 - Combined Inclinator Chain Chart of Si Values.....	100
Figure 67 - Topographic Benchmarks in Park Area.....	103
Figure 68 - Topographic Benchmark Section 1 Chart.....	104
Figure 69 - Topographic Benchmark Section 3 Chart.....	104
Figure 70 - Topographic Benchmark Section 5 Chart.....	105

LIST OF TABLES

Table 1 - Accelerometer Data	65
Table 2 - Tiltmeter Data	66
Table 3 - Inclinator Chain Data	68
Table 4 - Topographic Benchmark Data (S1-2)	69
Table 5 - Topographic Benchmark Data (S2-3)	70
Table 6 - Topographic Benchmark Data (S3-4)	71
Table 7 - Topographic Benchmark Data (S4-5)	72
Table 8 - Part of Phyton Code for sending data to Tandem from Jupyter	
Notebook	74

1. Introduction

In recent years, civil engineering has increasingly adopted digital tools to improve the design, monitoring, and management of infrastructure. Among these tools, Building Information Modeling (BIM) and Structural Health Monitoring (SHM) have become essential. BIM provides a 3D model enriched with technical information, while SHM collects data from sensors that record the real behavior of structures. When combined, they enable the creation of a Digital Twin: a virtual model directly connected to real time monitoring data. This approach allows engineers to better understand performance, predict problems, and support maintenance decisions.

Metro stations and tunnels are particularly suitable for such applications. These underground structures are exposed to complex conditions such as soil structure interaction, train induced vibrations, angular displacements, and potential settlements that may also influence nearby buildings. However, in practice, monitoring data and BIM models are often managed separately. This limits the possibility of using monitoring information effectively for predictive maintenance and safety assessments.

This thesis develops a BIM based workflow for SHM integration, applied to the Certosa Metro Station in Turin, in collaboration with Infra.To. The aim is to demonstrate how monitoring data, including accelerometers, tiltmeters, inclinometer chains, and topographic benchmarks, can be linked to BIM models and transferred to Autodesk Tandem, creating a functioning digital twin for metro infrastructure.

The first stage of the work was the creation of a georeferenced 3D model of the metro station and its surroundings using QGIS, CAD, Revit, and InfraWorks. The model included correct structural alignment, underground levels, and the representation of nearby terrain and buildings.

In the Certosa area, two adjacent buildings were selected for detailed monitoring with accelerometers and tiltmeters to evaluate vibrations and inclinations. An inclinometer chain was positioned under the railway line to capture ground settlements and shear deformations, while topographic benchmarks were installed at 10 m intervals across five sections to track surface movements. Other nearby buildings were not individually analyzed, since they were located at similar distances from the railway line and therefore expected to show comparable responses. The two chosen buildings, being the closest to the station, provided a more representative and efficient case study for the scope of this research.

The second stage focused on the data workflow. Synthetic datasets simulating vibration, tilt, settlement, and benchmark responses were first prepared in Excel. These datasets were then processed in Python using Jupyter Notebook, where scripts automated their conversion into JSON files and sent them to Tandem's API. In this way, each virtual sensor in the BIM model was linked to a corresponding time series stream in the digital twin. This setup allowed the visualization of sensor data in real time and demonstrated the potential of connecting monitoring systems to BIM.

The results confirm that BIM and SHM can be successfully combined to support the development of a digital twin. The study also highlights several challenges, such as parameter mapping, data formatting, and interoperability between different software platforms. Nevertheless, the methodology shows that it is possible to integrate monitoring data into BIM models and use them as the basis for real time digital twins.

The remainder of this thesis is structured as follows: Chapter 2 reviews the state of the art and relevant literature on BIM, SHM, digital twins and IoT sensors. Chapter 3 presents the case study definition, the modeling workflow, and the integration of sensors into BIM. Chapter 4 describes the data workflow and IoT simulation, including dataset generation, processing, and transfer to Tandem. Chapter 5 provides validation, testing, and analysis of sensor outputs, with risk assessments and recommendations for future work. Finally, Chapter 6 summarizes the conclusions and outlines potential future developments, including the use of real monitoring data and predictive simulations.

2. Literature Review

2.1 Building Information Modeling (BIM)

2.1.1 Definition

Building Information Modeling (BIM) is widely recognized as a transformative methodology in the construction and infrastructure sectors. It can be defined as a digital representation of the physical and functional characteristics of a facility, serving as a shared knowledge resource for information throughout the entire life cycle of a project, from planning and design to construction, operation, and maintenance. Unlike traditional 2D drawings, BIM integrates geometry, spatial relationships, quantities, material properties, and associated metadata into a single parametric model. This integration allows engineers and stakeholders not only to visualize designs in three dimensions but also to simulate construction processes, evaluate performance, and support facility management.

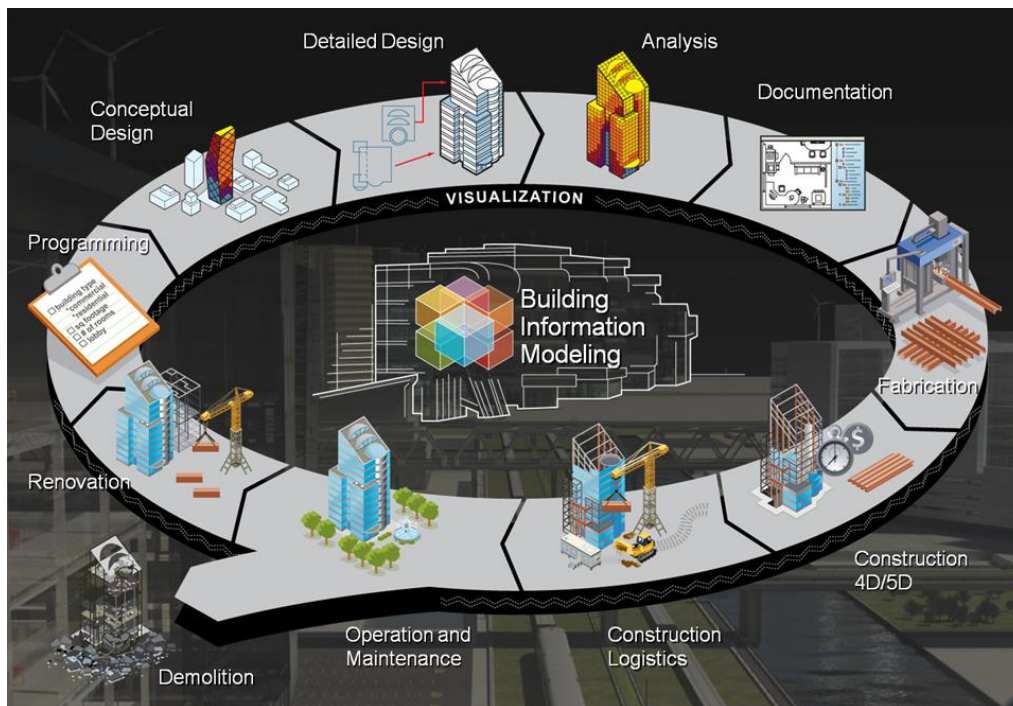


Figure 1 - Building Information Modelling (BIM)

BIM is not merely a software tool but a collaborative process that standardizes communication and decision-making across disciplines. Standardized file formats such as Industry Foundation Classes (IFC) ensure interoperability across diverse platforms, enabling architects, engineers, contractors, and owners to work within the same digital ecosystem. Beyond 3D modeling, BIM extends into 4D (time scheduling), 5D (cost estimation), and 6D (sustainability and facility management) dimensions, which broaden its scope from design documentation to lifecycle asset management.

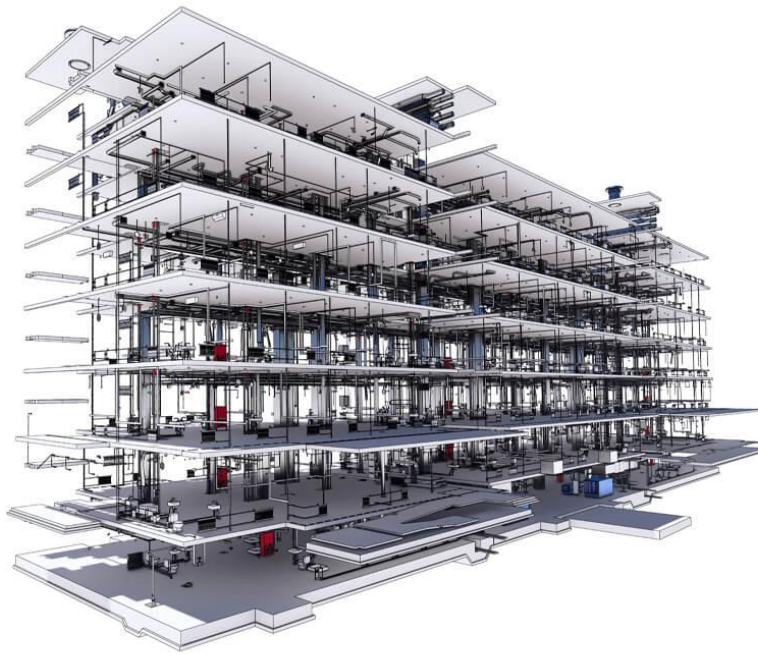


Figure 2 - BIM Example Building

2.1.2 Context in Infrastructure and Monitoring

In infrastructure projects, BIM has become critical for managing complex, multidisciplinary systems such as bridges, tunnels, and metro stations. For underground works like metro stations and tunneling, BIM facilitates the integration of geotechnical, structural, and architectural data into a unified model. This integration allows engineers to study soil-structure interaction, support systems, and excavation sequencing in a single environment, reducing design conflicts and improving construction safety.

Recent studies emphasize that BIM is now increasingly linked with Structural Health Monitoring (SHM) and Digital Twin technologies. For example, Hu et al. (2024) proposed an intelligent BIM-enabled digital twin framework that combines wireless IoT sensing, digital signal processing, and structural analysis to monitor infrastructure performance in real time. Similarly, Shafie Panah and Kioumars (2021) reviewed the integration of BIM in health monitoring workflows, highlighting its ability to host live sensor data, visualize structural responses, and support predictive maintenance. These works demonstrate that BIM is evolving beyond static design documentation to become a dynamic platform for real time decision support.

2.1.3 Previous Approaches and Relevance to This Study

Several previous approaches have successfully applied BIM to metro and tunnel environments. Early implementations primarily used BIM for coordination of underground utilities and geometry but did not integrate monitoring data. More recent frameworks, such as the BIM-SHM models discussed in Expert Systems with Applications (Hu et al., 2024), show that linking IoT sensors with BIM significantly improves risk management and operational planning. Shafie Panah & Kioumars (2021) also stressed that BIM based monitoring can detect anomalies earlier than traditional methods, reducing long term maintenance costs.

This thesis builds upon these approaches by using BIM not only for 3D geometric modeling of the Certosa Metro Station and surrounding buildings but also as a central hub for sensor metadata. Accelerometers, tiltmeters, inclinometer chains, and topographic benchmarks were virtually embedded in Autodesk Revit and InfraWorks, enriched with custom parameters to describe their technical properties. This approach demonstrates how BIM can serve as both a data container and a gateway for real time SHM integration, laying the foundation for the Digital Twin implemented in Autodesk Tandem.

2.2 Structural Health Monitoring (SHM)

Structural Health Monitoring (SHM) is a comprehensive methodology for continuously observing and assessing the condition of civil structures throughout their service life. It combines sensor technologies, data acquisition systems, and analytical models to detect performance changes, identify damage, and ensure safety and reliability. Unlike traditional inspections, which are often manual, periodic, and reactive, SHM provides continuous or high frequency measurements that enable early detection of anomalies and data driven maintenance planning.



Figure 3 - Structural Health Monitoring (SHM)

2.2.1 Definition and Principles

At its core, SHM involves three fundamental components:

1. Sensors that capture structural or environmental variables such as acceleration, strain, displacement, inclination, or temperature.
2. Data acquisition, transmission, and storage systems that collect, digitize, and organize these measurements in real time.
3. Data processing and interpretation tools , ranging from statistical analysis and machine learning to physics based models, that transform raw readings into actionable insights about structural performance.

This workflow allows engineers to track the evolution of structural responses under operational loads, environmental conditions, or extreme events. By providing near real time feedback, SHM supports proactive decision making, reduces risks of sudden failure, and extends the operational life of critical infrastructure.

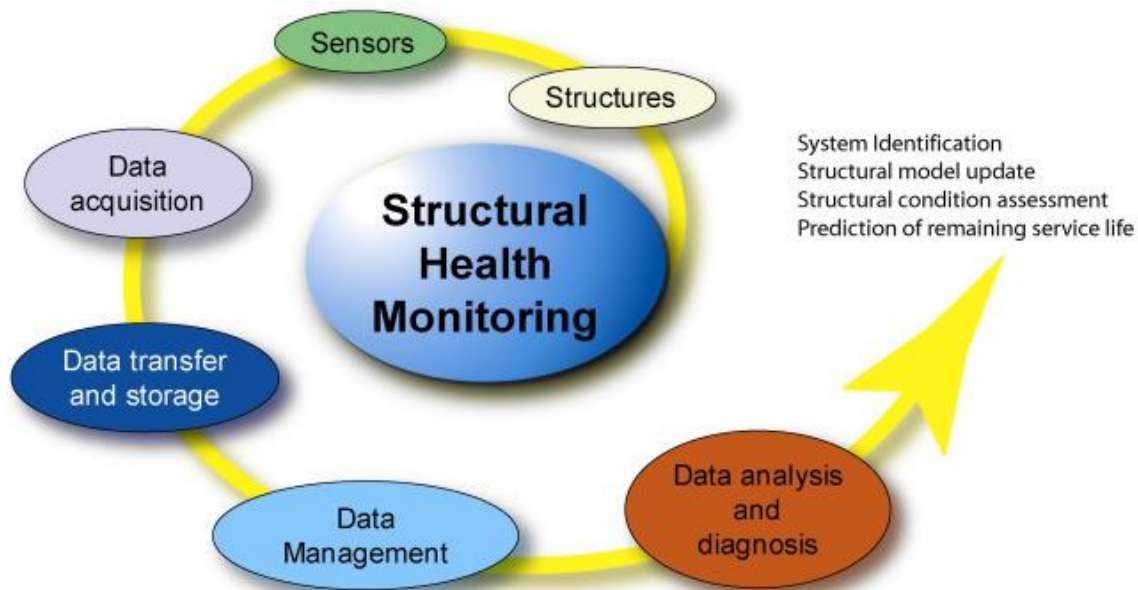


Figure 4 - Structural Health Monitoring (SHM) Workflow

2.2.2 Context in Infrastructure and Urban Projects

SHM has been widely adopted for bridges, high rise buildings, tunnels, metro systems, and dams, where structural integrity is critical for public safety. In underground transportation systems such as railways and metro tunnels, the method is particularly valuable: dynamic vibrations from trains, soil structure interaction, and quasi static settlements can impose stresses on both the tunnel lining and adjacent buildings.

Armijo and Zamora-Sánchez (2024) demonstrated how SHM integrated with IoT and digital twin platforms can connect monitoring data directly to operational decision making for railway bridges. Similarly, Doni (2021) showed that embedding monitoring parameters within BIM environments improves coordination between design and field measurements, reducing delays and unexpected costs. These studies emphasize that SHM is not only about damage detection but also about predictive maintenance and asset management optimization.

Furthermore, recent discussions (Li et al., 2024) underline the growing role of wireless sensing networks and cloud based platforms in SHM. These technologies enable large scale, distributed monitoring systems that are easier to deploy and maintain compared to traditional wired configurations. As civil engineering projects become more complex, such integrated SHM frameworks are increasingly viewed as essential components of resilient infrastructure planning.

2.2.3 Previous Approaches and Relevance to This Study

Traditional SHM campaigns often treated data collection and modeling as separate processes, leading to fragmented workflows where valuable monitoring information was underused. The shift toward real time SHM integrated with BIM and digital twins is a recent but growing trend. Previous research has demonstrated that connecting SHM data streams to 3D models provides engineers with a spatial and contextual understanding of structural behavior, which can significantly enhance risk assessment and decision making.

In this thesis, SHM principles are applied to the Certosa Metro Station in Turin, where underground excavation and railway operations could influence nearby buildings and ground stability. A representative sensor network, composed of accelerometers, tiltmeters, inclinometer chains, and topographic benchmarks, was selected to capture both dynamic (e.g., train induced vibrations) and quasi static (e.g., soil settlement and building rotation) effects. By embedding these sensors as virtual elements within Autodesk Revit and linking them to Tandem, SHM is transformed from a standalone monitoring effort into a fully integrated digital twin workflow.

This approach demonstrates how modern SHM not only safeguards structural performance but also creates continuous feedback loops between field measurements, design models, and asset management systems, pushing urban infrastructure projects toward smarter and more resilient operation.

2.3 Digital Twin and Autodesk Tandem

The concept of the Digital Twin (DT) originated in the early 2000s in the aerospace and manufacturing industries, where it was used to monitor and optimize the performance of complex systems. Over the last decade, this concept has been increasingly adopted in civil engineering and infrastructure management (Wu et al., 2025; Liu et al., 2020). A digital twin can be described as a virtual counterpart of a physical asset, system, or process, dynamically synchronized with real time data and operational conditions. Unlike traditional 3D models or BIM files, which remain static once created, digital twins are living systems: they evolve alongside their physical counterparts, providing continuous monitoring, advanced simulations, and predictive analytics.

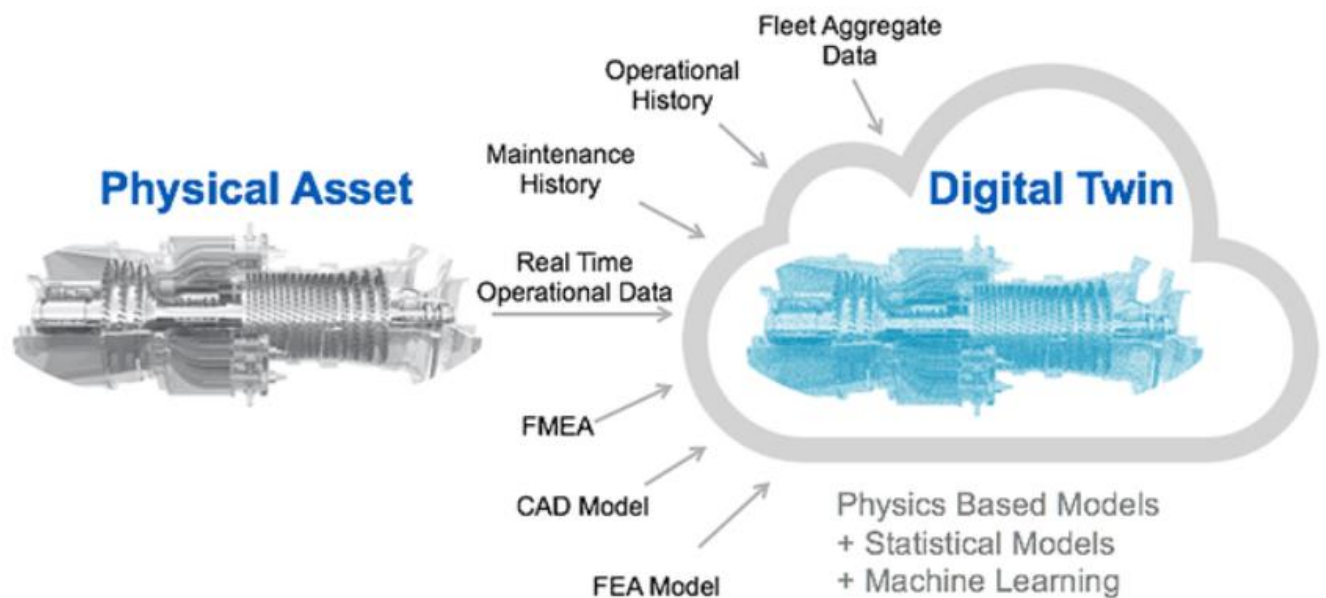


Figure 5 - Digital Twin Workflow

Digital twins integrate four essential components:

1. Geometric representation – typically developed through Building Information Modeling (BIM), which provides the structured, parametric framework for the virtual asset.
2. Sensor and IoT data streams – which feed the digital twin with live measurements such as vibrations, displacements, tilting, or temperature changes.
3. Data processing and analytics – including computational modeling, machine learning algorithms, and predictive simulations to interpret trends and forecast potential risks or maintenance needs.
4. Visualization and interaction platforms – enabling engineers, operators, and stakeholders to explore, query, and act upon the twin's information in real time.

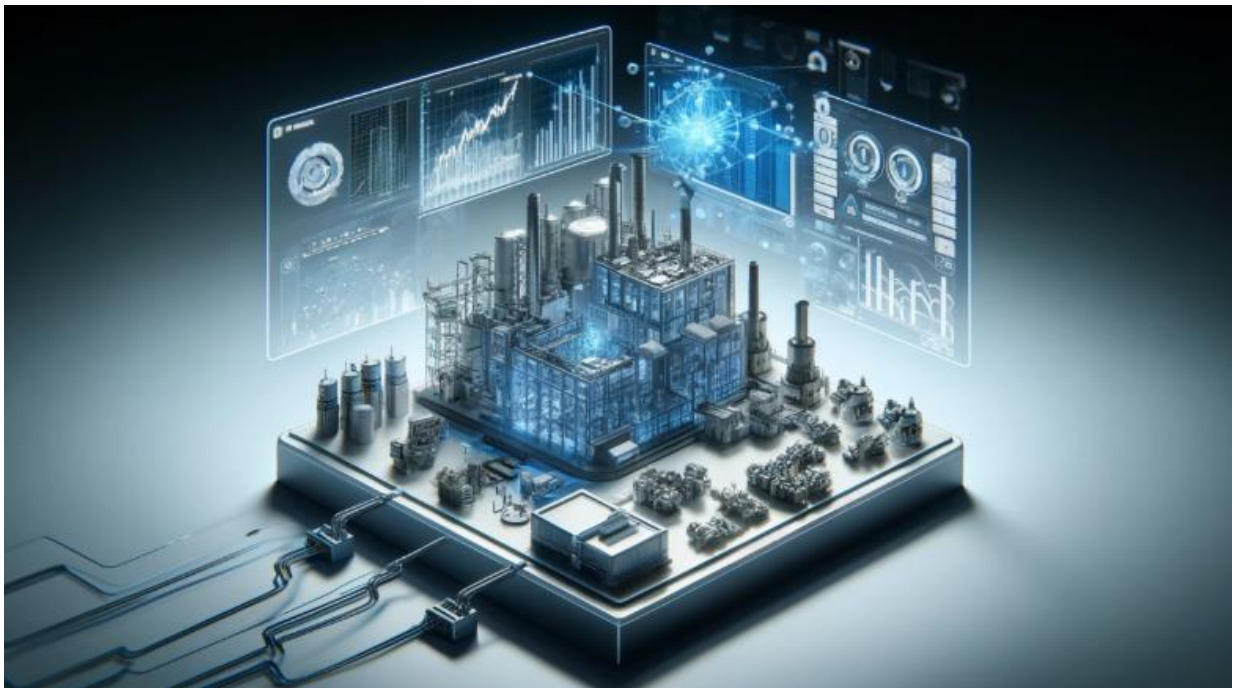


Figure 6 - Digital Twin Environment

Recent surveys on transportation and urban infrastructure (Wu et al., 2025) highlight that DTs are especially beneficial for metro tunnels, underground stations, and railway networks, where soil structure interaction, dynamic loading, and safety critical conditions require real time situational awareness. Case studies in offshore engineering (Liu et al., 2020) and railways have shown that digital twins can significantly reduce operational risks, improve emergency response, and optimize maintenance schedules. These findings emphasize that the DT paradigm is not just a visualization tool but a decision support system that bridges design, construction, and operation phases.

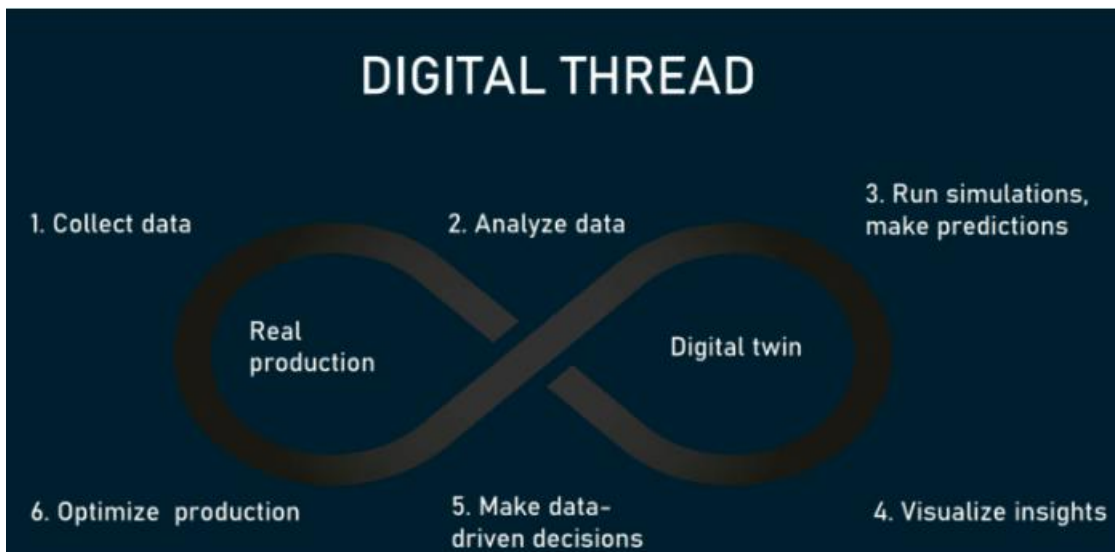


Figure 7 - Digital Thread Workflow

In urban environments, where underground works can influence surface structures and surrounding utilities, the combination of BIM and SHM forms the backbone of a functional digital twin. BIM provides the geometric and semantic structure, while SHM supplies the dynamic data needed to update and validate the model.

As the digital twin receives and processes sensor data, it becomes a “single source of truth” for engineers, operators, and stakeholders supporting not only monitoring but also predictive maintenance, risk assessment, and lifecycle management.

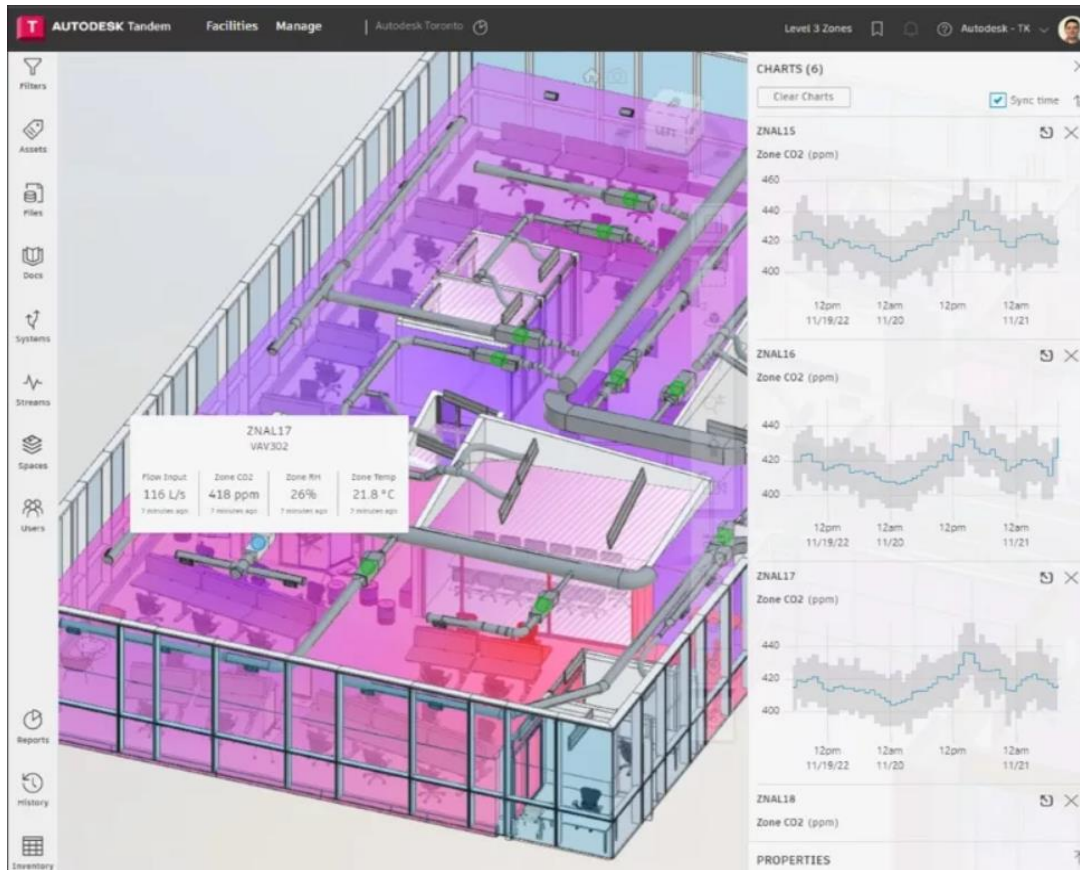


Figure 8 - Autodesk Tandem Example

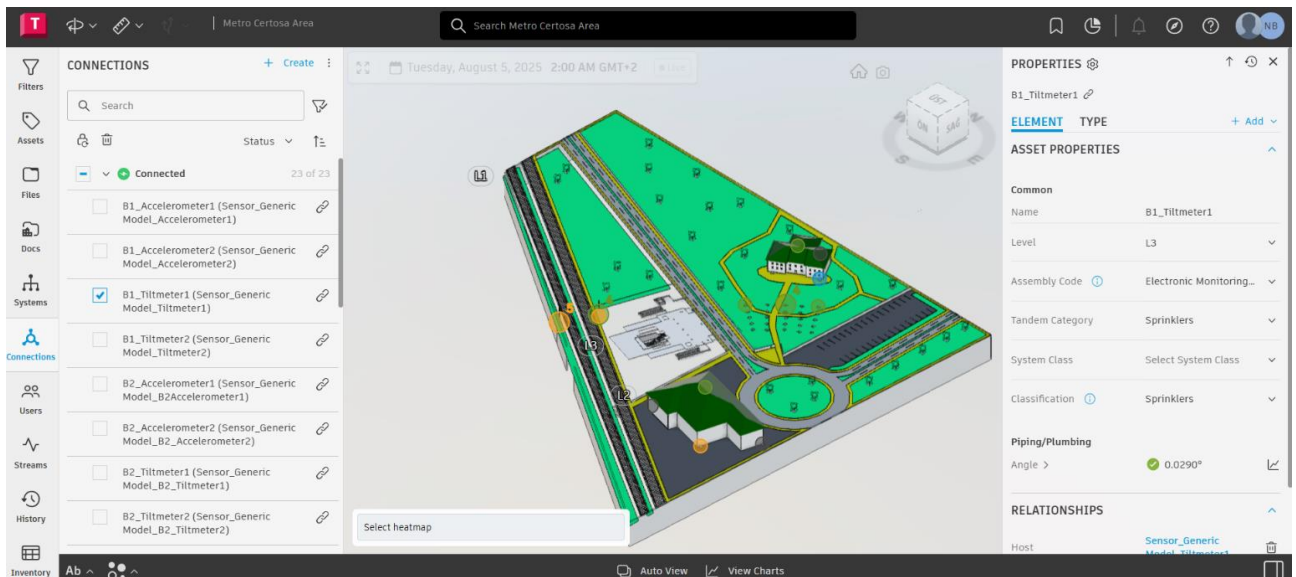


Figure 9 - Autodesk Tandem work of Certosa Metro Station Area

Autodesk Tandem represents one of the most recent advancements in cloud based DT platforms tailored for the construction industry. Tandem enables users to import BIM models from Revit, IFC, or other standard formats and assign custom parameters, asset hierarchies, and IoT data connections. A key feature is its ability to map JSON or CSV based IoT streams directly to BIM elements, allowing previously static models to become interactive, data driven twins. Users can visualize time series charts, overlay thresholds for alerts and warnings, and perform “what-if” analyses in a single environment. Its collaborative nature ensures that project teams, asset owners, and facility managers can access the same updated information remotely, which is particularly valuable for large scale and multi disciplinary infrastructure projects.

In digital twin systems, the communication between sensors, acquisition devices, and cloud platforms relies on standardized protocols. Commonly used options include MQTT (Message Queuing Telemetry Transport), designed for lightweight, low bandwidth communication in IoT networks; CoAP (Constrained Application Protocol), optimized for constrained devices and machine-to-machine

communication; and traditional cellular or NB-IoT networks, which allow large-scale deployment in urban environments. These protocols differ in latency, efficiency, and scalability: MQTT is well suited for real-time streams with limited resources, while CoAP enables fast machine-level interaction, and cellular solutions guarantee coverage in underground or remote sites.

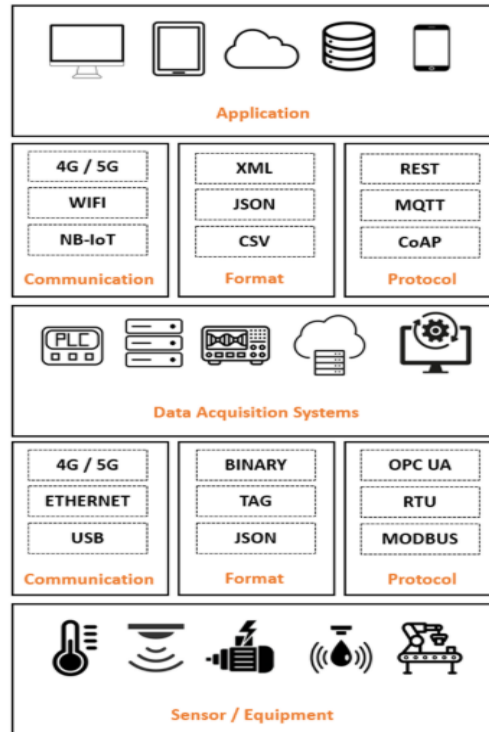


Figure 10 - Communication architecture for IoT-based Structural Health Monitoring systems

For this thesis, however, REST API (Representational State Transfer) was selected, in combination with the HTTP protocol and JSON format, because it is the method natively supported by Autodesk Tandem for data ingestion. While REST is not always the most efficient option for large-scale IoT deployments, it ensures straightforward integration, human readability of payloads, and compatibility with cloud-based services. This choice reflects a pragmatic balance: although MQTT or CoAP could reduce bandwidth and latency, REST provided the most reliable and accessible interface for testing digital twin workflows under controlled conditions.

In this thesis, Autodesk Tandem was used as the target platform for developing the digital twin of the Certosa Metro Station area in Turin. The georeferenced BIM model created in Revit and InfraWorks was imported into Tandem, where virtual sensors, including accelerometers, tiltmeters, topographic benchmarks, and inclinometer chains, were linked to synthetic datasets.

Python scripts executed in Jupyter Notebook automated the transformation of Excel based datasets into JSON streams compatible with Tandem's API. Once uploaded, these data streams updated the virtual sensors in real time, enabling interactive visualizations, threshold based alerts, and cross verification between spatial locations and temporal trends.

The application of Tandem in this case study demonstrates a critical transition: from traditional BIM, which primarily supports design documentation, to a fully functional digital twin capable of real time monitoring and operational insights. This approach highlights both the potential and current limitations of emerging DT platforms. As noted during testing, Tandem occasionally displayed inconsistencies and data loss due to system bugs, a reminder that, while promising, digital twin technology in construction is still in its early stages of maturity. Identifying these issues was part of the aim of this research: to evaluate Tandem's robustness and reliability under controlled conditions and to provide insights for its refinement.

Ultimately, the Certosa Metro Station case study confirms that combining BIM, SHM, and Autodesk Tandem can enhance risk management, support predictive maintenance, and streamline lifecycle management for urban infrastructure. As digital twins become more mature, they are expected to transform static engineering documentation into dynamic decision support ecosystems, significantly improving safety, efficiency, and sustainability in civil engineering practice.

2.4 IoT Sensors for Structural Health Monitoring

The selection of appropriate sensors is a critical step in the design of any Structural Health Monitoring (SHM) system. Each sensor type captures different physical responses, and only their combined use can provide a comprehensive picture of both structural performance and geotechnical behavior.

In recent years, the integration of Internet of Things (IoT) technologies with SHM has significantly advanced the way data are collected, transmitted, and analyzed (Lamonaca et al., 2018; Abdelgawad & Yelamarthi, 2017; Mahmud et al., 2018). Wireless IoT based monitoring allows continuous and remote observation of infrastructures, reducing the need for manual inspections and enabling real time decision making.

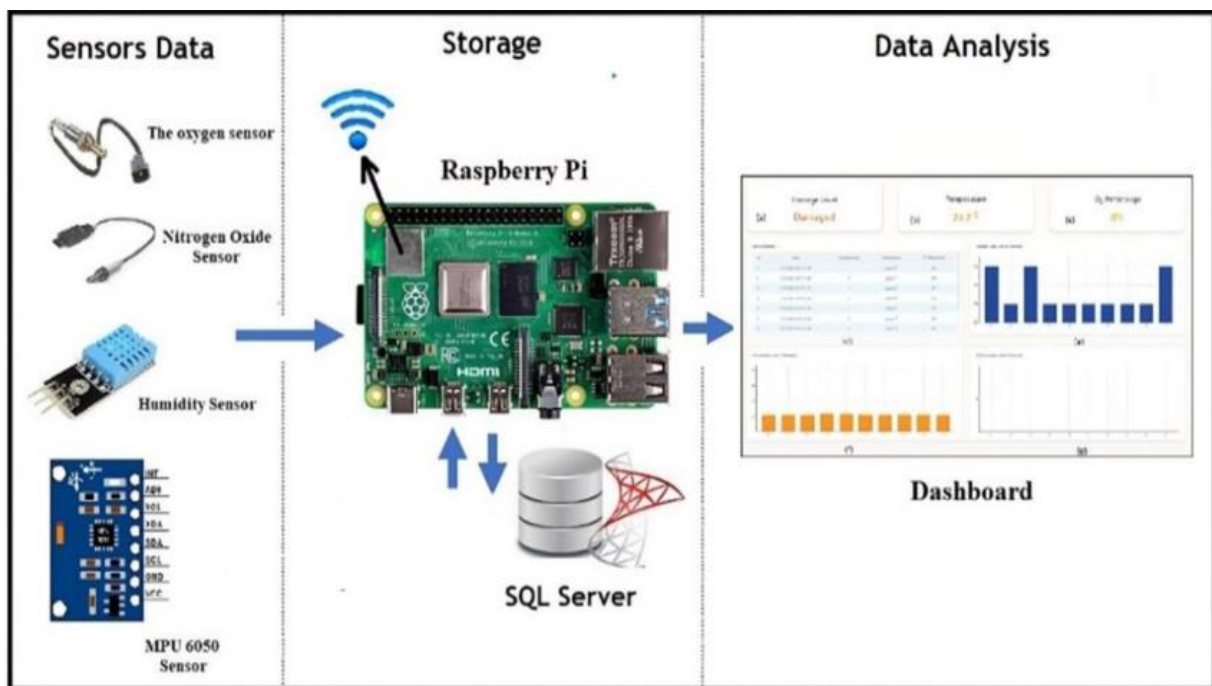


Figure 11 - IoT sensors workflow

IoT enabled SHM systems typically consist of smart sensors, low power microcontrollers, wireless communication protocols (e.g., ZigBee, LoRa, or Wi-Fi), and cloud based platforms for data storage and analytics. Additionally, higher-level data transfer from acquisition systems to cloud platforms often relies on standardized protocols such as MQTT, CoAP, or REST APIs. In this project, REST was adopted as it is the native protocol supported by Autodesk Tandem for JSON data ingestion. Compared to traditional wired networks, these systems are more flexible, scalable, and cost effective, especially for urban infrastructure projects where sensor deployment conditions may be challenging.

Researchers have demonstrated the successful use of IoT sensors to detect vibrations in bridges, monitor tilt in high rise buildings, and track ground movements near tunnels, applications directly relevant to metro construction and operation.

For the Certosa Metro Station area, three sensor types were selected based on their ability to capture the most critical behaviors:

1. Accelerometers – used to record dynamic responses such as train induced vibrations transmitted through the ground and into adjacent buildings. These sensors help assess comfort levels, potential structural fatigue, and compliance with vibration limits.
2. Tiltmeters – designed to measure small angular rotations of building elements or surface structures. They are particularly useful for identifying slow tilting or differential settlement that may precede visible damage.
3. Inclinator chains – installed below ground to detect lateral soil movements and shear deformations near the tunnel excavation. By capturing deformation profiles with depth, they provide insights into soil-structure interaction and the stability of the surrounding ground.

This multi-sensor approach ensures that both dynamic phenomena (e.g., transient vibrations) and quasi-static phenomena (e.g., progressive settlements or lateral soil displacements) are effectively monitored. The combination of these devices creates a redundant and complementary monitoring network, increasing the reliability of the system and reducing the risk of undetected issues.

Furthermore, linking these IoT enabled sensors to a digital twin platform like Autodesk Tandem allows engineers to visualize live measurements within the BIM model, facilitating cross checks between spatial locations and temporal trends. The use of IoT sensors in SHM not only improves data quality and accessibility but also supports predictive maintenance strategies. Instead of relying solely on scheduled inspections, operators can adopt condition based maintenance, intervening only when sensor data indicate abnormal behavior.

This approach reduces operational costs, minimizes downtime, and increases the safety and resilience of metro infrastructure. In the context of the Certosa Metro project, such a strategy is particularly important, as underground works and nearby structures are subject to dynamic loads, soil settlements, and complex geotechnical interactions.

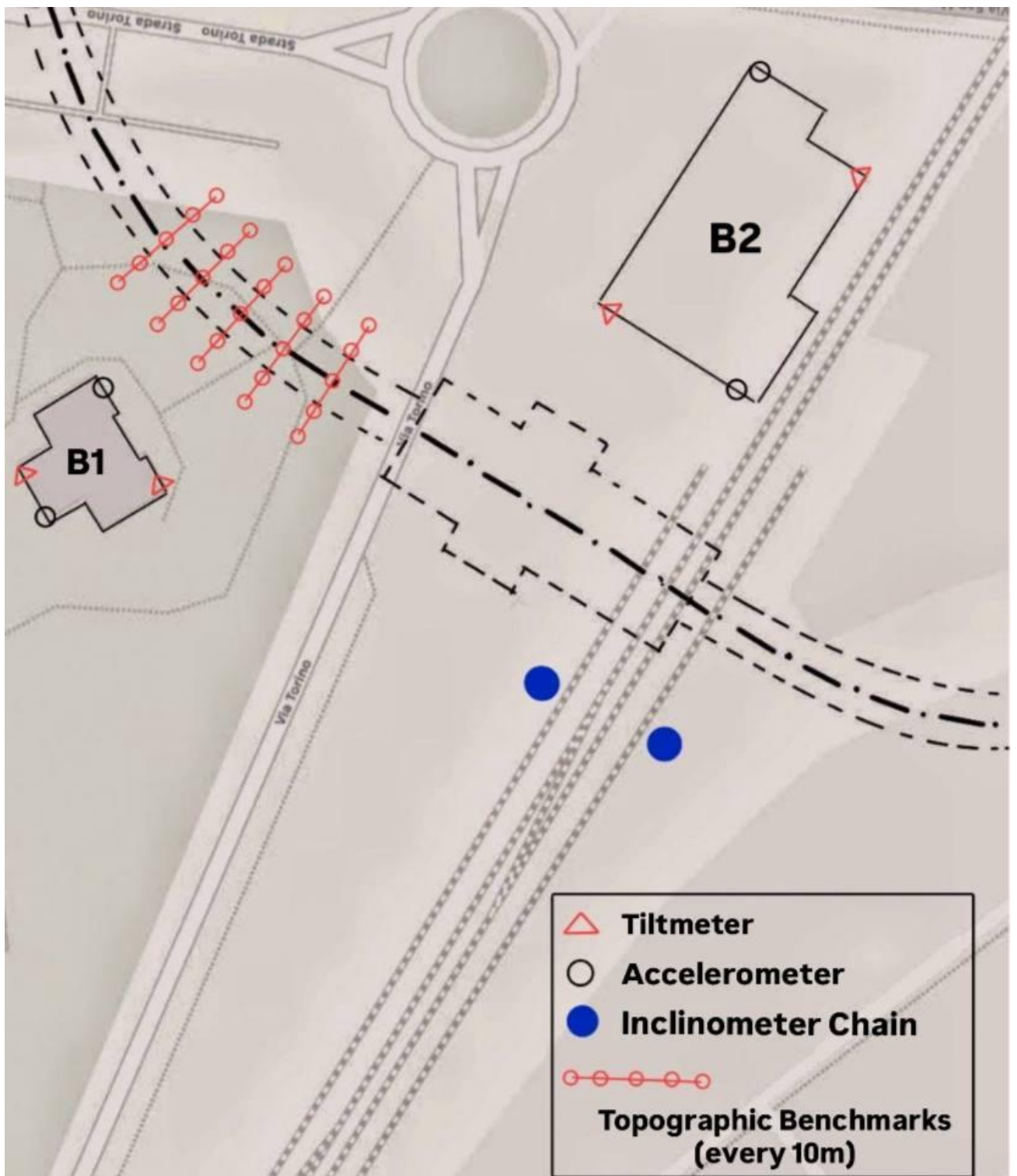


Figure 12 - Certosa Metro Area Sensors Placement Scheme

2.4.1 Accelerometers

Accelerometers are widely used in vibration monitoring because they directly measure acceleration over time. The data, usually recorded in m/s^2 or in fractions of gravity (g), can later be processed to obtain velocity and displacement. In metro infrastructure, accelerometers are typically installed on ground surfaces near the track, as well as on structural elements of adjacent buildings. Their main purpose is to record the propagation of vibrations caused by train passages and to assess whether these vibrations might affect structural safety or user comfort.

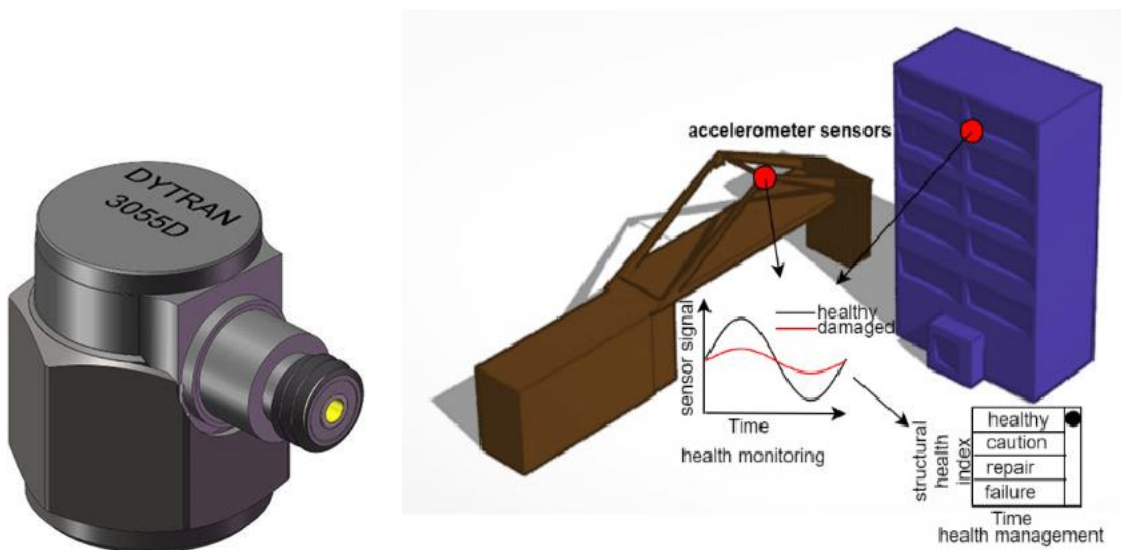


Figure 13 - Accelerometers

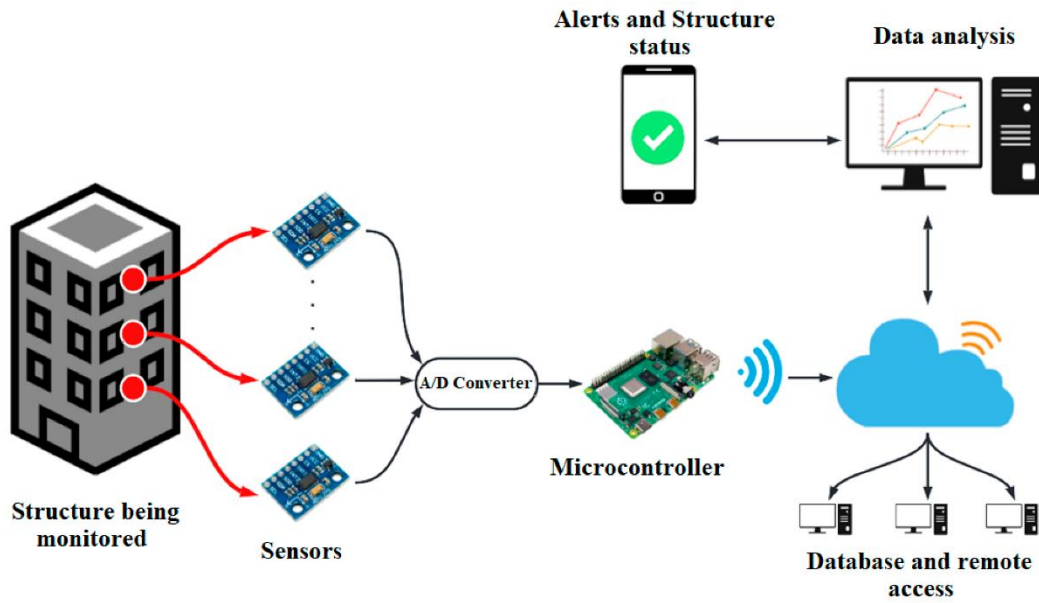


Figure 14 - Accelerometers Workflow

Train induced ground vibrations are usually in the range of 0.01 to 0.5 m/s^2 , while building responses are typically lower, around 0.001 to 0.05 m/s^2 . These values, although small, may accumulate or resonate with building frequencies, making accelerometers essential for dynamic analysis. In the Certosa case study, accelerometers were virtually positioned both in the soil and on the façades of two adjacent buildings, chosen as the closest and most representative structures.

- Gruppo CIDIU building: 2 accelerometers were positioned, one on the front façade and one on the rear façade, both at the ground floor level, fixed on rigid elements (columns/walls) to maximize contact with the structural response.
- Abandoned building adjacent to the station: 2 accelerometers were installed in the same configuration (front and rear façades) to record the propagation of vibrations into a different structural typology.

2.4.2 Tiltmeters

Tiltmeters measure angular changes (rotations) in structures, expressed in degrees or milliradians. They are sensitive to very small inclinations, often in the order of 0.001° to 0.05° , which makes them useful for detecting building settlements or rotations caused by tunneling activities, ground subsidence, or vibration effects.

In practice, tiltmeters are mounted on structural members such as walls or columns. For metro environments, tiltmeters complement accelerometers by capturing low frequency or long term deformations, such as tilting due to soil settlement.



Figure 15 - Tiltmeter SISGEO

In the Certosa case study:

- Gruppo CIDIU building: 2 tiltmeters were placed, one on the front side wall and one on the rear wall, in correspondence with the accelerometer locations, to correlate angular rotation with vibration data.
- Abandoned building: 2 tiltmeters were also installed on the front and rear façades, ensuring consistency in monitoring between the two buildings.

By positioning tiltmeters on both sides of the buildings, it was possible to capture potential differential rotations, which are more critical than uniform tilting in terms of structural damage.

2.4.3 Inclinometer Chains

Inclinometer chains are among the most effective tools for monitoring subsurface soil deformations. They consist of a borehole with a casing, inside which a chain of sensors is installed at fixed intervals. Each node of the chain measures angular variations relative to the vertical, and by integrating these inclinations, a horizontal displacement profile of the soil can be reconstructed.



Figure 16 - Inclinometer Chain

2.4.3.1 Theoretical Basis of Inclinator Chains

The inclinometer chain technology adopted in this thesis is based on the MUMS system (Modular Underground Monitoring System) developed at the University of Parma (Segalini et al., 2014). The system consists of a series of nodes installed along a flexible rope at known intervals inside a vertical borehole. Each node is equipped with:

- a 3D MEMS accelerometer, which measures orientation relative to gravity;
- a 3D magnetometer, which provides heading relative to magnetic north;
- and a temperature sensor for environmental compensation.

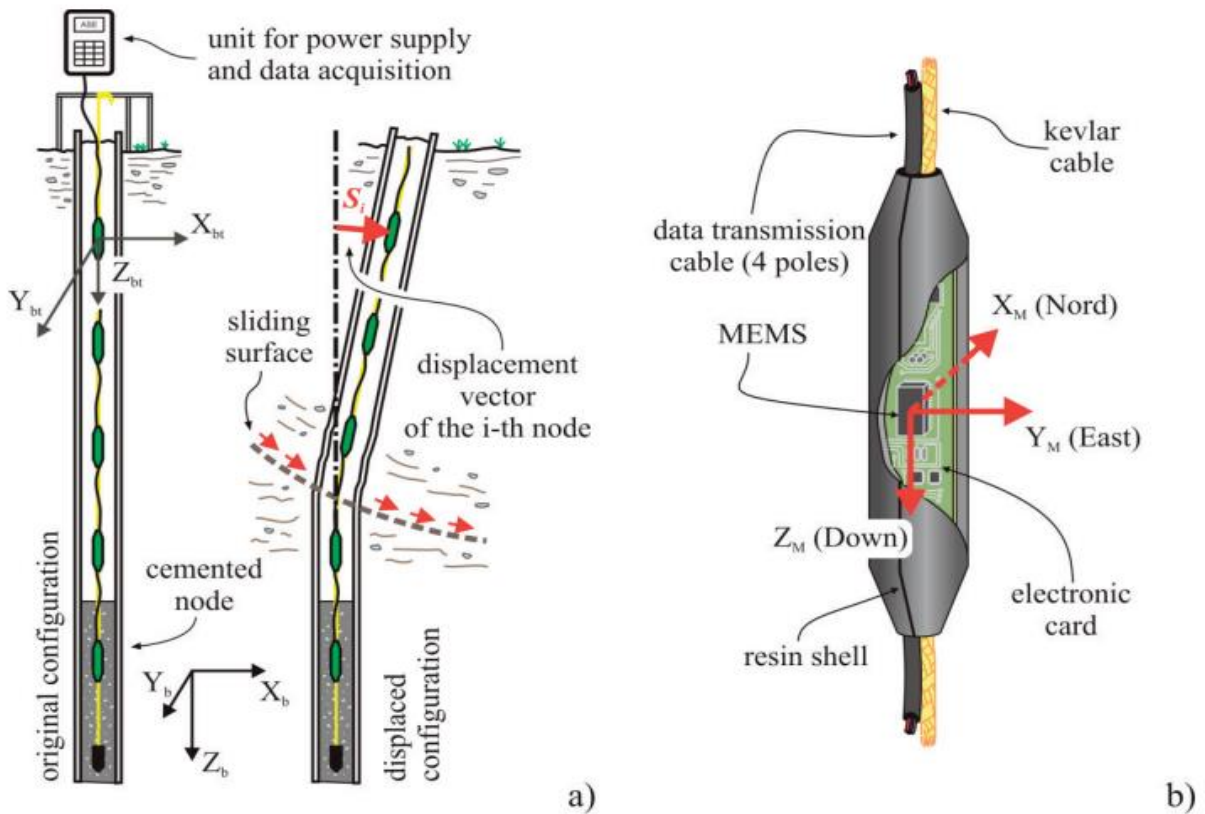


Figure 17 - Modular Underground Monitoring System (MUMS)

When installed, the lower nodes are cemented into a stable soil layer, serving as a benchmark, while the upper nodes are free to move with the deforming soil. This configuration allows the reconstruction of the lateral displacement profile of the soil column, which is essential for detecting shear zones and settlement patterns near underground infrastructure such as metro tunnels.

2.4.3.2 Theoretical Principle

Each MEMS accelerometer measures the components of gravitational acceleration along its local axes. When the node tilts, the projection of gravity on the vertical axis changes. From this variation, the lateral displacement of the i -th node, S_i , can be derived.

Neglecting the azimuthal direction and focusing on the vertical component of gravity (a_z), the displacement of node i can be expressed as:

$$S_i = L \cdot \Delta a_z$$

where:

- S_i = lateral displacement of node i
- L = length of the chain portion between the fixed reference and node i
- Δa_z = variation of the vertical acceleration component relative to the initial (zero) reading

A more complete formulation, considering trigonometric contributions, is expressed in Segalini et al. (2014) as:

$$S_i = L \cdot (\sin(\Delta a_z) \cos(a_{z1}) - \sin(a_{z1}) \cos(\Delta a_z))$$

where a_{z1} is the initial vertical component at the time of installation, and Δa_z represents the change over time.

This formula highlights an important aspect: small variations in acceleration components can induce significant apparent displacements, especially if the sensor's initial orientation is close to vertical. Therefore, sensor calibration and signal filtering (e.g., moving average, detrending) are required to reduce drift and noise, distinguishing real soil movements from instrumental artifacts.

In the Certosa Metro Station case study, two inclinometer chains, each with five nodes, were virtually installed in boreholes on both sides of the railway alignment. The lower nodes were assumed fixed in the stable soil layers, while the upper nodes recorded deformations induced by tunnel excavation and train operations.

The theoretical framework described above allowed the simulated datasets to reproduce realistic displacement profiles. By applying the relationship between Δa_z and S_i the generated inclinometer data reflected possible soil displacements of tenths of millimeters to a few millimeters, consistent with the expected range for the site geology and excavation type. These synthetic signals, once processed and filtered, were integrated into the BIM environment and visualized in Autodesk Tandem as part of the digital twin.

2.4.4 Topographic Benchmarks

Topographic benchmarks are fixed reference points used to monitor long term ground deformations such as settlement, uplift, and lateral displacement. They provide a stable surface level reference that complements dynamic vibration sensors by capturing slow movements that develop over extended periods.

In the Certosa Metro Station area, benchmarks were positioned across the park to cover the monitoring zone most exposed to potential ground settlement. A total of five sections (S1–S5) were arranged along the park area, spaced at 10-meter intervals. Each section contains a row of benchmarks placed orthogonally to the pedestrian paths, forming a systematic grid that allows differential movements to be compared across the site. This layout ensures that any localized ground deformation can be identified by comparing displacement trends between neighboring sections.



Figure 18 - Topographic Benchmark

For the purpose of this thesis, synthetic benchmark measurements were created to simulate periodic surveying. The sampling interval was set to 5 minutes, which is denser than typical field campaigns but useful for testing the data pipeline and validating the digital twin. Each benchmark reading records the vertical displacement (ΔZ) relative to its initial elevation, and minor horizontal shifts where applicable.

In the BIM model, the benchmarks were represented as point assets and assigned unique IDs, section numbers, and coordinates as shared parameters. These were then imported into Autodesk Tandem, where the benchmark time series were visualized alongside accelerometer, tiltmeter, and inclinometer data. Including benchmarks in the monitoring system strengthens the overall analysis by providing a surface level confirmation of settlement patterns and by linking long term ground movements with building tilts and subsurface deformations.

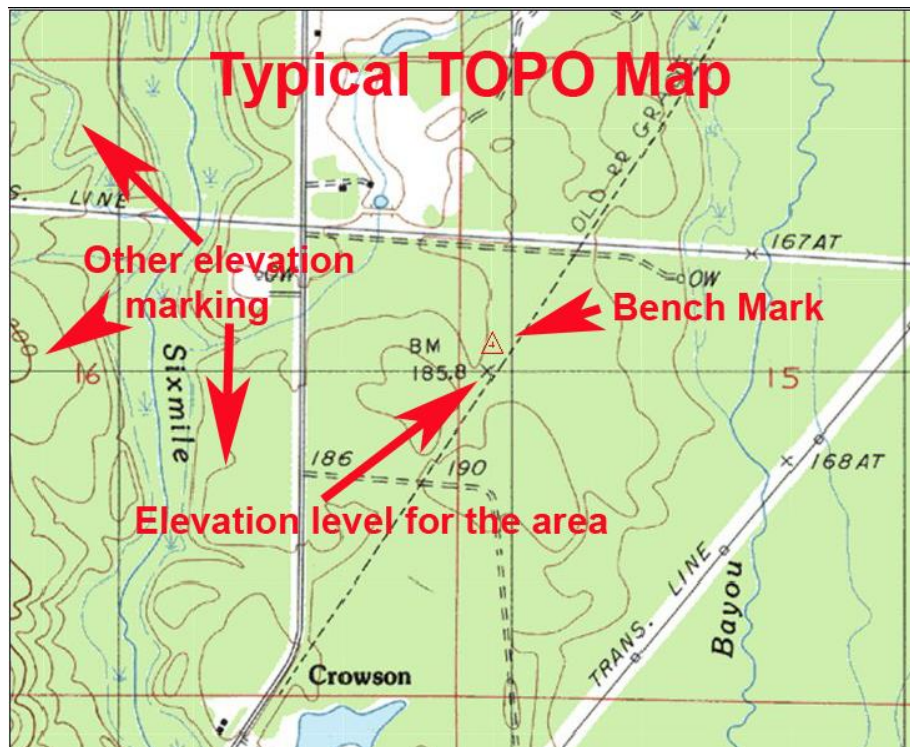


Figure 19 - Benchmark TOPO Map Example

3. Methodology

The methodology of this thesis is based on a step-by-step workflow that connects Building Information Modeling (BIM) with Structural Health Monitoring (SHM) to build a functional digital twin of the Certosa Metro Station area. The process combines modeling, sensor integration, data generation, and digital twin implementation. Each stage was designed to ensure interoperability between different platforms and to demonstrate how monitoring data can be linked to a BIM environment and visualized in real time.

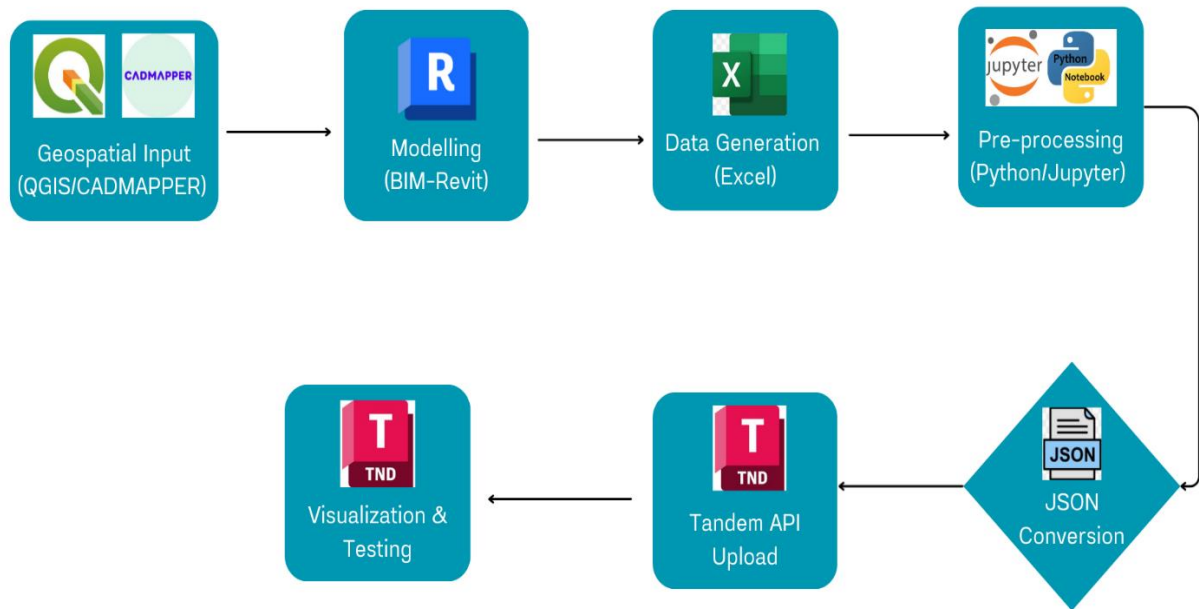


Figure 20 - Workflow of Project

The main phases of the methodology are:

1. Case Study Definition

- Introduction of the Certosa Metro Station project and description of its relevance.
- Justification for selecting two nearby buildings and the railway area for monitoring.

2. Modeling Workflow

- Preparation of a georeferenced 3D environment.
- Integration of QGIS, CAD, Revit, and InfraWorks to model the metro station, terrain, and surrounding buildings.

3. Sensor Integration in BIM

- Creation of parametric sensor families in Revit.
- Definition of shared/project parameters.
- Placement of accelerometers, tiltmeters, and inclinometer chains in the selected locations.

4. Data Workflow and IoT Simulation

- Generation of synthetic datasets in Excel.
- Adaptation of data using manufacturer technical sheets, values from similar projects, and expected conditions of the site.
- Processing in Python (Jupyter Notebook) to convert datasets into JSON and link them to Tandem.

5. Validation and Testing in Autodesk Tandem

- Connection of data streams to digital sensors.
- Visualization of vibration, inclination, and settlement in real time.
- Discussion of technical challenges (data formatting, parameter mapping, interoperability).

This structured methodology demonstrates the process of moving from a traditional BIM model to an operational digital twin, which can later be extended with real sensor data and predictive analysis.

3.1 Case Study Definition

The case study of this thesis is the Certosa Metro Station in Turin, which is part of the new metro extension under development by Infra.To. The station is located in a densely built urban area and plays a crucial role in connecting residential and industrial districts to the wider metropolitan transport network. Due to the underground excavation and proximity of existing buildings, the site presents several challenges in terms of soil structure interaction, train induced vibrations, and potential settlements. These factors make the Certosa area a suitable and meaningful case study for testing the integration of BIM and SHM within a digital twin framework.



Figure 21 - The Region Around the Certosa Metro Area Studied

Area: 0.043 km²

Buildings: 2 total, 0 with height value (0%)

Topography: Included, 298.00 m above sea level

Settings: Road outlines (highways 10.0, major 8.0, minor 6.0, paths 4.0), 3D buildings (no value = 3.0 m), 4 m contours

Spatial Reference System: Meters; UTM zone: 32, easting: 388080.49, northing: 4992389.09

DOWNLOAD (16.8 KB)

Download available on site for 1 month.

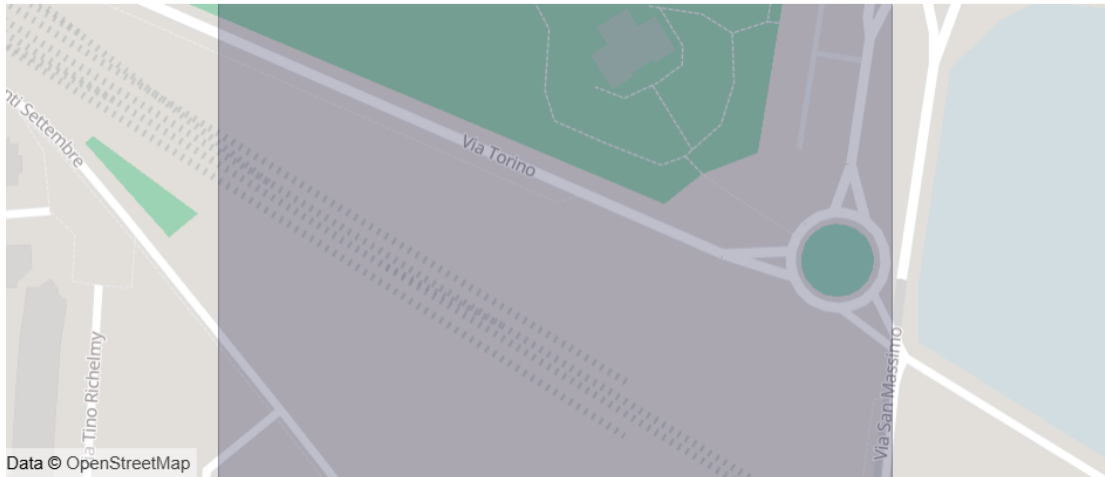


Figure 22 - Downloaded region in CADmapper

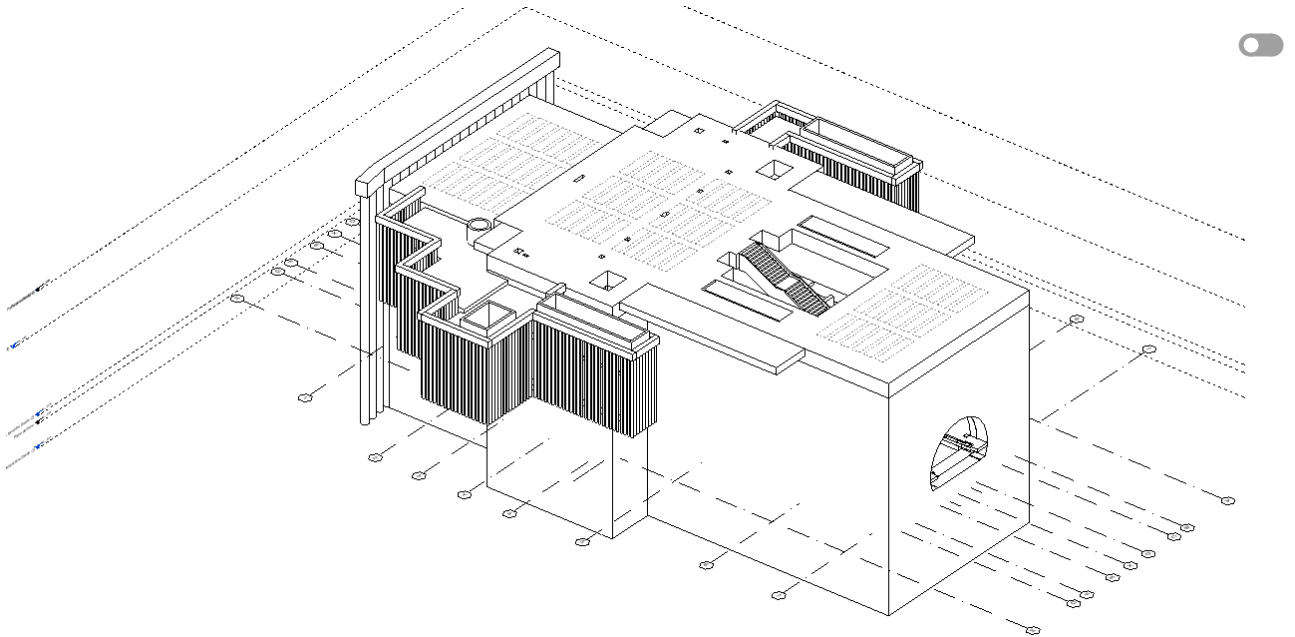


Figure 23 - The BIM model of the station provided by Infra.To

The BIM model of the station was originally provided by Infra.To, ensuring that the geometry and main structural elements were accurate and consistent with the design project. For the purpose of this research, the model was further complemented with the surrounding terrain, adjacent buildings, and the integration of virtual sensors. This extension allowed the digital model to represent not only the station itself but also the broader environment that could be affected by metro operations.

In defining the monitoring system, two specific buildings were selected for sensor placement:

- Gruppo CIDIU building, located closest to the metro alignment and representing a functional urban structure in active use.
- An abandoned building, situated immediately adjacent to the metro site, chosen as a second representative structure to compare responses across different building conditions.

Other nearby buildings were excluded from the analysis because they were located at similar distances from the railway line and therefore expected to show comparable responses. Focusing on the two closest buildings allowed for a more efficient and representative assessment of the effects of metro induced vibrations and ground deformations.

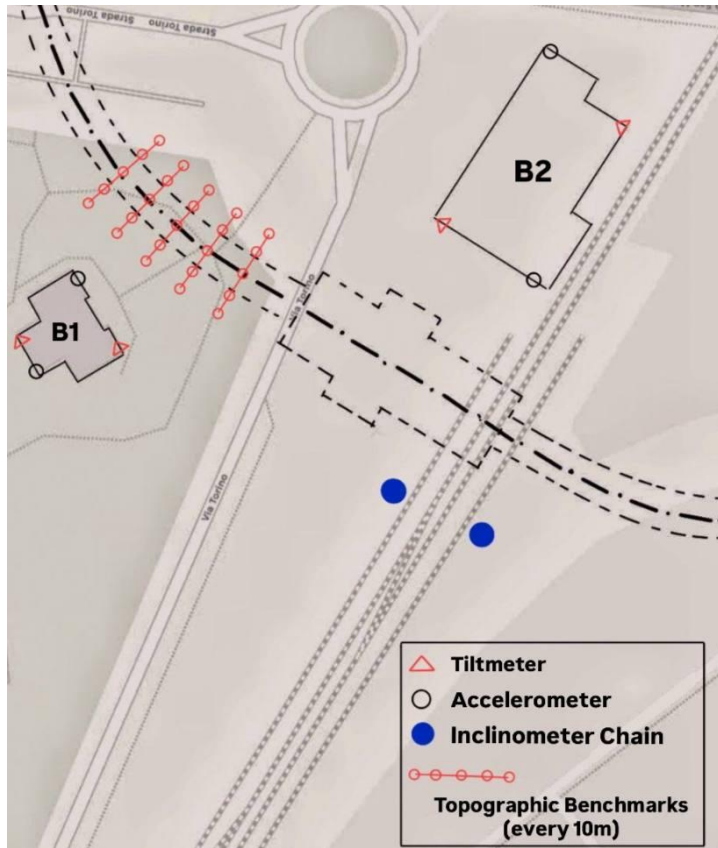


Figure 24 - Certosa Metro Area Plan

For the geotechnical component, two inclinometer chains were positioned virtually in the soil on both sides of the railway alignment. Each chain included five nodes distributed along the depth of the boreholes, enabling the detection of horizontal displacements and shear zones that might develop around the tunnel. Together with the building sensors, these devices formed a complementary monitoring system: accelerometers to capture dynamic vibrations, tiltmeters to record building inclinations, inclinometer chains to evaluate subsurface soil deformations, and topographic benchmarks to monitor long term surface settlements and lateral ground movements.

In addition to building and subsurface monitoring, topographic benchmarks were arranged across the Certosa park area in five sections spaced 10 meters apart. These benchmarks form a regular grid designed to detect long term settlement and lateral ground movements, providing surface level confirmation of trends observed in the accelerometer, tiltmeter, and inclinometer chain data.

This case study definition ensured that the monitoring design was both targeted and representative: targeted because it focused on the most critical assets (the nearest buildings and the railway area), and representative because the results could reasonably be extended to similar nearby structures and conditions.

3.2 Modeling Workflow

The development of the digital environment for the Certosa Metro Station followed a multi-platform workflow, combining geospatial data with BIM and infrastructure modeling tools. The objective was to create a georeferenced, realistic, and information-rich model that could serve as the foundation for sensor integration and digital twin implementation.

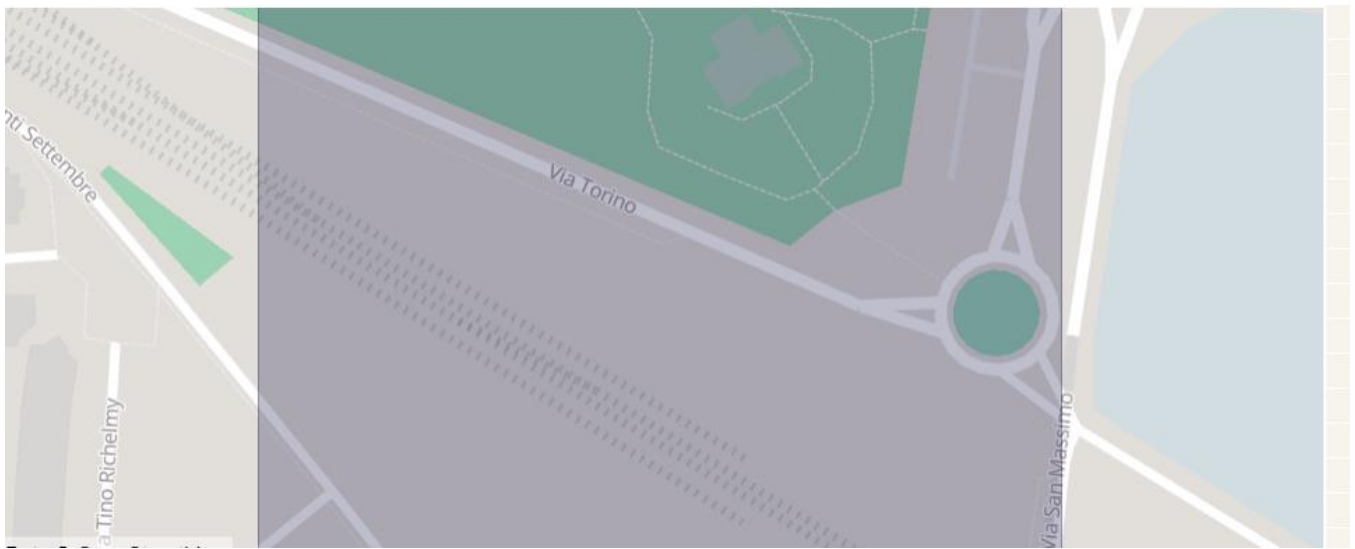


Figure 25 - QGIS topographic data of the Certosa area

The workflow began with QGIS, where cadastral and topographic data of the Certosa area were processed. Vector and raster datasets were analyzed, and relevant boundaries of the station area were extracted.

This step ensured that the project operated within the correct coordinate system and maintained consistency with the georeferenced data available from municipal and regional sources. The processed datasets were exported in CAD formats (DXF/DWG) to allow interoperability with BIM software.

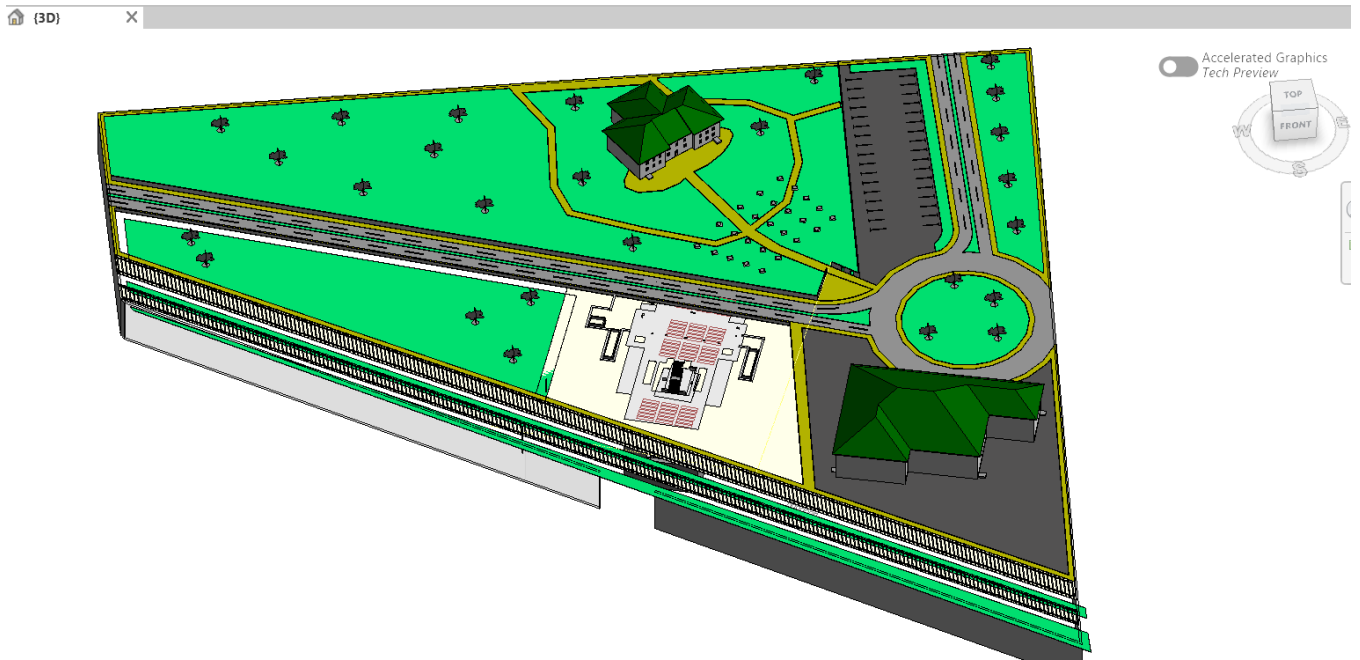


Figure 26 - Certosa region BIM model designed in Revit

The next step was carried out in Autodesk Revit, where the BIM model of the Certosa Metro Station provided by Infra.To was imported. This model contained the main structural and architectural elements of the station, including underground levels, alignments, and station geometry. To extend the scope of the model, the surrounding environment was added: terrain features were traced from the QGIS/CAD data, and adjacent buildings, including the Gruppo CIDIU building and the abandoned structure, were modeled to reflect the urban context. This integration allowed the Revit model to represent not only the metro station itself but also its interaction with nearby assets.

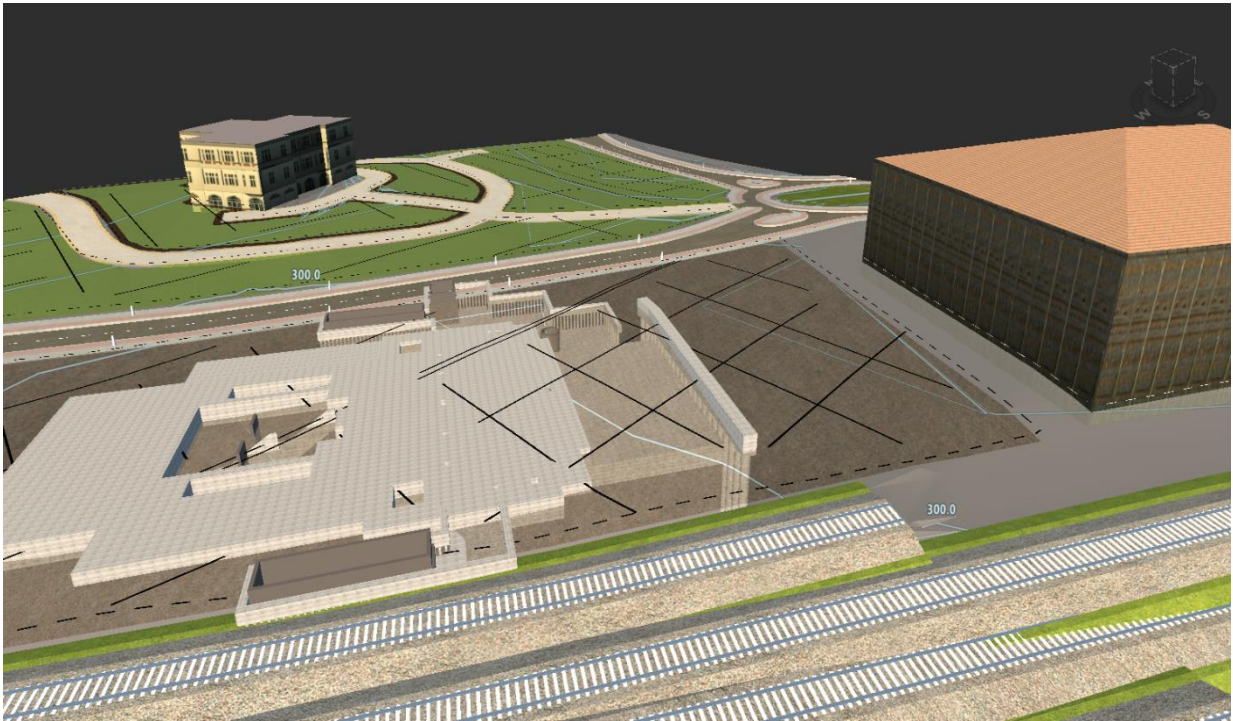


Figure 27 - Region of Certosa created in InfraWorks

To further enhance the realism of the environment, Autodesk InfraWorks was used. InfraWorks enabled the creation of a 3D topographic context by incorporating elevation data and surface models. The station model developed in Revit was then imported into InfraWorks, where the surrounding terrain, roads, and existing infrastructure were refined. This step provided a visually realistic urban environment that could later be exported and linked back to Revit, ensuring consistency between detailed BIM modeling and large-scale infrastructure representation.

A critical aspect of the workflow was the alignment of coordinate systems across platforms. QGIS provided the georeferenced base, which was preserved during the CAD export and maintained during Revit and InfraWorks integration. This ensured that the position of the metro station, the surrounding buildings, and the sensor locations corresponded accurately to the real world site.

The final outcome of this workflow was a georeferenced BIM model enriched with urban context, suitable for hosting monitoring devices and serving as the backbone for the digital twin. This model allowed both structural and environmental conditions to be represented in a single framework, providing the necessary foundation for the subsequent stages of sensor integration and data connection.

3.3 Sensor Integration in BIM

The integration of sensors within the BIM model represents a fundamental step for transforming a static digital representation into a monitoring oriented environment. In this study, Autodesk Revit was used to host virtual sensors that correspond to accelerometers, tiltmeters, inclinometer chains, and topographic benchmarks.

3.3.1 Creation of Sensor Families

Custom Revit families were developed to represent each type of sensor. These families were modeled as simplified 3D geometries to ensure visibility in the model without adding unnecessary complexity. The geometric representation was complemented with parameters that defined the identity and function of each device. For example, accelerometer families included fields for ID, type, frequency range, and installation location, while tiltmeters and inclinometer chains included parameters related to angular resolution, depth, and measurement units. Topographic benchmarks were represented as point elements with parameters for section ID, benchmark ID, and precise coordinates.

3.3.2 Definition of Parameters

To standardize the information structure, a combination of shared parameters and project parameters was employed. Shared parameters ensured consistency across different projects and compatibility with Autodesk Tandem, while project parameters allowed flexibility in adapting to the specific needs of the Certosa case study. The parameters were organized into categories such as:

- Identification (Sensor ID, Type, Manufacturer Reference, Section for benchmarks)
- Technical specifications (Measurement range, Accuracy, Units)
- Location (Building, Façade, Depth, Coordinate reference, Benchmark section coordinates)
- Connection (Tandem mapping field, Stream ID)

This approach enabled a smooth transition from BIM modeling to digital twin implementation, since each virtual sensor in Revit already contained the metadata required for mapping to Tandem.

3.3.3 Placement of Sensors

The virtual sensors were strategically positioned in the model according to the monitoring design:

- Gruppo CIDIU building: Two accelerometers and two tiltmeters were placed, one set on the front façade and one on the rear façade at ground floor level. Accelerometers were fixed to rigid structural elements (walls or columns) to ensure accurate vibration transmission, while tiltmeters were positioned to capture angular changes in the same locations.

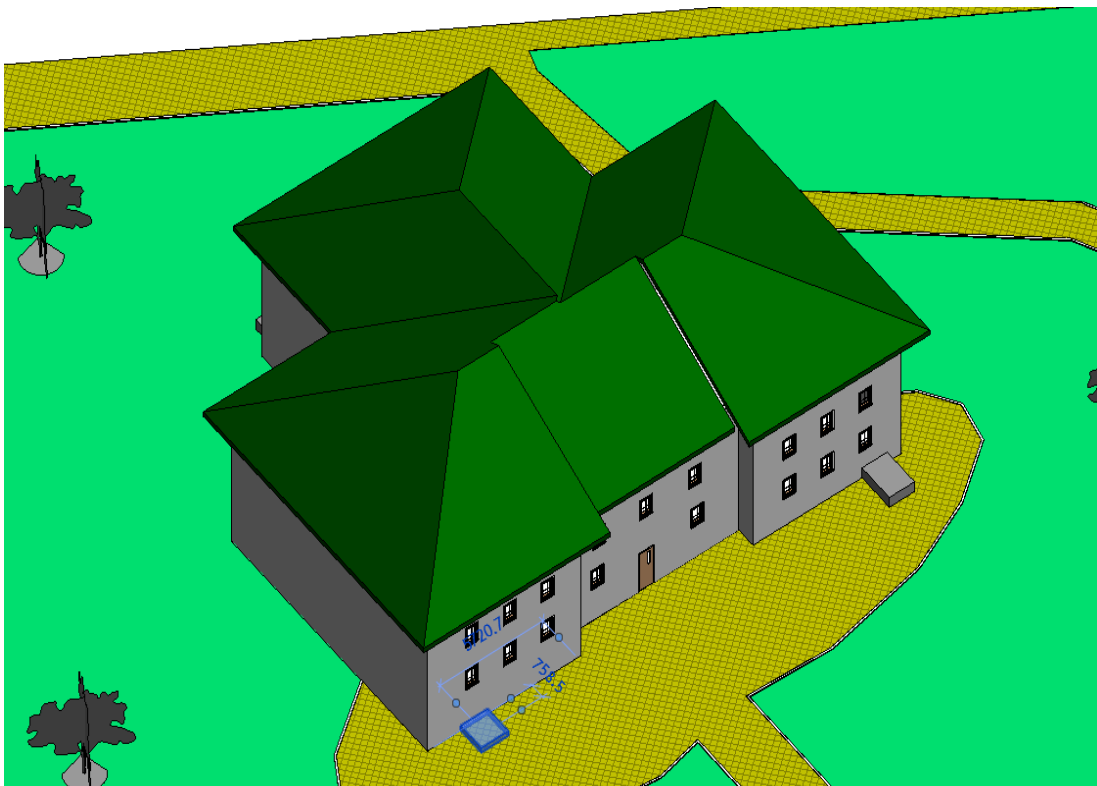


Figure 28 - Gruppo CIDIU Building (B1) Revit Model Front View Sensors Placement

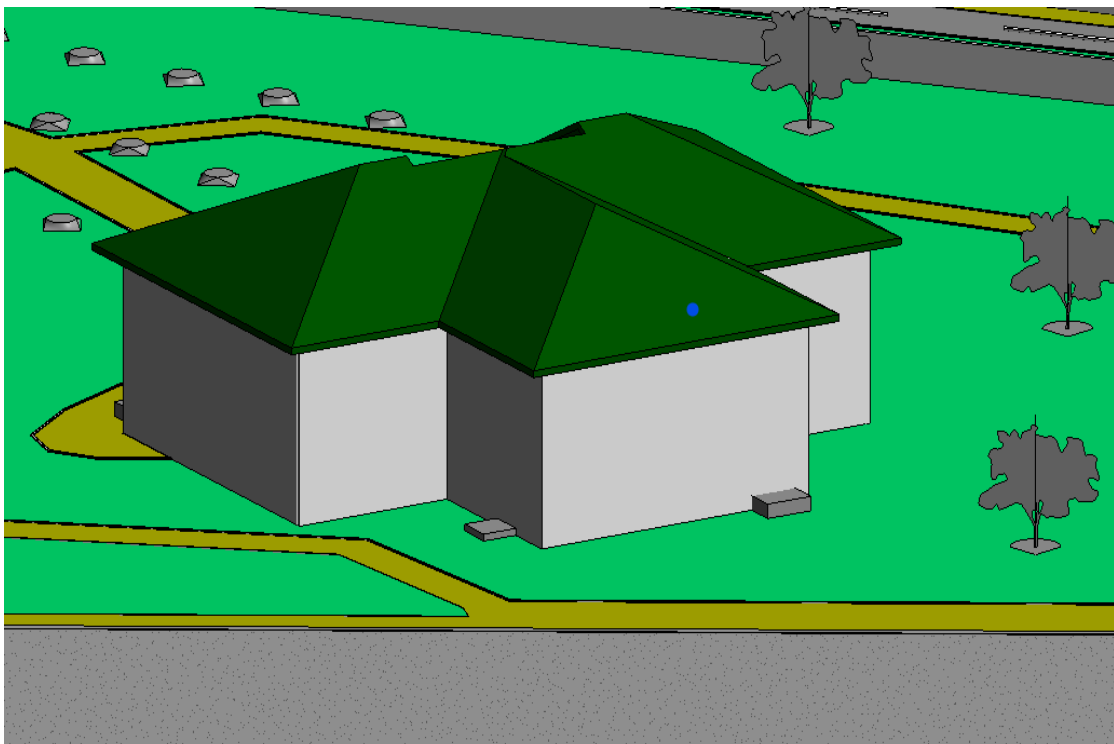


Figure 29 - Gruppo CIDIU Building (B1) Revit Model Back View Sensors Placement

- Abandoned building: Similarly, two accelerometers and two tiltmeters were installed on the front and rear façades. Consistency in placement between the two buildings allowed for direct comparison of responses in different structural conditions.

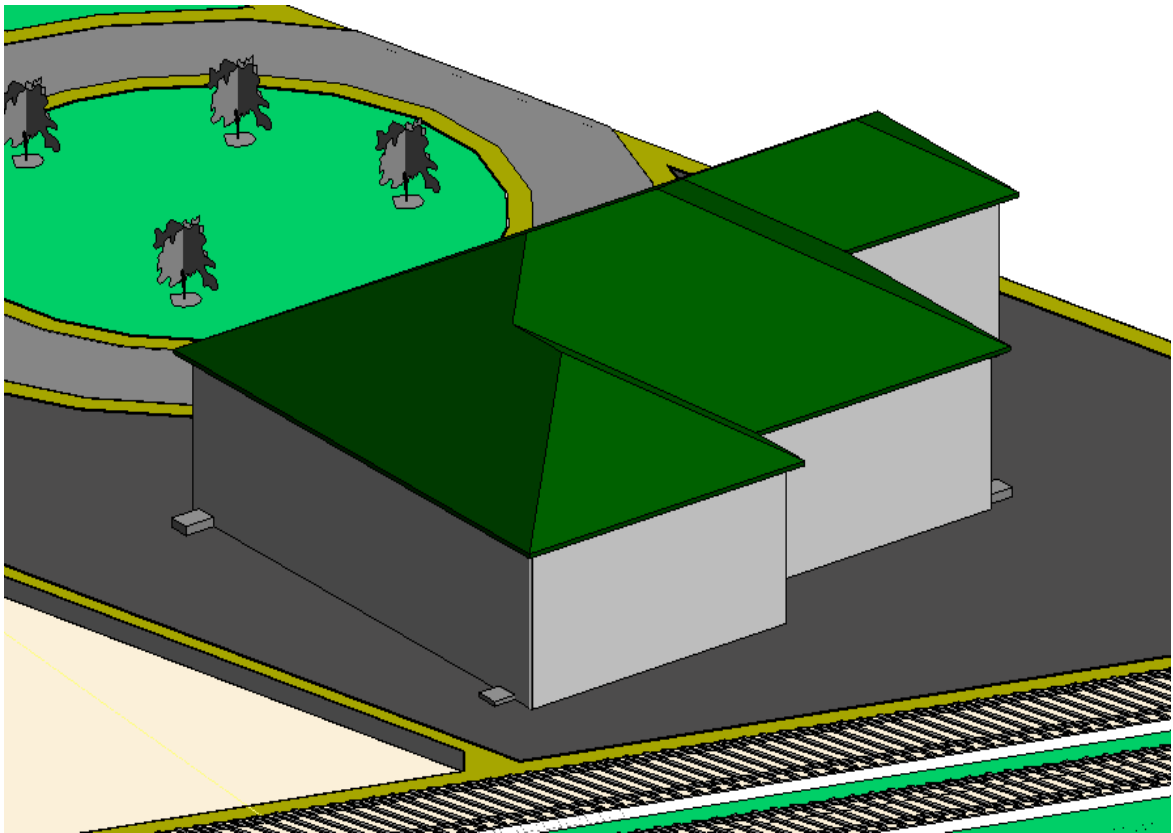


Figure 30 - Abandoned Building (B2) Side View of Sensors Placement

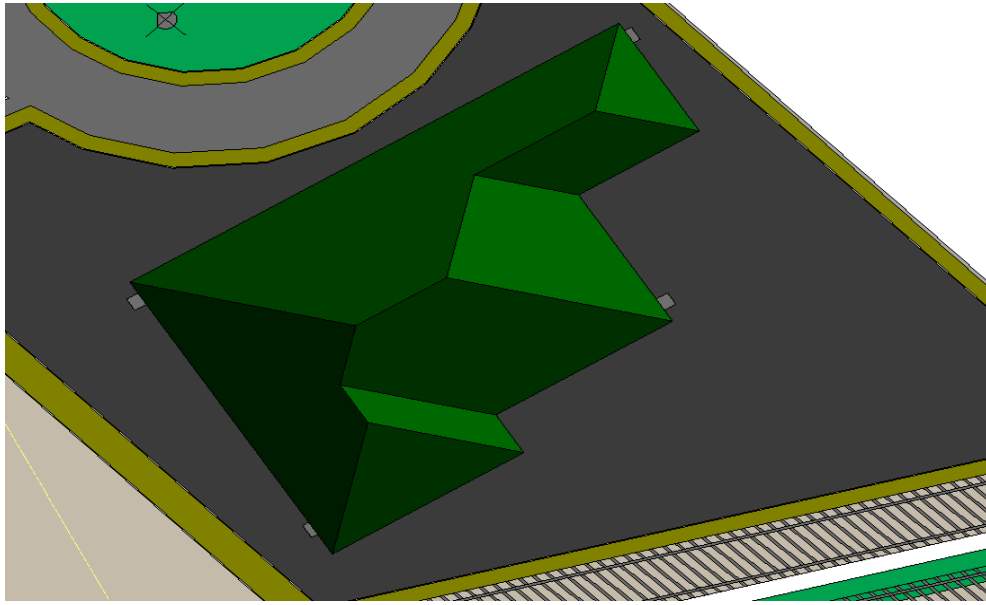


Figure 31 - Abandoned Building (B2) Top View of Sensors Placement

- **Railway alignment:** Two inclinometer chains were virtually placed in the soil, one on each side of the track. Each chain consisted of five nodes, spaced regularly along the borehole depth. The lower nodes were fixed into stable soil layers to serve as reference points, while the upper nodes recorded deformations closer to the tunnel and surface.

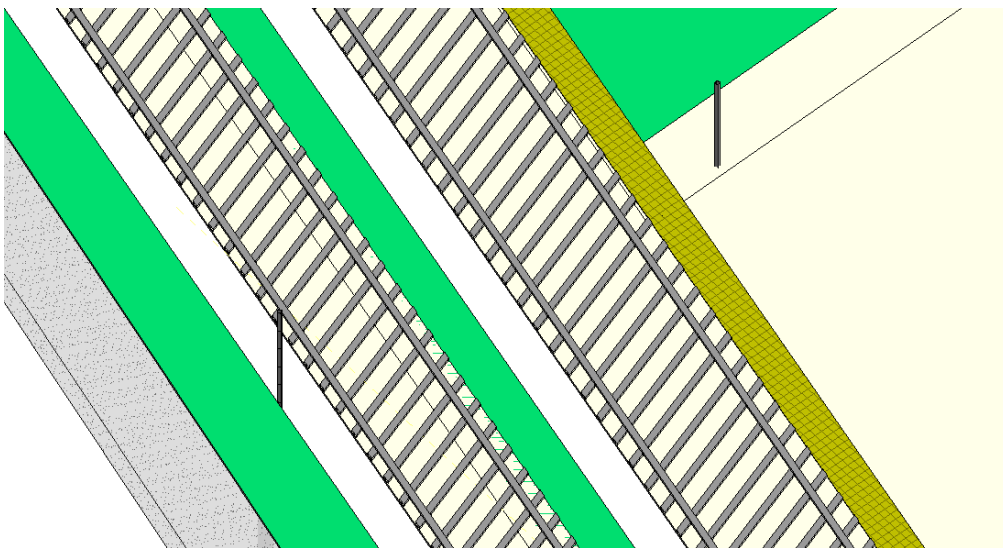


Figure 32 - Inclinometer Chains Placement in Railway Alignment

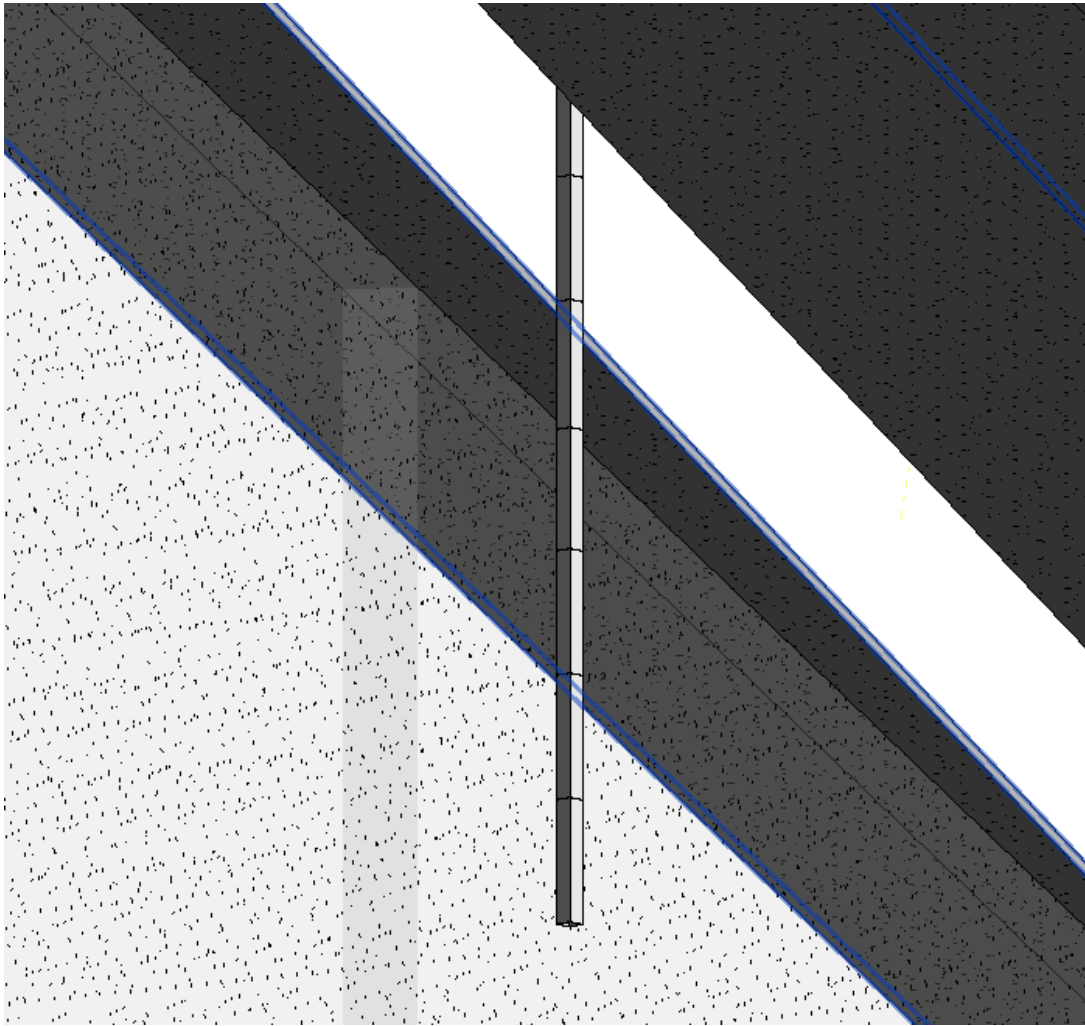


Figure 33 - Inclinometer Chain 1 underground view of nodes

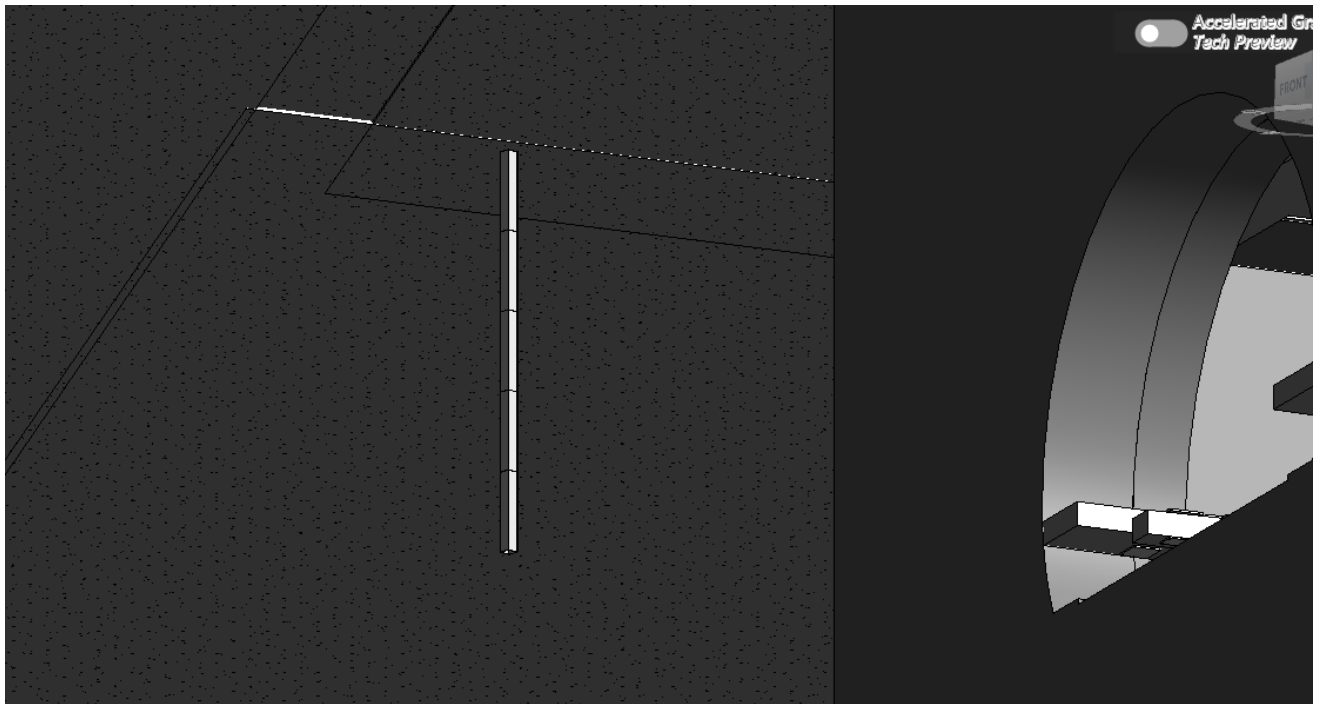


Figure 34 - Inclinometer Chain 2 underground view of nodes

- Park area benchmarks: Five sections of topographic benchmarks were arranged across the park area at 10 meter intervals. Each section consisted of multiple benchmark points placed along orthogonal transects to capture surface level settlement and lateral movements. The benchmarks were positioned in open areas clear of obstructions to allow accurate surveying and were represented in Revit with their IDs and section references for easy mapping to measurement data.

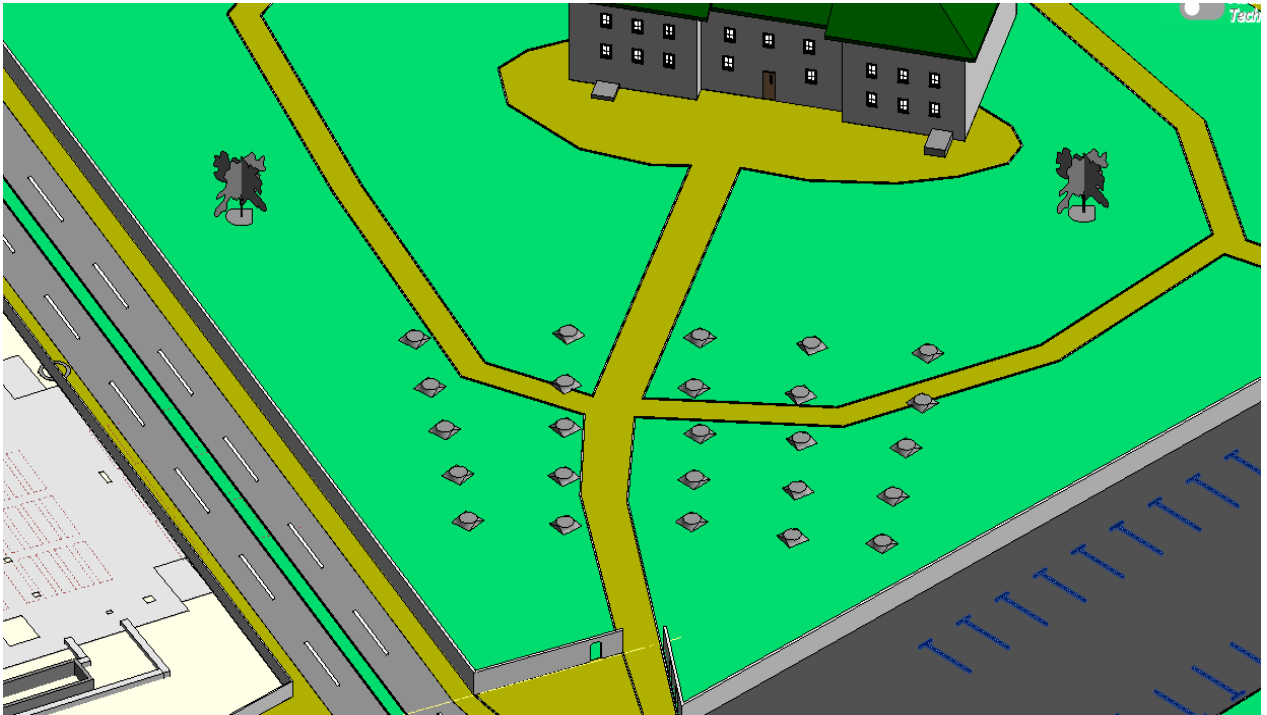


Figure 35 - Topographic Benchmark Placement in Park Area

By positioning sensors on both façades of the buildings, the system was able to capture differential vibrations and rotations, which are critical indicators of structural stress. Similarly, the placement of inclinometer chains near the railway provided a geotechnical perspective to complement the structural monitoring, while the park area topographic benchmarks added a surface level reference for long term settlement trends and ground movements across multiple sections.

3.3.4 Interoperability Considerations

The use of shared parameters and standardized family templates ensured that the Revit model was fully interoperable with Autodesk Tandem. Each sensor family, including the benchmarks contained a unique ID and connection field, which allowed direct mapping to incoming data streams. This step transformed the BIM model into a monitoring ready environment, bridging the gap between design documentation and real time SHM integration.

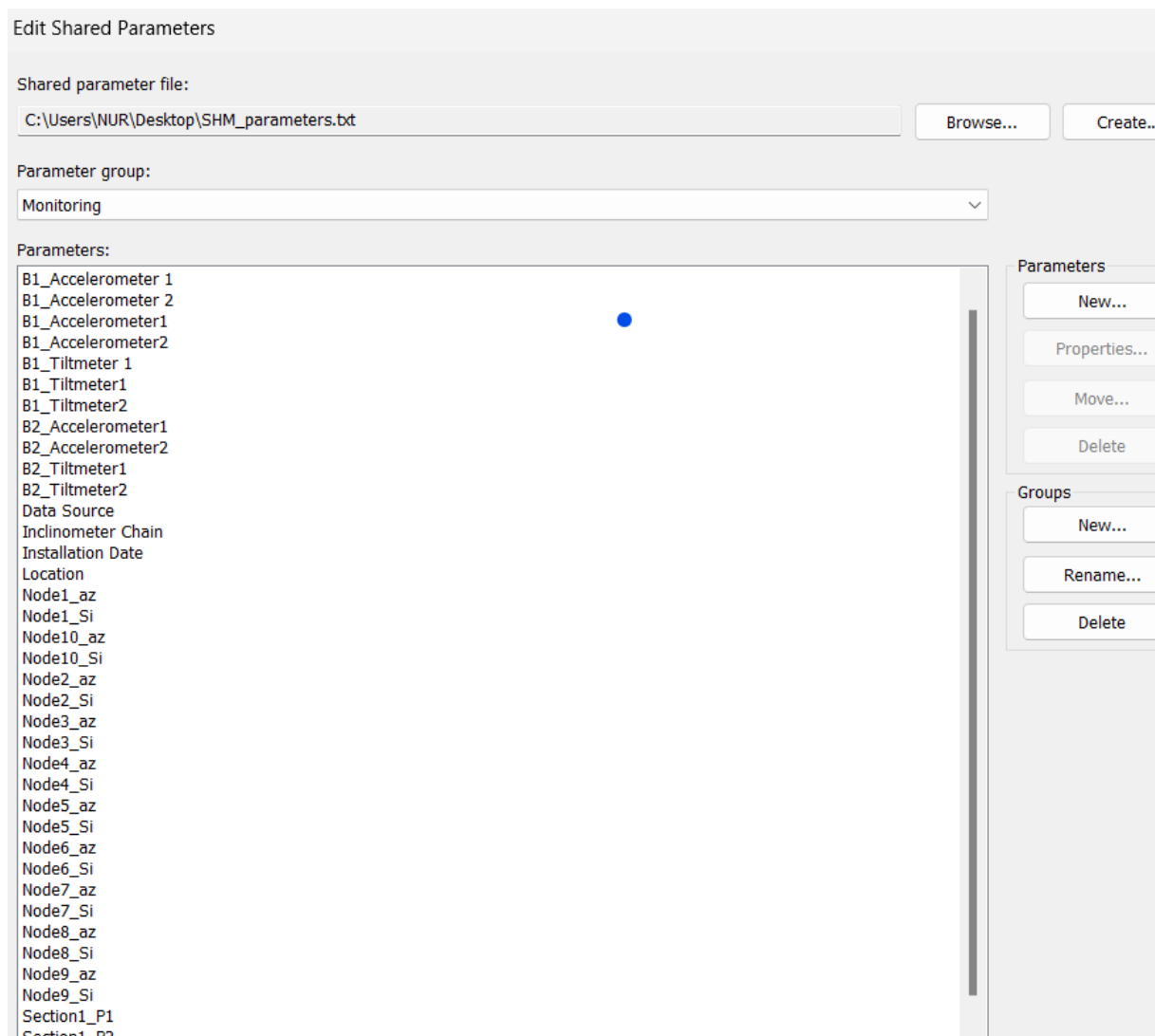


Figure 36 - Shared Parameters in Revit

3.4 Data Workflow and IoT Simulation

The integration of monitoring data into the digital twin required a complete and robust data pipeline capable of transforming synthetic measurements into formats compatible with Autodesk Tandem. Because real sensor data were not yet available at the time of this study, artificial datasets were generated to emulate realistic field conditions for accelerometers, tiltmeters, inclinometer chains, and topographic benchmarks. This simulation approach allowed the testing and validation of the digital workflow under controlled and repeatable conditions, ensuring that the procedures developed here can later be applied to live data streams without modification.

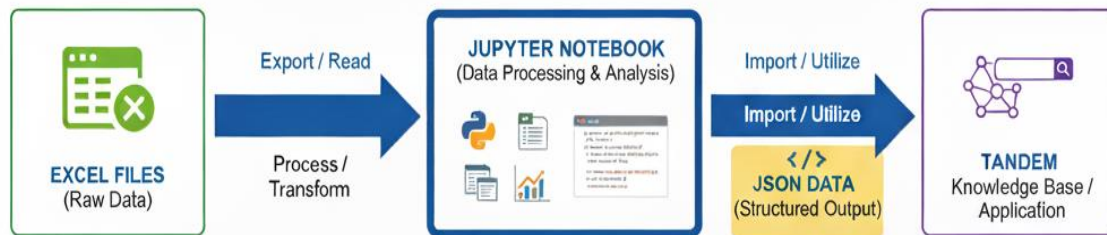


Figure 37 - Workflow of sending data to Tandem

The workflow began with Excel as the primary environment for generating synthetic data tables. Each dataset was carefully designed rather than randomly assigned: values were chosen based on examples from similar metro and tunneling monitoring projects, on the technical specifications provided by the sensor manufacturers, and on typical ranges of soil response and building behavior for the ground and excavation type present in the Certosa area. For example, accelerometer signals were created to reproduce train induced vibration peaks between 0.001–0.05 m/s² for the monitored buildings and up to 0.5 m/s² near the railway track, reflecting amplitudes reported in comparable SHM studies. Tiltmeter readings were modeled to display gradual angular drifts superimposed with small, high frequency

fluctuations, simulating the combination of long term settlement and short term construction disturbances. Inclinator chains were assigned lateral displacement profiles that increased with depth to replicate the shear deformation typically expected adjacent to tunneling activity, while topographic benchmarks were given small vertical displacements to mimic surface settlement gradients across the park area. In addition, for inclinometer chains, the simulated values were generated as a function of the excavation front position. When the excavation was closer to a monitored sensor, displacement and acceleration values were increased, while they gradually decreased as the excavation moved further away. This correlation with excavation distance reflects realistic tunneling behavior, where soil deformation and settlement effects are strongest in proximity to the advancing front and attenuate with distance.

Once the synthetic values were prepared, they were validated for physical plausibility, checking units, limits, and trends, before further processing. The data were then imported into Jupyter Notebook, where Python scripts automated the conversion of the Excel sheets into JSON streams. These scripts also handled timestamp formatting, ensured consistent units, and added unique sensor IDs corresponding to the parameters previously defined in Revit. By adopting this automated step, potential human error in manual formatting was avoided, and the workflow was prepared for future expansion to real time IoT feeds.

The JSON files generated in Jupyter were subsequently tested for Tandem compatibility using small trial uploads. Any formatting inconsistencies or mismatched keys were corrected, and the final datasets were organized by sensor category and location (e.g., B1-Front-Accelerometer, B2-Rear-Tiltmeter, InclinatorChain1_Node5). This organization mirrored the structure of the BIM model, enabling straightforward mapping once imported into Tandem.

Finally, metadata tables summarizing the sensor type, ID, location, measurement units, and thresholds were prepared alongside the datasets. These tables acted as a reference for both the mapping process and later validation, ensuring that every virtual sensor in Autodesk Tandem corresponded to a clearly defined data stream. By structuring the synthetic measurements in this systematic way, the project not only replicated realistic monitoring conditions but also stress tested the entire BIM-IoT integration pipeline, confirming that the digital twin could process, display, and analyze live structural health monitoring data once real sensors are installed.

Timestamp	B1_Accelerometer1[m/s ²]	B1_Accelerometer 2 [m/s ²]	B2_Accelerometer1 [m/s ²]	B2_Accelerometer 2 [m/s ²]
2025-07-22 00:00:00	0,0339	0,035	-0,0586	-0,0541
2025-07-22 00:00:01	0,0648	-0,0146	0,1463	0,0002
2025-07-22 00:00:02	0,0201	0,0317	0,0383	0,0082
2025-07-22 00:00:03	-0,0011	0,0355	0,1035	-0,0262
2025-07-22 00:00:04	-0,0643	0,0646	-0,06	0,0529
2025-07-22 00:00:05	0,0474	0,0178	-0,0018	0,0191
2025-07-22 00:00:06	-0,0244	-0,011	0,074	-0,1061
2025-07-22 00:00:07	-0,0105	0,0429	0,0984	-0,0732
2025-07-22 00:00:08	-0,0086	-0,0389	0,0457	-0,0443
2025-07-22 00:00:09	0,0303	0,0132	0,0656	0,037
2025-07-22 00:00:10	0,0372	0,0552	0,0373	0,0857
2025-07-22 00:00:11	0,0255	-0,023	0,0004	0,1067
2025-07-22 00:00:12	0,0451	0,0096	0,0637	-0,0912
2025-07-22 00:00:13	0,0532	-0,0724	0,0405	0,0538
2025-07-22 00:00:14	0,0439	0,0625	0,0474	-0,0284
2025-07-22 00:00:15	0,0631	0,0899	0,065	-0,0392
2025-07-22 00:00:16	0,0009	0,0014	-0,063	0,0025
2025-07-22 00:00:17	0,0118	-0,0522	-0,0286	0,0655
2025-07-22 00:00:18	0,0678	-0,0318	0,0409	-0,0529
2025-07-22 00:00:19	-0,0597	0,0828	-0,0306	-0,0754
2025-07-22 00:00:20	0,0041	0,0421	0,0251	-0,0705
2025-07-22 00:00:21	-0,0078	0,0381	0,0235	0,0219
2025-07-22 00:00:22	-0,0229	0,056	0,0883	-0,0886
2025-07-22 00:00:23	-0,029	0,0116	0,1406	0,0523
2025-07-22 00:00:24	-0,0319	0,034	0,0036	0,0086
2025-07-22 00:00:25	-0,0528	-0,038	0,0075	0,0355
2025-07-22 00:00:26	0,0616	-0,0112	0,0822	0,0342
2025-07-22 00:00:27	-0,0269	-0,1203	0,0245	-0,057
2025-07-22 00:00:28	0,014	0,0371	-0,0423	-0,0946
2025-07-22 00:00:29	-0,0039	0,0506	-0,0142	0,0046
2025-07-22 00:00:30	0,0109	0,0253	0,0653	-0,0062
2025-07-22 00:00:31	-0,02	0,0248	-0,0272	-0,0596
2025-07-22 00:00:32	0,001	0,075	-0,0216	0,0145
2025-07-22 00:00:33	0,0324	-0,004	-0,0151	0,0831
2025-07-22 00:00:34	0,0234	-0,0758	-0,0202	0,046
2025-07-22 00:00:35	-0,0188	0,0053	0,045	0,0128
2025-07-22 00:00:36	0,0533	-0,0234	-0,041	0,02
2025-07-22 00:00:37	0,0137	-0,0079	0,0935	0,0334
2025-07-22 00:00:38	-0,0082	0,0145	-0,0406	0,0483
2025-07-22 00:00:39	-0,01	0,0538	0,0225	-0,0287
2025-07-22 00:00:40	-0,043	0,0015	-0,0277	0,0625
2025-07-22 00:00:41	0,0371	0,033	0,0775	0,0276
2025-07-22 00:00:42	0,0314	0,0582	0,08	-0,0179
2025-07-22 00:00:43	0,1147	-0,0025	-0,0048	-0,1512
2025-07-22 00:00:44	0,0161	-0,0393	-0,0793	0,0065
2025-07-22 00:00:45	-0,0466	-0,0104	-0,035	-0,0345
2025-07-22 00:00:46	0,0233	0,0202	0,0577	0,0113
2025-07-22 00:00:47	0,0197	0,0585	0,1026	0,0273
2025-07-22 00:00:48	0,0064	0,0418	0,0779	-0,035

Table 1 - Accelerometer Data

Timestamp	B1_Tiltmeter 1 θ [°]	B1_Tiltmeter 2 θ [°]	B2_Tiltmeter 1 θ [°]	B2_Tiltmeter 2 θ [°]
2025-07-22 00:00:00	0,021	0,044	0,031	0,042
2025-07-22 00:05:00	0,045	0,048	0,026	0,037
2025-07-22 00:10:00	0,015	0,029	0,035	0,04
2025-07-22 00:15:00	0,014	0,021	0,032	0,04
2025-07-22 00:20:00	0	0,013	0,044	0,013
2025-07-22 00:25:00	0,026	0,023	0,027	0,012
2025-07-22 00:30:00	0,008	0,043	0,015	0,019
2025-07-22 00:35:00	0,013	0,019	0,015	0,004
2025-07-22 00:40:00	0,019	0,014	0,05	0,041
2025-07-22 00:45:00	0,018	0,031	0,033	0,026
2025-07-22 00:50:00	0,006	0,015	0,044	0,047
2025-07-22 00:55:00	0,038	0,047	0,046	0,045
2025-07-22 01:00:00	0,029	0,042	0,011	0,011
2025-07-22 01:05:00	0,028	0,022	0,024	0,018
2025-07-22 01:10:00	0,014	0,015	0,011	0,033
2025-07-22 01:15:00	0,005	0,047	0,031	0,034
2025-07-22 01:20:00	0,029	0,016	0,016	0,039
2025-07-22 01:25:00	0,007	0,024	0,001	0,006
2025-07-22 01:30:00	0,019	0,024	0,044	0,012
2025-07-22 01:35:00	0,024	0,049	0,037	0,037
2025-07-22 01:40:00	0,028	0,018	0,029	0,006
2025-07-22 01:45:00	0,007	0,042	0,002	0,007
2025-07-22 01:50:00	0,011	0,028	0,002	0,024
2025-07-22 01:55:00	0,038	0,001	0,028	0,046
2025-07-22 02:00:00	0,049	0,024	0,019	0,001
2025-07-22 02:05:00	0,042	0,013	0,017	0,004
2025-07-22 02:10:00	0,01	0,002	0,006	0,009
2025-07-22 02:15:00	0,006	0,015	0,033	0,008
2025-07-22 02:20:00	0,034	0,048	0,017	0,011
2025-07-22 02:25:00	0,049	0,01	0,008	0,025
2025-07-22 02:30:00	0,03	0,024	0,032	0,016
2025-07-22 02:35:00	0,03	0,024	0,001	0,008
2025-07-22 02:40:00	0,003	0,027	0,009	0,038
2025-07-22 02:45:00	0,003	0,045	0,003	0,048
2025-07-22 02:50:00	0,026	0,012	0,011	0,043
2025-07-22 02:55:00	0,022	0,006	0,044	0,049
2025-07-22 03:00:00	0,005	0,05	0,023	0,036
2025-07-22 03:05:00	0,043	0,015	0,039	0,017
2025-07-22 03:10:00	0,043	0,008	0,036	0,033
2025-07-22 03:15:00	0,021	0,008	0,031	0,038
2025-07-22 03:20:00	0,047	0,025	0,014	0,032
2025-07-22 03:25:00	0,048	0,034	0,033	0,015
2025-07-22 03:30:00	0,029	0,016	0,033	0,043
2025-07-22 03:35:00	0,044	0,006	0,05	0,018
2025-07-22 03:40:00	0,046	0,001	0,038	0,013
2025-07-22 03:45:00	0,022	0,032	0,003	0,001
2025-07-22 03:50:00	0,048	0,019	0,016	0,023
2025-07-22 03:55:00	0,02	0,018	0,039	0,003
2025-07-22 04:00:00	0,038	0,033	0,032	0,049

Table 2 - Tiltmeter Data

Timestamp	Excavation front	Distance to monitored sensor (m)	Node1_az [m/s ²]	Node1_Si [mm]	Node2_az [m/s ²]	Node2_Si [mm]
2025-07-22 00:00:00	West	60	0,9666	0,001479467	0,9935	0,001520452
2025-07-22 00:30:00	West	59,95	0,973	0,001489265	0,9662	0,00147871
2025-07-22 01:00:00	West	59,9	0,975	0,001492282	0,9704	0,001485462
2025-07-22 01:30:00	West	59,85	0,9902	0,00151539	0,9878	0,001512003
2025-07-22 02:00:00	West	59,8	0,9966	0,001525221	0,9867	0,001510071
2025-07-22 02:30:00	West	59,75	0,9954	0,001523545	0,9898	0,001515097
2025-07-22 03:00:00	West	59,7	0,9895	0,001514495	0,9853	0,001508076
2025-07-22 03:30:00	West	59,65	0,9909	0,001516616	0,9934	0,001520417
2025-07-22 04:00:00	West	59,6	0,9914	0,001517509	0,9929	0,001519683
2025-07-22 04:30:00	West	59,55	0,9745	0,001491377	0,9749	0,001492098
2025-07-22 05:00:00	West	59,5	0,9675	0,001480757	0,9688	0,00148302
2025-07-22 05:30:00	West	59,45	0,9738	0,001490303	0,9779	0,001496671
2025-07-22 06:00:00	West	59,4	0,9657	0,001478295	0,9985	0,001528185
2025-07-22 06:30:00	West	59,35	0,9699	0,001484643	0,9778	0,001496446
2025-07-22 07:00:00	West	59,3	0,9754	0,001492928	0,9831	0,00150489
2025-07-22 07:30:00	West	59,25	0,9693	0,0014834	0,9961	0,001524628
2025-07-22 08:00:00	West	59,2	0,9903	0,001515631	0,9655	0,001477762
2025-07-22 08:30:00	West	59,15	0,9787	0,001498055	0,9629	0,001473902
2025-07-22 09:00:00	West	59,1	0,9657	0,001477894	0,9771	0,001495484
2025-07-22 09:30:00	West	59,05	0,9762	0,001493979	0,9657	0,001477981
2025-07-22 10:00:00	West	59	0,9855	0,001508355	0,9654	0,001477744
2025-07-22 10:30:00	West	58,95	0,9682	0,001481746	0,9774	0,001496041
2025-07-22 11:00:00	West	58,9	0,9762	0,001494401	0,995	0,001522995
2025-07-22 11:30:00	West	58,85	1	0,001530393	0,9978	0,001527358
2025-07-22 12:00:00	West	58,8	0,9958	0,001523994	0,982	0,001502855
2025-07-22 12:30:00	West	58,75	0,9645	0,00147623	0,9723	0,001488168
2025-07-22 13:00:00	West	58,7	0,9705	0,001485277	0,9607	0,001470391
2025-07-22 13:30:00	West	58,65	0,9764	0,001494588	0,9671	0,001480417

Node3_az [m/s ²]	Node3_Si [mm]	Node4_az [m/s ²]	Node4_Si [mm]	Node5_az [m/s ²]	Node5_Si [mm]	Node6_az [m/s ²]	Node6_Si [mm]
0,9932	0,001520012	0,9908	0,001516326	0,9776	0,001496248	0,9714	0,001486932
0,9612	0,001471145	0,9747	0,001491829	0,9755	0,00149294	0,9743	0,001491356
0,9883	0,001512692	0,994	0,001521349	0,9799	0,001499991	0,9691	0,001483338
0,9825	0,001503925	0,9632	0,001474395	0,9856	0,001508515	0,9899	0,001515194
0,9853	0,001508143	0,9832	0,001504785	0,9793	0,001499197	0,9764	0,001494352
0,9612	0,001471452	0,9968	0,001525687	0,9712	0,001486325	0,985	0,001507752
0,9868	0,001510223	0,9699	0,001484765	0,9923	0,001518942	0,9762	0,001494024
0,9641	0,001475502	0,9861	0,001509164	0,9786	0,001497991	0,9811	0,001501601
0,9966	0,001525512	0,9684	0,001482197	0,961	0,001470778	0,9882	0,001512504
0,9948	0,001522793	0,9929	0,001519768	0,9674	0,001480771	0,975	0,001492272
0,9734	0,001489825	0,9893	0,00151429	0,9694	0,001483553	0,9618	0,001472323
0,9779	0,00149665	0,9734	0,001489969	0,9857	0,001508532	0,9791	0,001498571
0,9625	0,001473183	0,9928	0,001519706	0,9657	0,001478272	0,9869	0,001510561
0,9726	0,001488869	0,9795	0,001499388	0,9601	0,001469612	0,9983	0,001527894
0,9905	0,001515982	0,9811	0,001501735	0,9727	0,001488867	0,9696	0,001484205
0,9715	0,001487159	0,9792	0,001498732	0,9965	0,001525283	0,9607	0,001470266
0,9889	0,001513647	0,9751	0,001492563	0,9807	0,001501037	0,9679	0,00148145
0,9609	0,00147064	0,9834	0,001505234	0,9605	0,001470261	0,993	0,001519921
0,9793	0,001498795	0,9961	0,001524621	0,9841	0,001506208	0,9671	0,001480064
0,9741	0,001491015	0,9926	0,001519567	0,9947	0,001522397	0,9866	0,001510209
0,9996	0,001529927	0,9976	0,001527086	0,9664	0,001479291	0,9733	0,001489773
0,9778	0,001496484	0,9998	0,001530219	0,9851	0,001507582	0,9756	0,001493182
0,9686	0,001482585	0,9854	0,001508058	0,961	0,001470863	0,9922	0,00151846
0,9995	0,001529878	0,9835	0,001505409	0,9815	0,00150212	0,9723	0,001488042
0,9894	0,001514277	0,9947	0,001522356	0,9641	0,001475437	0,9688	0,00148268
0,9624	0,001473168	0,9778	0,001496819	0,9892	0,001514111	0,994	0,001521214
0,982	0,001503065	0,9795	0,001499184	0,9699	0,001484325	0,9797	0,001499427
0,9905	0,001516159	0,9776	0,001496205	0,988	0,001512364	0,9971	0,001526116

Node7_az [m/s ²]	Node7_Si [mm]	Node8_az [m/s ²]	Node8_Si [mm]	Node9_az [m/s ²]	Node9_Si [mm]	Node10_az [m/s ²]	Node10_Si [mm]
0,9937	0,001520833	0,9674	0,001480635	0,9817	0,001502491	0,9755	0,001493234
0,9949	0,001522899	0,9928	0,001519842	0,9715	0,001487136	0,9772	0,001496008
0,9755	0,001493239	0,9631	0,001474118	0,9771	0,001495371	0,9887	0,001513179
0,993	0,001520033	0,985	0,001507655	0,9902	0,001515533	0,9701	0,001484936
0,9873	0,001511122	0,9785	0,001497619	0,9962	0,001524862	0,971	0,001486468
0,9736	0,001490009	0,9938	0,00152107	0,9756	0,001493145	0,9746	0,001491616
0,9752	0,00149245	0,9911	0,001517024	0,9897	0,001514874	0,9888	0,001513255
0,9918	0,001517922	0,9707	0,001485582	0,9976	0,001526832	0,9899	0,001515421
0,9941	0,001521639	0,982	0,00150295	0,9975	0,001526856	0,9944	0,001521885
0,9793	0,001499039	0,9686	0,00148234	0,9886	0,001513214	0,9689	0,001482944
0,9978	0,001527108	0,9967	0,001525635	0,9736	0,001490153	0,9723	0,001488294
0,9925	0,001518981	0,9923	0,001518645	0,9781	0,001497065	0,9989	0,00152913
0,9627	0,001473433	0,972	0,001487844	0,9692	0,001483445	0,9626	0,001473189
0,9868	0,001510695	0,9936	0,001520582	0,9694	0,001483788	0,9832	0,0015047
0,9676	0,001480862	0,9903	0,001515828	0,9857	0,001508671	0,9752	0,001492618
0,9955	0,00152376	0,9698	0,001484375	0,9715	0,001486828	0,9788	0,001498107
0,995	0,00152303	0,9635	0,00147464	0,9838	0,001505844	0,9985	0,001528199
0,9934	0,001520376	0,9915	0,001517568	0,998	0,001527357	0,998	0,001527569
0,9901	0,001515288	0,985	0,001507727	0,995	0,001522829	0,9771	0,001495744
0,9926	0,001519277	0,9952	0,001523088	0,999	0,00152913	0,9703	0,001484979
0,9611	0,001471056	0,9735	0,001490064	0,9687	0,001482709	0,9952	0,00152314
0,993	0,001519923	0,9842	0,001506475	0,9997	0,001530046	0,9975	0,001526999
0,9754	0,001493032	0,989	0,001513619	0,9603	0,00146979	0,9836	0,001505341
0,9952	0,001523183	0,983	0,001504749	0,9918	0,001518004	0,995	0,001522964
0,9619	0,001472383	0,9744	0,001491199	0,9689	0,001483068	0,9761	0,001493802
0,9952	0,001523219	0,9902	0,001515635	0,9872	0,001510948	0,989	0,001513683
0,9675	0,001480986	0,9968	0,001525529	0,9992	0,00152941	0,9693	0,001483771
0,9885	0,001512921	0,9745	0,001491511	0,9805	0,001500804	0,9912	0,001517173

Table 3 - Inclinator Chain Data

The synthetic values were generated as a function of the excavation front position. When the excavation was closer to a monitored node, the simulated lateral displacements (Si) and accelerations (Az) were slightly increased, while values gradually decreased as the excavation front moved away. This approach reflects realistic tunneling behavior, where ground deformations and soil-structure interaction effects are stronger in proximity to the advancing excavation face and attenuate with distance.

For the topographic benchmarks, measurements were created to represent surface settlement trends across the park area. A total of five benchmark sections (S1–S5) spaced 10 meters apart were included in the model. Benchmark readings were defined at 5-minute intervals over a two week simulated period. This sampling rate is denser than typical field practice but was selected to stress test the data workflow and ensure smooth integration into the Tandem environment. Each benchmark record included a unique ID, section reference, timestamp, and vertical displacement relative to its initial elevation.

Timestamp	Section1_P1 [mm]	Section1_P2 [mm]	Section1_P3 [mm]	Section1_P4 [mm]	Section1_P5 [mm]	Section2_P1 [mm]
2025-07-22 00:00:00	0,0039	0,0033	0,0024	0,0044	0,0018	0,0017
2025-07-22 00:05:00	0,0043	0,002	0,0042	0,0033	0,0005	0,0022
2025-07-22 00:10:00	0,0038	0,0042	0,0037	0,004	0,0001	0,0046
2025-07-22 00:15:00	0,0043	0,0024	0,0002	0,0017	0,0027	0,0002
2025-07-22 00:20:00	0,0032	0,0001	0,002	0,0005	0,0015	0,0023
2025-07-22 00:25:00	0,0026	0,0027	0	0,0033	0,0047	0,0006
2025-07-22 00:30:00	0,0047	0,0025	0,0032	0,0018	0,0046	0,002
2025-07-22 00:35:00	0,0026	0,0005	0,0004	0,0045	0,0022	0,0012
2025-07-22 00:40:00	0,0001	0,0041	0,0029	0,0023	0,0034	0,0001
2025-07-22 00:45:00	0,0014	0,0015	0,0025	0,0031	0,0045	0,0025
2025-07-22 00:50:00	0,0031	0,0024	0,0046	0,0031	0,002	0,0025
2025-07-22 00:55:00	0,0002	0,0032	0,0013	0,0036	0,0034	0,0031
2025-07-22 01:00:00	0,0015	0,0003	0,002	0,0022	0,0045	0,0025
2025-07-22 01:05:00	0,0021	0,0027	0,0027	0,0044	0,0006	0,0011
2025-07-22 01:10:00	0,0013	0,0034	0,0007	0,0033	0,0007	0,0026
2025-07-22 01:15:00	0,0048	0,0039	0,0031	0,0045	0,0003	0,0016
2025-07-22 01:20:00	0,0035	0,0028	0,0003	0,0017	0,0028	0,0018
2025-07-22 01:25:00	0,0041	0,0023	0,0044	0,0042	0,0024	0,0011
2025-07-22 01:30:00	0,0023	0,0013	0,0009	0,0022	0,0015	0,0048
2025-07-22 01:35:00	0,0005	0,0048	0,0014	0,0032	0,0027	0,0004
2025-07-22 01:40:00	0,0044	0,0008	0,0019	0,0034	0,0031	0,0006
2025-07-22 01:45:00	0,004	0,0043	0,003	0,0031	0,0022	0,0034
2025-07-22 01:50:00	0,0045	0,0035	0,0014	0,0041	0,0045	0,0015
2025-07-22 01:55:00	0,0042	0,002	0,0036	0,005	0,0049	0,0049
2025-07-22 02:00:00	0,0021	0,0005	0,0027	0,004	0,004	0,0022
2025-07-22 02:05:00	0,0039	0,0032	0,0007	0,0047	0,0017	0,003
2025-07-22 02:10:00	0,0042	0,0028	0,0033	0,0037	0,0029	0,0026
2025-07-22 02:15:00	0,0014	0,0023	0,0008	0,0002	0,0026	0,0029

Table 4 - Topographic Benchmark Data (S1-2)

Section2_P2 [mm]	Section2_P3 [mm]	Section2_P4 [mm]	Section2_P5 [mm]	Section3_P1 [mm]	Section3_P2 [mm]	Section3_P3 [mm]
0	0,0002	0,0042	0,0024	0,0012	0,0011	0,0002
0,0017	0,0033	0	0,0035	0,0015	0,0044	0,0037
0,0039	0,002	0,0032	0,0022	0,0023	0,0024	0,0006
0,0043	0,0003	0,0015	0,0017	0,0006	0,004	0,0023
0,0046	0,004	0,0004	0,002	0,0037	0,0018	0,0039
0,0037	0,0025	0,0005	0,0007	0,0024	0,0025	0,0012
0,0045	0,0033	0,0009	0,0044	0,0003	0,0044	0,0016
0,0026	0,0044	0,0019	0,0007	0,0027	0,0026	0,0018
0,004	0,002	0,0021	0,0035	0,0037	0,0035	0,0019
0,0041	0,0046	0,0034	0,0017	0,0013	0,0018	0,0021
0,0017	0,0046	0,0003	0,0044	0,0003	0,0029	0,0007
0,0028	0,0021	0,0021	0,0008	0,0032	0,0049	0,0044
0,0039	0,0035	0,0045	0,0004	0,0002	0,0033	0,0021
0,0017	0,0038	0,0039	0,0024	0,0016	0,0004	0,0004
0,0044	0,0019	0,0023	0,0022	0,0014	0,0034	0,0034
0,0007	0,0038	0,0044	0,0021	0,0036	0,003	0,0014
0,0002	0,0008	0,001	0,0049	0,0003	0,0028	0,0043
0,0002	0,0007	0,0026	0,0018	0,0039	0,0013	0,0017
0,0002	0,0001	0,0018	0,0044	0,005	0,0005	0,0017
0,0004	0,0002	0,0011	0,0022	0,0014	0,0043	0,0033
0,001	0,0008	0,004	0,0003	0,002	0,0015	0,0043
0,0004	0,0045	0,0034	0,0039	0,0026	0,0001	0,0022
0,0014	0,0033	0,0011	0,004	0,0046	0,0037	0,0048
0,0023	0,0016	0,0029	0,0039	0,0022	0,0018	0,0046
0,0007	0,0046	0,0027	0,0027	0,0027	0,0024	0,0036
0,0014	0,0036	0,0027	0,0036	0,0027	0,0026	0,0045
0,0032	0,0033	0,0005	0,0035	0,0033	0,0025	0,0017
0,0022	0,0019	0,0007	0,0032	0,0045	0,0018	0,0038

Table 5 - Topographic Benchmark Data (S2-3)

Section3_P4 [mm]	Section3_P5 [mm]	Section4_P1 [mm]	Section4_P2 [mm]	Section4_P3 [mm]	Section4_P4 [mm]
0,0047	0,0009	0,0041	0,0042	0,0015	0,0016
0,0028	0,0006	0,0012	0,0028	0,0002	0,0022
0,0011	0,0027	0,0003	0,0016	0,0009	0,0038
0,0005	0,0018	0,0015	0,0033	0,0019	0,0015
0,003	0,0013	0,001	0,002	0,0016	0,0012
0,0016	0,0034	0,0037	0,003	0,0013	0,0004
0,0015	0,0001	0,0049	0,0021	0,0019	0,0024
0,0036	0,0034	0,0037	0,0006	0,0012	0,0039
0,0049	0,0047	0,0046	0,0036	0,0001	0,0036
0,003	0,0018	0,0002	0,0039	0,0026	0,002
0,0046	0,001	0,0036	0,0019	0,0028	0
0,0013	0,0017	0,0011	0,0031	0,0016	0,0003
0,0049	0,0015	0,0043	0,0009	0,0033	0,0037
0,0026	0,0046	0,0041	0,0042	0,0029	0,0043
0,0016	0,0008	0,0013	0,0048	0,003	0,0037
0,0009	0,0037	0,0004	0,0002	0,0017	0,0014
0,0034	0,0018	0,0026	0,0026	0,0014	0,0047
0,0045	0,0011	0,0005	0,0049	0,0003	0,004
0,0042	0,0005	0,0036	0,0035	0,0015	0,0024
0,0049	0,0049	0,0029	0,0039	0,0024	0,003
0,0035	0,0023	0,0011	0,003	0,0025	0,0025
0,0008	0,0026	0	0,0046	0,0017	0,0017
0,0039	0,0009	0,0032	0,0015	0,0021	0,0016
0,0044	0,0029	0,003	0,0015	0,0033	0,0003
0,003	0,0024	0,0036	0,0024	0,0033	0,0044
0,0021	0,0048	0,004	0,0022	0,0047	0,0038
0,003	0,0007	0,0027	0,0004	0,0021	0,003
0,0013	0,0043	0,0024	0,0048	0,0041	0,0003
0	0,0014	0,0007	0,0022	0,0033	0,0047
0,0036	0,0015	0,0014	0,0048	0,0043	0,0025
0,001	0,002	0,0013	0,0001	0,0029	0,0025

Table 6 - Topographic Benchmark Data (S3-4)

Section4_P5 [mm]	Section5_P1 [mm]	Section5_P2 [mm]	Section5_P3 [mm]	Section5_P4 [mm]	Section5_P5 [mm]
0,0029	0,0005	0,0035	0,0048	0,0033	0,0023
0,0001	0,0037	0,0027	0,0001	0,0029	0,0005
0,0046	0,0039	0,0004	0,0017	0,0023	0,0033
0,0047	0,0005	0,0029	0,0016	0,0028	0,0048
0,0024	0,0007	0,0006	0,0001	0,0046	0,0045
0,0023	0,0011	0,0018	0,002	0,0026	0,0003
0,0008	0,0011	0,0021	0,0041	0,0026	0,0041
0,0015	0,0011	0,0023	0,0021	0,0027	0,0042
0,0021	0,0027	0,0049	0,0012	0,0037	0,0027
0	0,004	0,0049	0,0047	0,0029	0,005
0,0049	0,0001	0,0021	0,0017	0,0043	0,0016
0,0021	0,0005	0,0004	0,0028	0,0048	0,0029
0,0027	0,0022	0,0044	0,0008	0,0015	0,004
0,0019	0,005	0,0035	0,0014	0,0016	0,0032
0,0021	0,0022	0,0019	0,0026	0,0011	0,0032
0,0034	0,0048	0,0037	0,0013	0,0016	0,0007
0,0021	0,0019	0,0005	0,0027	0,0017	0,0048
0,0006	0,0029	0,0046	0,0004	0,005	0,0023
0,0043	0,0013	0,0041	0,0008	0,002	0,0015
0,0002	0,0005	0,0026	0,0009	0,0039	0,0005
0,0006	0,0031	0,0022	0,0014	0,0044	0,0003
0,0006	0,0006	0,001	0,0008	0,0025	0,0036
0,004	0,0022	0,0025	0,0034	0,0013	0,0016
0,0048	0,0012	0,002	0,0018	0,0003	0,0007
0,003	0,0034	0,0026	0,0048	0,0002	0,0015
0	0,0012	0,0046	0,0036	0,0044	0,0015
0,0017	0,0017	0,0043	0,0022	0	0,0026
0,0007	0,0026	0,002	0,0003	0,0002	0,0001
0,0022	0,0034	0,0036	0,0047	0,0041	0,0012
0,0012	0,0021	0,0038	0,0029	0,003	0,0037
0,0011	0,0006	0,0026	0,0016	0,0015	0,0043

Table 7 - Topographic Benchmark Data (S4-5)

After preparing the synthetic datasets in Excel, Python scripts running in Jupyter Notebook were used to transform and upload the data to Autodesk Tandem. The workflow ensured that all measurements, representing accelerometers, tiltmeters, inclinometer chains, and topographic benchmarks, were properly formatted, validated, and linked to their virtual sensors.

First, the scripts imported the raw time series data from Excel using *pandas*, verifying timestamps, units, and column structures. A validation check followed to identify missing values, duplicated rows, or unrealistic readings (e.g., accelerations above 1.0 m/s^2 or angles beyond $\pm 0.2^\circ$). This step ensured that only reliable data progressed to the next stage.

Validated values were then converted into JSON objects following Tandem API requirements. Each dataset was mapped to its corresponding virtual sensor using unique IDs and a reference table created during Revit parameterization. This automated mapping avoided manual errors and maintained consistency between the datasets and the 3D model elements.

Finally, a batch upload routine sent multiple data streams to Tandem in a single process, simulating real world Structural Health Monitoring conditions where numerous sensors continuously provide input. This approach allowed quick repetition of tests when thresholds or configurations were adjusted, confirming that the pipeline could reliably handle large scale monitoring scenarios.

```
[ ]: # ===== SETTINGS =====
CSV_PATH = "C:/Users/NUR/Desktop/CSV/Accelerometer3.csv" # Use CSV instead of CSV/XLSX
COL_NAME = "B1_Accelerometer1 [m/s²]" # The column name you will send
KEY_NAME = "value1" # The JSON field mapped in Tandem (e.g., "value", "value_acc_b2_2", ...)
URL = "https://UbnV2tp8Rtm_Sw3ZhjIRKw@eu.tandem.autodesk.com/api/v1/timeseries/models/urn:adsk.dtm:L3T7ekoyQLKycU2IdbbhUw/streams/AQAAANVLqz

# Optional
START_AT = 0 # Index to start from if resuming
STOP_AT = 21601 # Up to a specific row (None = until the end)
LOG_EVERY = 1000 # Print status every N rows
SLEEP_BETWEEN = 0.0 # Wait time (sec) after each POST
TIMEOUT = 8 # HTTP timeout (sec)
# =====

import pandas as pd
import numpy as np
import requests, time

def read_csv_auto(path):
    # Automatically handle BOM and delimiter
    try:
        df = pd.read_csv(path, sep=None, engine="python", encoding="utf-8-sig")
        if df.shape[1] == 1:
            df = pd.read_csv(path, sep=";", engine="python", encoding="utf-8-sig")
    except Exception:
        df = pd.read_csv(path, sep=";", engine="python", encoding="utf-8-sig")
    # Normalize column names, drop 'Unnamed'
    df.columns = (df.columns.astype(str)
                  .str.replace("\uffff", "", regex=False)
                  .str.strip())
    df = df.loc[~df.columns.str.startswith("Unnamed")]
```

Table 8 – Part of Python Code for sending data to Tandem from Jupyter Notebook

The JSON payloads were then uploaded to Autodesk Tandem, where they were linked to the virtual sensors representing accelerometers, tiltmeters, inclinometer chains, and benchmarks. Benchmark streams were visualized alongside the other sensors, providing surface level confirmation of settlement patterns. Tandem's time series dashboard was used to check that accelerometer peaks coincided with small tiltmeter oscillations, inclinometer profiles showed depth dependent displacements, and benchmark trends revealed gradual surface movements across the five sections.

This workflow demonstrated the end-to-end integration of monitoring data into a BIM-based digital twin. Even though the values were synthetic, using realistic sampling intervals and durations particularly the 5 minute benchmark measurements over two weeks validated the feasibility of real time streaming and visualization. The pipeline also highlighted practical considerations such as data formatting, parameter mapping, and interoperability, which are essential for scaling the system to future deployments with live sensor data.

3.5 Validation and Testing in Autodesk Tandem

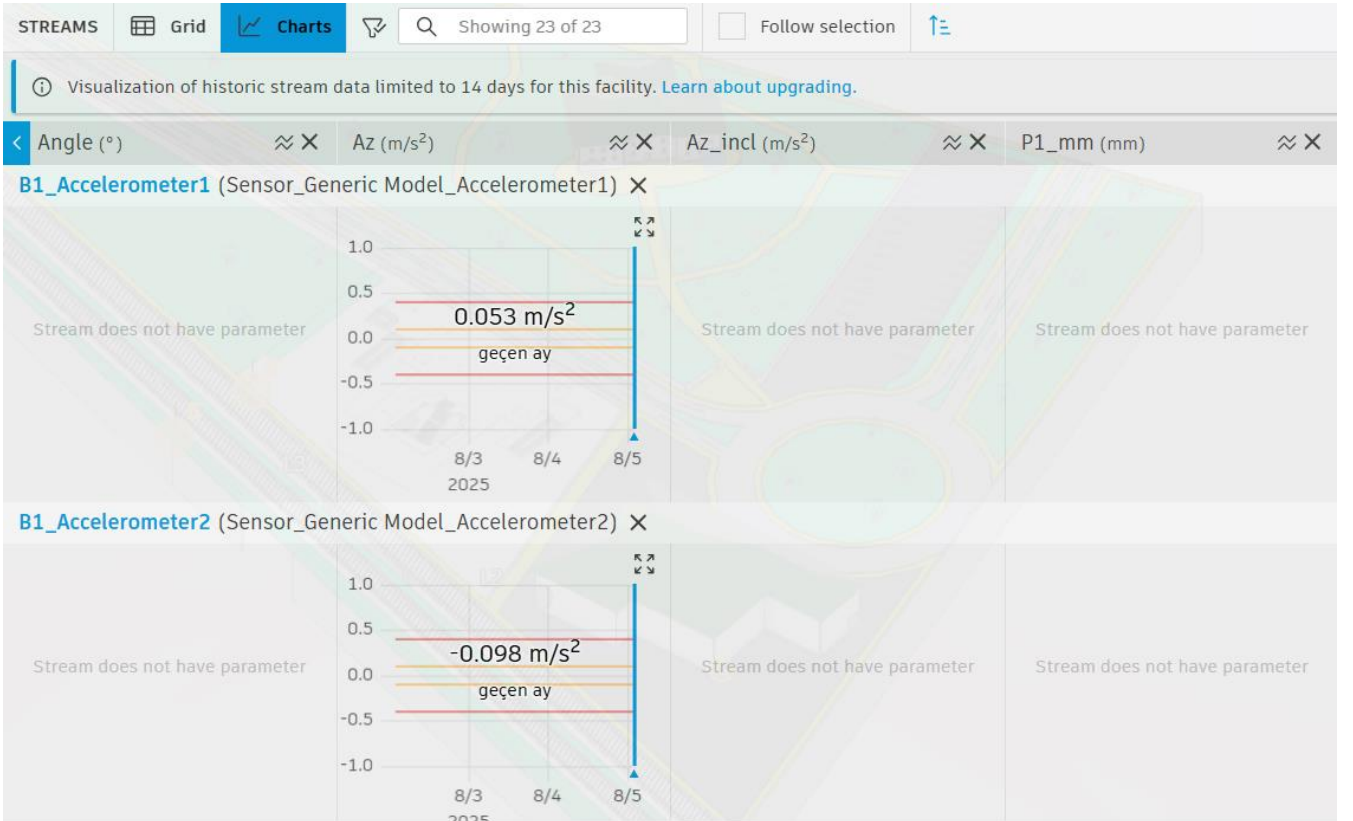
The validation and testing stage within Autodesk Tandem was a critical step in confirming that the BIM based digital twin could accurately represent the structural monitoring system. After creating and parameterizing virtual sensors in Revit accelerometers, tiltmeters, inclinometer chains, and topographic benchmarks, these elements were exported with unique shared parameter IDs that served as links between the Revit model and incoming JSON data streams. The sensor readings, pre-processed and formatted externally, were uploaded to Tandem and mapped to their respective assets using these identifiers.

Within Tandem, I configured connections for each virtual device, ensuring that all sensors were correctly linked to their geographic positions within the Certosa Metro area model. Threshold values for warnings and alerts were set for every parameter (e.g., inclination, acceleration, displacement, and tilt angle) to enable real time detection of unusual behavior.

Once configured, the live grid and chart tools allowed the verification of each data stream over time. This included cross checking inclinometer acceleration values, benchmark displacements, and tilt angles to ensure the system was receiving data without gaps, corrupted payloads, or incorrect units.

Name	Tandem Categories	Category	Data Type	Context
Angle	P.Sp Sprinklers	Piping/Plumbing	Number	Element
Az	M.CD Control Device	Eptura Asset Data	Number	Element
Az_incl	E.Eq Equipment	Electrical	Number	Element
P1_mm	B.Wa Wall	Architecture	Number	Element
P2_mm	B.Wa Wall	Architecture	Number	Element
P3_mm	B.Wa Wall	Architecture	Number	Element
P4_mm	B.Wa Wall	Architecture	Number	Element
P5_mm	B.Wa Wall	Architecture	Number	Element
Si	E.Eq Equipment	Electrical	Number	Element

Figure 38 - Autodesk Tandem Parameters



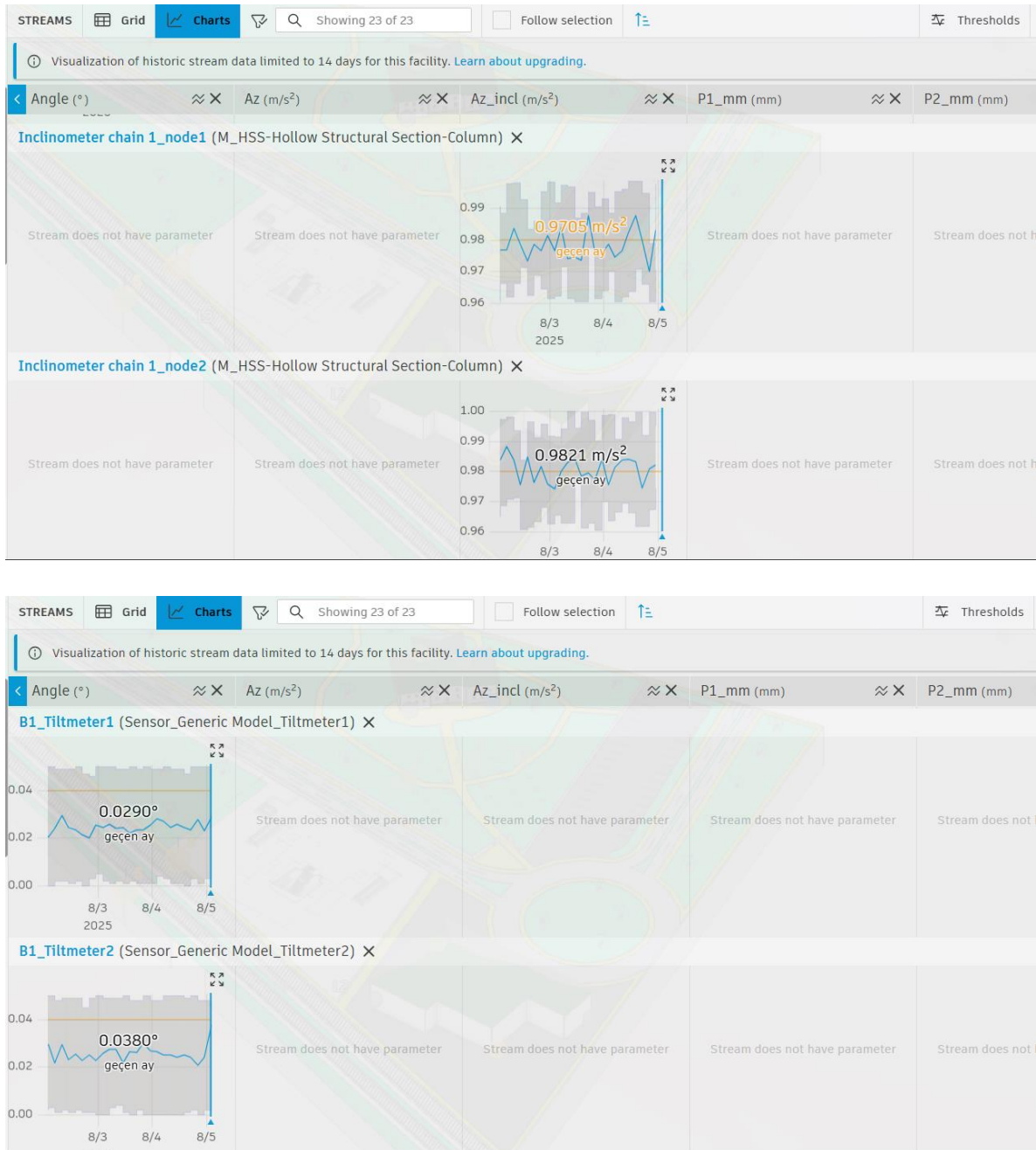


Figure 39 - Tandem Charts

Angle	Streams	Number	° > Angle	3	Tiltmeter
Angle	Piping/Plumbing	Number	° > Angle	4	Tiltmeter
Asset Tag	REC Asset	Text			REC Asset
Az	Eptura Asset Data	Number	m/s ² > Accelerat...	3	
Az_incl	Electrical	Number	m/s ² > Accelerat...	4	Inclinometer

P1_mm	Architecture	Number	mm > Length	4	Section1_P1
P2_mm	Architecture	Number	mm > Length	4	Section2_P1
P3_mm	Architecture	Number	mm > Length	4	Section3_P1
P4_mm	Architecture	Number	mm > Length	4	Section4_P4
P5_mm	Architecture	Number	mm > Length	4	Section5_P1

Figure 40 - Parameters

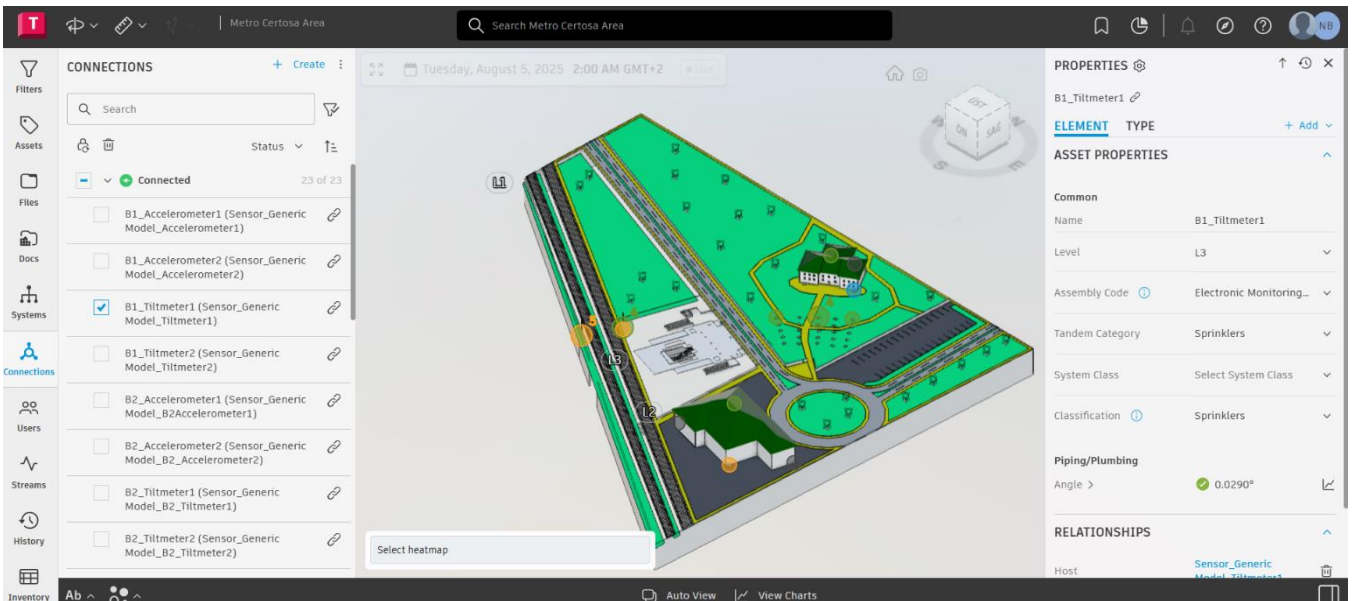


Figure 41 - Tandem Overview

Thresholds		Threshold values				Applied to		
Angle (°)	Tiltmeter Limits	● ≤ -0.1	● ≤ -0.04	● ≥ 0.04	● ≥ 0.1	4 connections		
Az (m/s ²)	Acceleration Limits	● ≤ -0.4	● ≤ -0.1	● ≥ 0.1	● ≥ 0.4	4 connections		
Az_incl (m/s ²)	Incline Limit	● ≤ 0.95	● ≤ 0.98	● ≥ 1.02	● ≥ 1.05	10 connections		
P1_mm (mm)	Benchmark Limits	● ≤ -5	● ≤ -3	● ≥ 3	● ≥ 5	1 connection		
P2_mm (mm)	Benchmark P2	● ≤ -5	● ≤ -3	● ≥ 3	● ≥ 5	1 connection		
P3_mm (mm)	Benchmark P3	● ≤ -5	● ≤ -3	● ≥ 3	● ≥ 5	1 connection		
P4_mm (mm)	Benchmark P4	● ≤ -5	● ≤ -3	● ≥ 3	● ≥ 5	1 connection		
P5_mm (mm)	Benchmark P5	● ≤ -5	● ≤ -3	● ≥ 3	● ≥ 5	1 connection		
Si (mm)	Settlement Limit	● ≤ -5	● ≤ -3	● ≥ 3	● ≥ 5	10 connections		

Create threshold

Figure 42 – Thresholds

The threshold configuration within Autodesk Tandem was a critical step to ensure that the digital twin could automatically flag abnormal structural or geotechnical behavior. Specific warning and alert values were assigned to each monitored parameter based on industry standards, manufacturer recommendations, and precedent studies of metro tunnel monitoring. For tiltmeters, angular deviations were set to trigger warnings at $\pm 0.04^\circ$ and alerts at $\pm 0.10^\circ$, representing the limits beyond which localized rotation of building elements could indicate potential structural stress. Accelerometer thresholds were defined at $\pm 0.10 \text{ m/s}^2$ for warnings and $\pm 0.40 \text{ m/s}^2$ for alerts, reflecting the expected vibration range during regular train operations versus values associated with excessive ground movement or mechanical impacts.

For inclinometer chains, acceleration components (Az_{incl}) were assigned warning levels between $0.98\text{--}1.02\text{ m/s}^2$ and alert boundaries at $\leq 0.95\text{ m/s}^2$ or $\geq 1.05\text{ m/s}^2$ to capture subtle subsurface shear deformations. Topographic benchmarks (P1–P5) and settlement indicators (Si) used displacement thresholds of $\pm 3\text{ mm}$ for warnings and $\pm 5\text{ mm}$ for alerts, values chosen to align with common practice for urban tunneling projects where millimetric settlements may still be acceptable but larger displacements could jeopardize surface infrastructure. By mapping these thresholds to their respective sensor connections, the system could visually highlight any excursions in real time, allowing engineers to distinguish normal construction induced fluctuations from conditions that warrant immediate attention. This configuration not only validated the reliability of the monitoring framework but also demonstrated Tandem’s capability to function as a proactive decision-support tool for risk management.

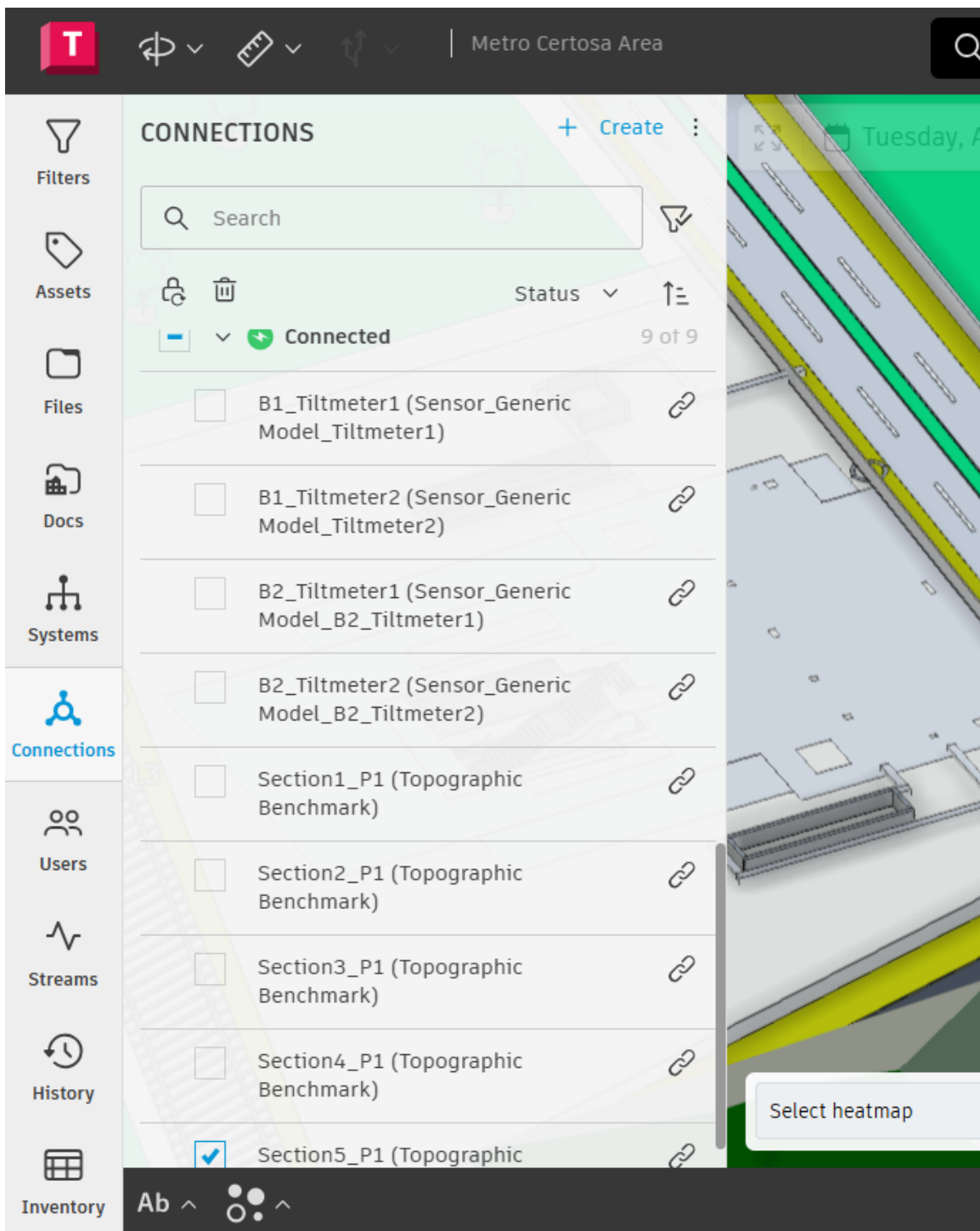


Figure 43 - Tandem Connections



Figure 44 – Connection of Sensors in Certosa Area

During testing, Autodesk Tandem occasionally displayed unexpected behavior. Tandem is still an emerging platform within the construction industry, and bugs or data losses can occur after upload. In several cases, previously confirmed streams temporarily disappeared or were delayed before becoming visible again. These issues did not compromise the overall validation but highlighted that digital twins for structural health monitoring are still under active development, making robustness testing an essential part of this research.

Despite these limitations, the system successfully demonstrated the end-to-end workflow from creating parameterized BIM elements, linking them to external sensor data, applying thresholds, and finally visualizing and analyzing results directly within the 3D context of the metro site. This testing confirmed that Tandem can already function as a practical digital twin platform for real time monitoring, even if further refinement and increased reliability are required for widespread adoption in the construction sector. This outcome directly aligns with the thesis's goal of evaluating the viability and challenges of emerging digital twin technologies for infrastructure monitoring.

3.5.1 Accelerometer Data Interpretation and Risk Assessment

The accelerometer measurements were taken over a six-hour period with one-second intervals. They record the vibrations affecting the two monitored buildings. The warning threshold was set at $\pm 0.10 \text{ m/s}^2$, and the alert threshold at $\pm 0.40 \text{ m/s}^2$. Most readings from the four accelerometers stayed between -0.08 m/s^2 and $+0.08 \text{ m/s}^2$, which represents normal background vibration.

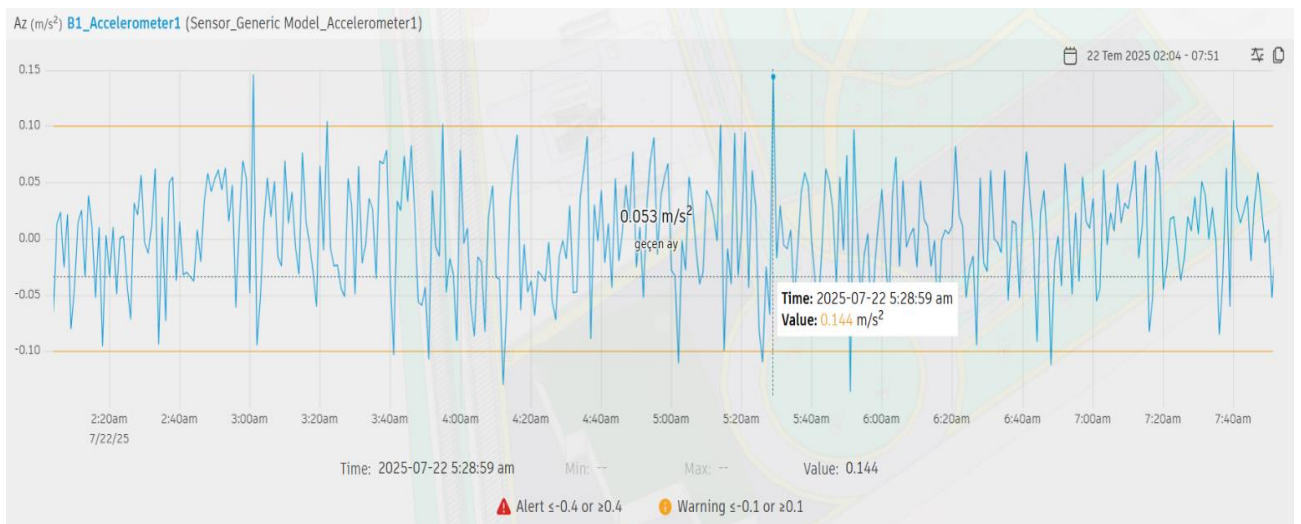


Figure 45 - B1_Accelerometer1 Chart

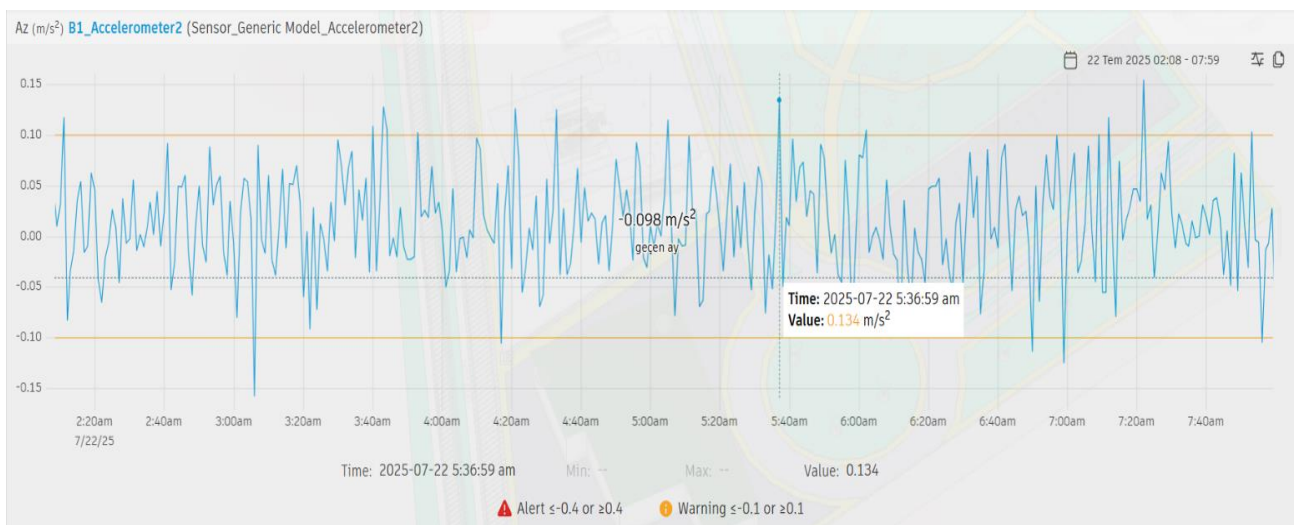


Figure 46 - B1_Accelerometer 2 Chart

For B1 (Gruppo CIDIU), which is very close to the metro line inside the park, B1_Accelerometer1 showed a maximum value of 0.144 m/s^2 at 05:28:59 on 22 July, and B1_Accelerometer2 reached 0.134 m/s^2 at 05:36:59. These values went above the warning limit but were still far below the alert limit. The peaks were short and occurred during expected train activity, so they are likely normal operational vibrations rather than a sign of structural damage. The higher frequency and amplitude at B1 confirm that its close distance to the metro exposes it to stronger vibrations.

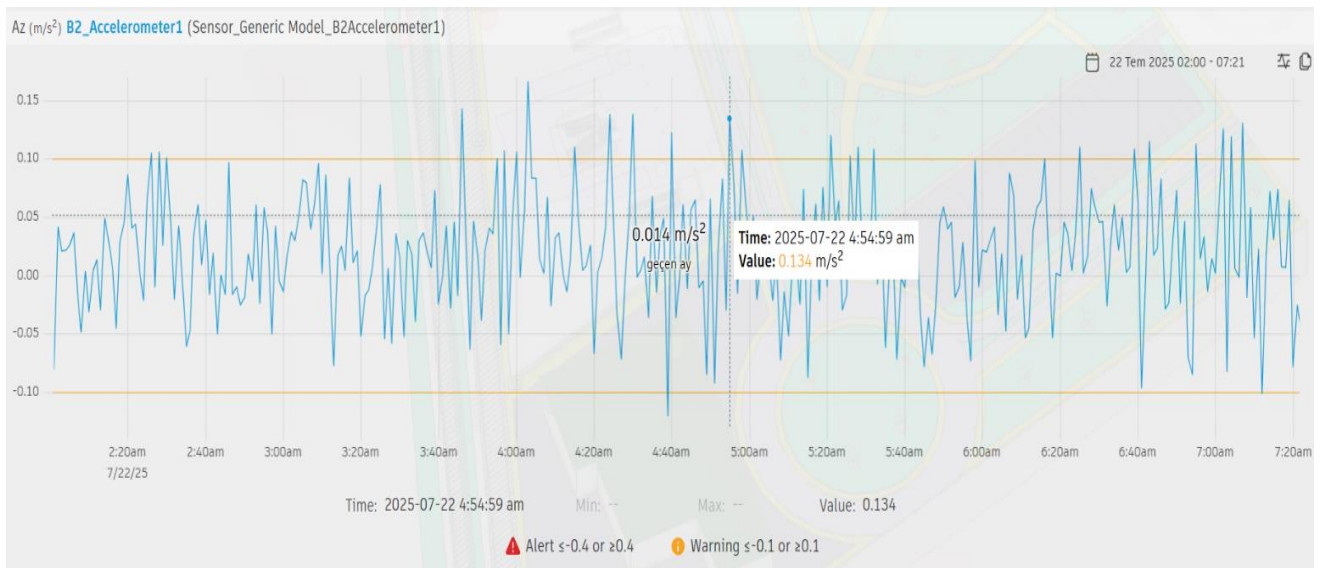


Figure 47 - B2_Accelerometer1 Chart

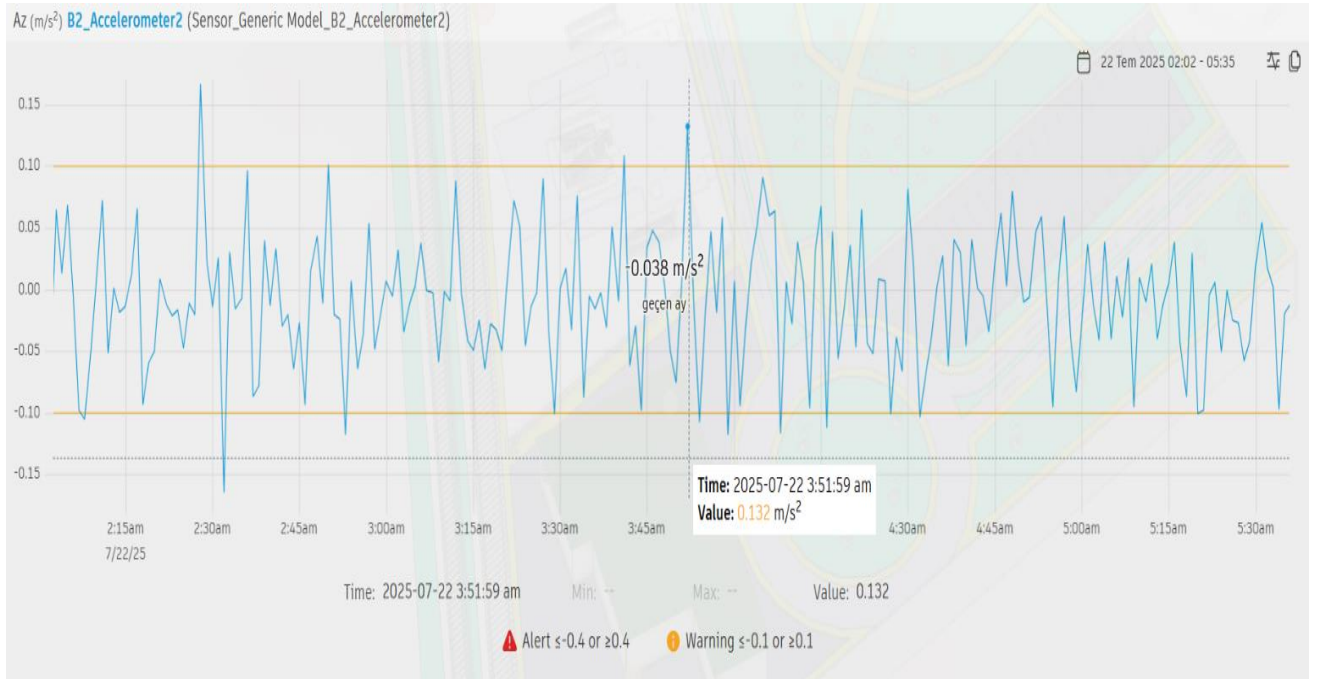


Figure 48 - B2_Accelerometer2 Chart

In comparison, B2, the abandoned building farther from the tracks, showed slightly smaller peaks. B2_Accelerometer1 peaked at 0.134 m/s^2 , and B2_Accelerometer2 reached 0.132 m/s^2 . These warning level events were less frequent and smaller in size, which matches the reduced vibration expected at a greater distance from the metro.

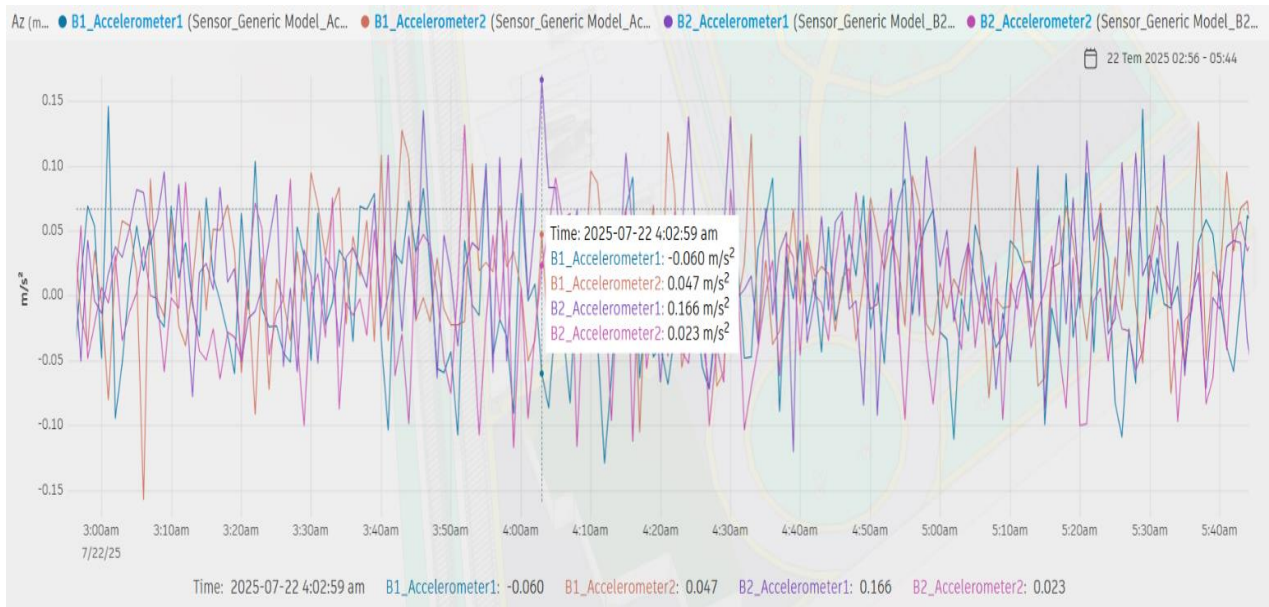


Figure 49 - Combined Chart of Accelerometers

When comparing all four accelerometers together, B2's readings are narrower and show fewer high peaks, confirming that the vibration intensity decreases with distance.

No sensor on either building reached the $\pm 0.40 \text{ m/s}^2$ alert threshold, meaning there is no immediate structural risk. However, the repeated short warnings at B1 mean that close observation is still important. If these peaks become more frequent or increase in size, they could over time affect non-structural parts such as façade connections or interior finishes. They might also interact with ground movement detected by the tiltmeters and inclinometer chains.

To maintain reliable monitoring, accelerometer measurements should continue at high-frequency sampling (one second intervals) during metro operations. Peaks that pass the $\pm 0.10 \text{ m/s}^2$ warning limit should be checked against tiltmeter readings on the same façade and cross referenced with topographic benchmarks to see if ground settlement or rotation is influencing vibration levels. Applying a basic frequency analysis (FFT) can help detect dominant vibration frequencies and identify whether they are close to the natural frequencies of the buildings, which

could lead to resonance effects.

Because B1 is closer to the metro line and therefore experiences stronger vibrations, regular visual inspections of its façades, joints, and non-structural elements are recommended. Any repeated warning-level events or visible signs of distress (e.g., cracks or loosened cladding) should trigger further checks or minor preventive measures. Logging all warning-level exceedances over time will help reveal patterns and improve future risk assessment.

From a critical perspective, the measurable quantity in the accelerometer records is the façade-level vibration response expressed as acceleration over time. The critical point is not only defined by the alert threshold of $\pm 0.40 \text{ m/s}^2$, but also by the pattern of repeated warnings around $\pm 0.10 \text{ m/s}^2$, especially when they cluster during train passages. While single peaks may not represent direct damage, the frequency and persistence of warnings are more relevant indicators for long-term performance.

The trade-off with accelerometers is clear: they are highly effective for capturing dynamic responses at high resolution and relatively low cost, but they provide only an indirect link to structural safety, as they cannot measure damage directly. In practical applications, engineers must balance these advantages against limitations such as sensor noise and environmental sensitivity. In this case, accelerometers serve primarily as an early-warning tool, highlighting potential vibration issues that should be cross-checked with tiltmeters and benchmarks before drawing conclusions about structural condition.

3.5.2 Tiltmeter Data Interpretation and Risk Assessment

Tiltmeters were installed on the front and rear façades of B1 (Gruppo CIDIU) and B2 (abandoned building) in a cross pattern to record angular changes on both sides of each structure. Measurements were taken every 5 minutes over a two-week period, ensuring that both daytime and nighttime metro activity was captured. The warning threshold for inclination was defined as $\pm 0.04^\circ$, while $\pm 0.10^\circ$ was set as the alert level for potential structural concern.

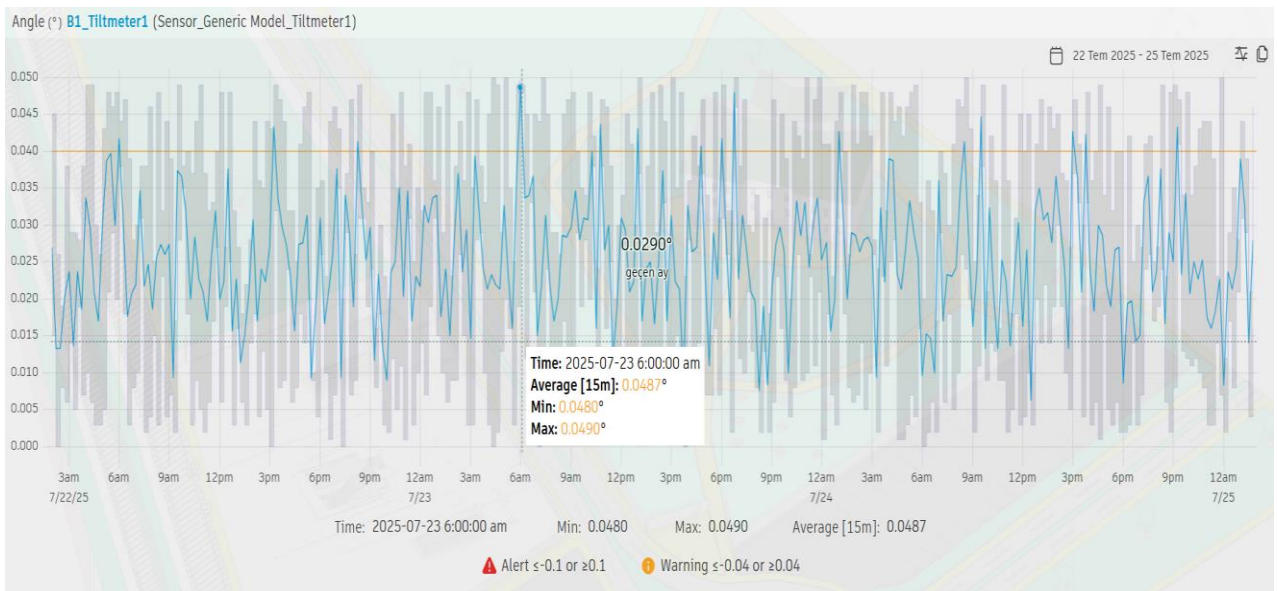


Figure 50 - B1_Tiltmeter1 Chart

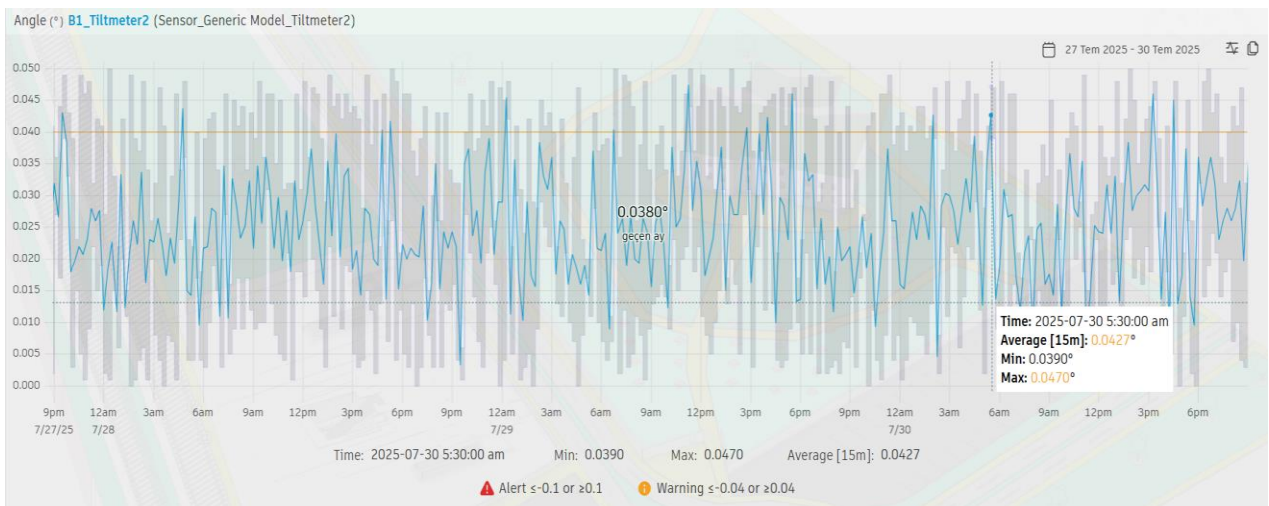


Figure 51 - B1_Tiltmeter2 Chart

For B1_Tiltmeter1 (Figure 48), a maximum of 0.0490° was observed on 23 July, crossing the warning limit by approximately 0.009° . This event corresponds to short-duration peaks rather than sustained drift, suggesting transient excitation, possibly simulated train vibrations or minor ground settlement. B1_Tiltmeter2 (Figure 49) reached 0.0470° on 30 July, again crossing the warning band but not approaching alert conditions.

Both instruments show a consistent average near $0.042\text{--}0.048^\circ$, meaning these warnings are frequent but not severe.

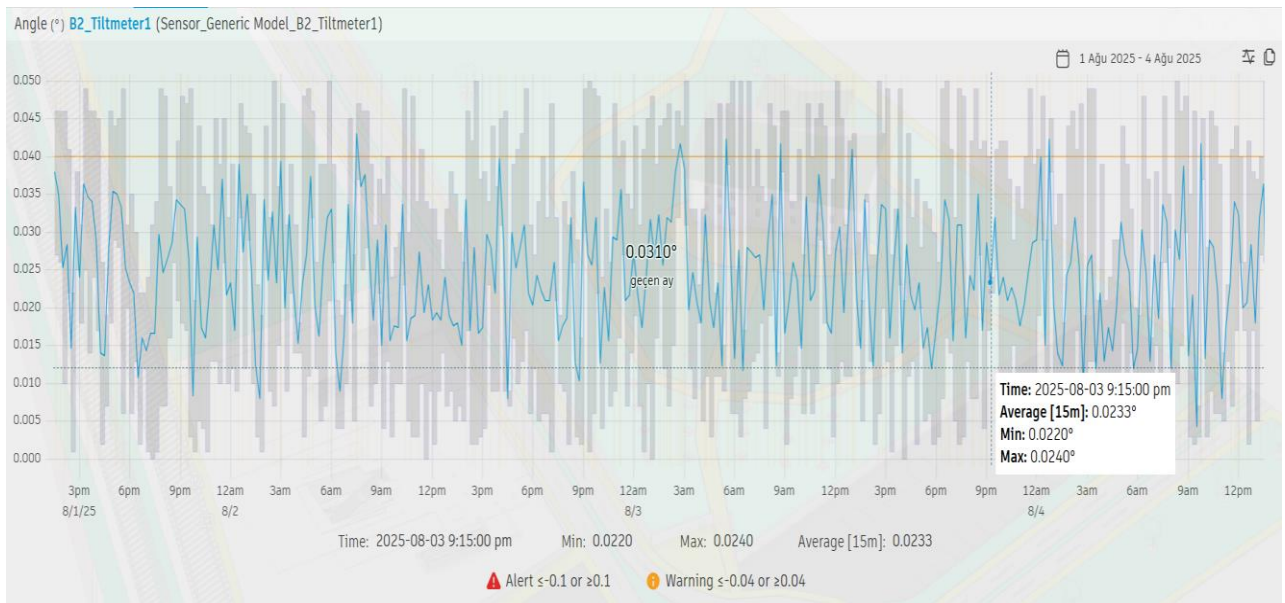


Figure 52 - B2_Tiltmeter1 Chart

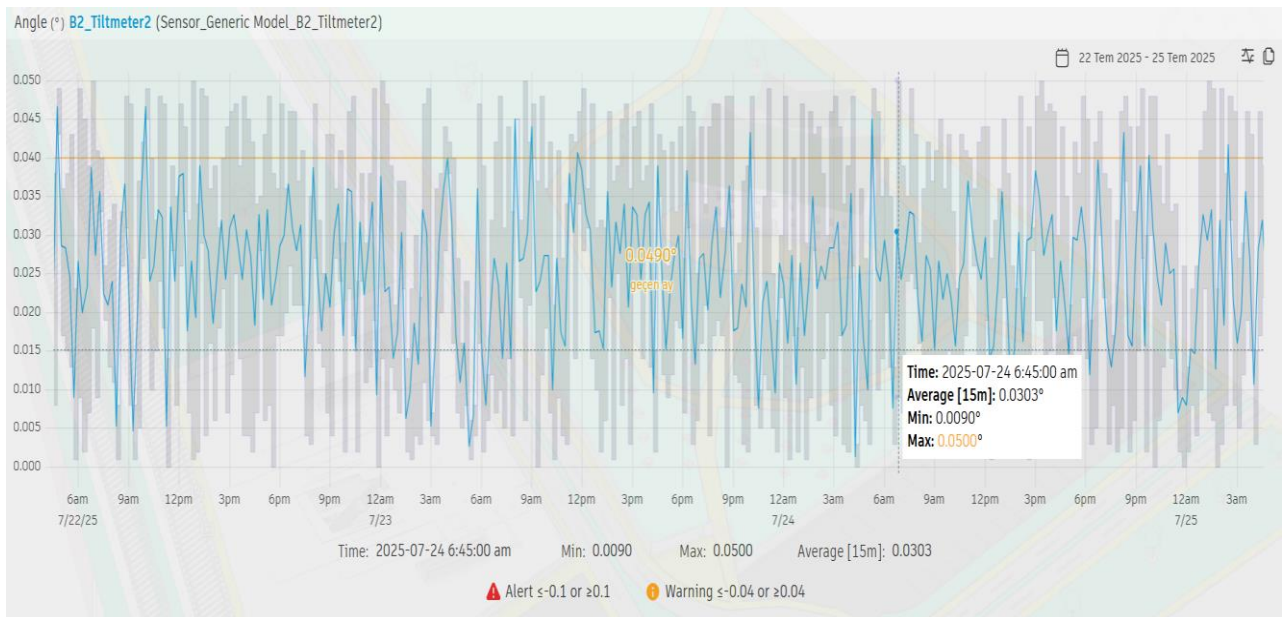


Figure 53 - B2_Tiltmeter2 Chart

The sensors installed on the second building (B2) exhibit lower angular changes overall. B2_Tiltmeter1 (Figure 50) has a maximum of 0.0240°, comfortably within the warning range, and averages of 0.023–0.031°. B2_Tiltmeter2 (Figure 51) briefly peaks at 0.0500° on 24 July, crossing the warning limit but without sustained exceedances.



Figure 54 - Combined Chart of Tiltmeters

The comparative plot of all four tiltmeters (Figure 52) confirms that the two sensors on B1 tend to register slightly larger angular oscillations than those on B2, consistent with their closer proximity to the metro alignment and therefore greater exposure to vibration and settlement effects.

From a risk perspective, no alert-level angular rotations ($\geq 0.10^\circ$) were recorded, meaning that structural safety is not immediately threatened. However, the repeated short-duration warnings on B1 merit closer observation. If similar exceedances persist or increase in frequency, they could indicate emerging differential settlement or façade rotation, especially if confirmed by accelerometer spikes or inclinometer chain anomalies.

Recommended actions include maintaining the current 5-minute sampling interval to preserve temporal resolution, cross-referencing warning events with accelerometer data to identify possible vibration sources, and comparing benchmark settlement data for corroboration.

It may also be advisable to extend monitoring duration or refine thresholds by applying a duration criterion, for example, only classifying warnings as significant if they persist for ≥ 30 –45 minutes. Proactive structural inspections (visual checks for façade cracks or joint openings) could be scheduled if repeated warnings cluster spatially on B1's façades.

In summary, the tiltmeters confirm low-to-moderate risk: the angular changes remain small and mostly transient, yet their concentration on the building closest to the tunnel suggests that ongoing observation is justified to prevent unnoticed progression of structural rotation or settlement effects.

The measurable parameter in the tiltmeter system is the façade rotation $\theta(t)$, expressed in degrees. The critical point is not only the absolute alert threshold of $\pm 0.10^\circ$, but also the trend over time, since a gradual but consistent increase, even if below thresholds, may point to developing differential settlement. This makes tiltmeters particularly valuable as they provide a direct measure of angular rotation, unlike accelerometers which capture only dynamic excitation.

The trade-off is that tiltmeters are relatively easy to install and cost-effective, offering continuous tracking of structural inclination, yet they can be influenced by thermal drift and sensor calibration issues. In practice, their strength lies in long-term monitoring of slow processes, while short-term fluctuations must be carefully filtered to avoid false alarms. In this project, tiltmeters act as a bridge between accelerometer dynamics and benchmark settlement data, giving a clearer picture of whether vibrations are translating into cumulative rotation or whether the building remains stable over time.

3.5.3 Inclinator Chain Analysis and Interpretation

Two inclinometer chains were installed parallel to the railway alignment, one on each side of the track, to monitor subsurface deformation during underground works. Each chain consisted of five nodes spaced evenly along the borehole depth. To streamline the analysis, only Node 5 (the shallowest, closest to the surface) and Node 1 (the deepest anchor point) were selected for evaluation. This choice was based on preliminary screening, which showed that intermediate nodes (Nodes 2–4) displayed stable readings without notable anomalies. Assessing the topmost and bottommost nodes provides an effective picture of potential surface effects and deep ground stability while reducing redundant data interpretation. The monitoring period covered two weeks, with measurements recorded every 30 minutes, and the data were processed and plotted in Excel.

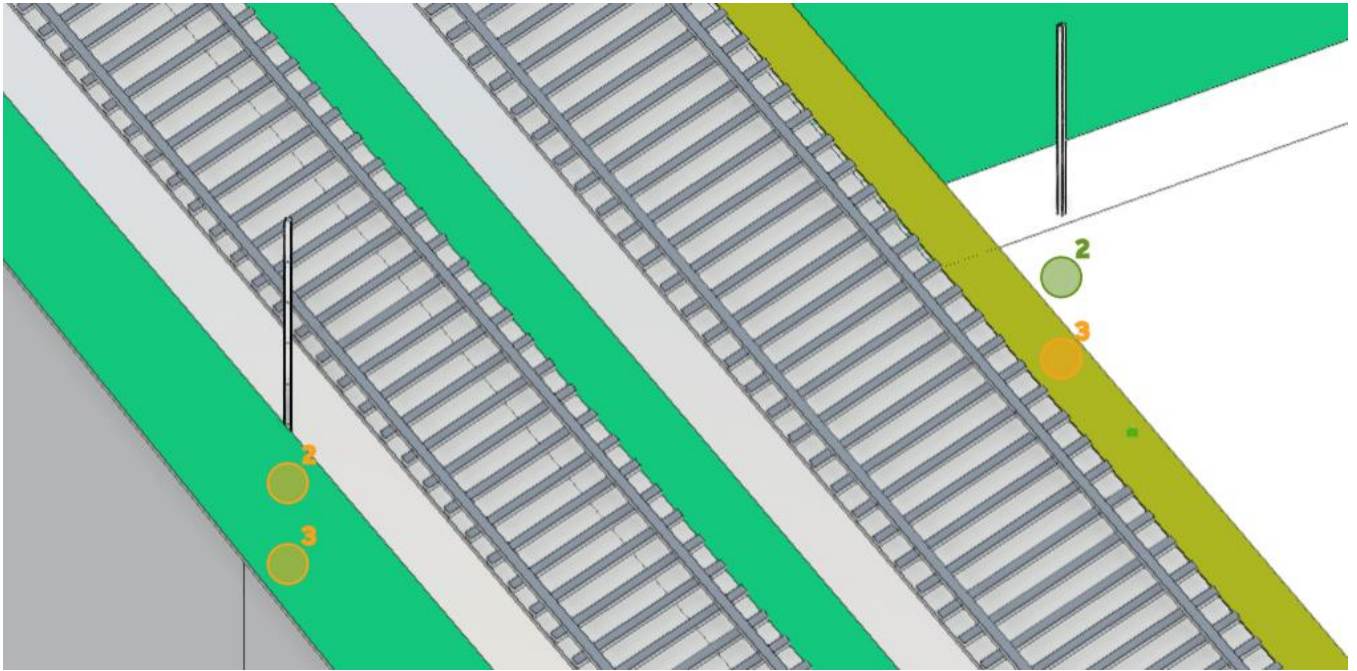


Figure 55 - Inclinator Chains Aligned in Railway

3.5.3.1 Az (Acceleration) Measurements

The Az acceleration graphs for Chain 1 – Node 1 and Node 5 and Chain 2 – Node 1 and Node 5 reveal values fluctuating between approximately 0.960 m/s^2 and 0.985 m/s^2 . All readings remained comfortably within the warning thresholds ($0.98\text{--}1.02 \text{ m/s}^2$) and far from the alert limits ($\leq 0.95 \text{ m/s}^2$ or $\geq 1.05 \text{ m/s}^2$).

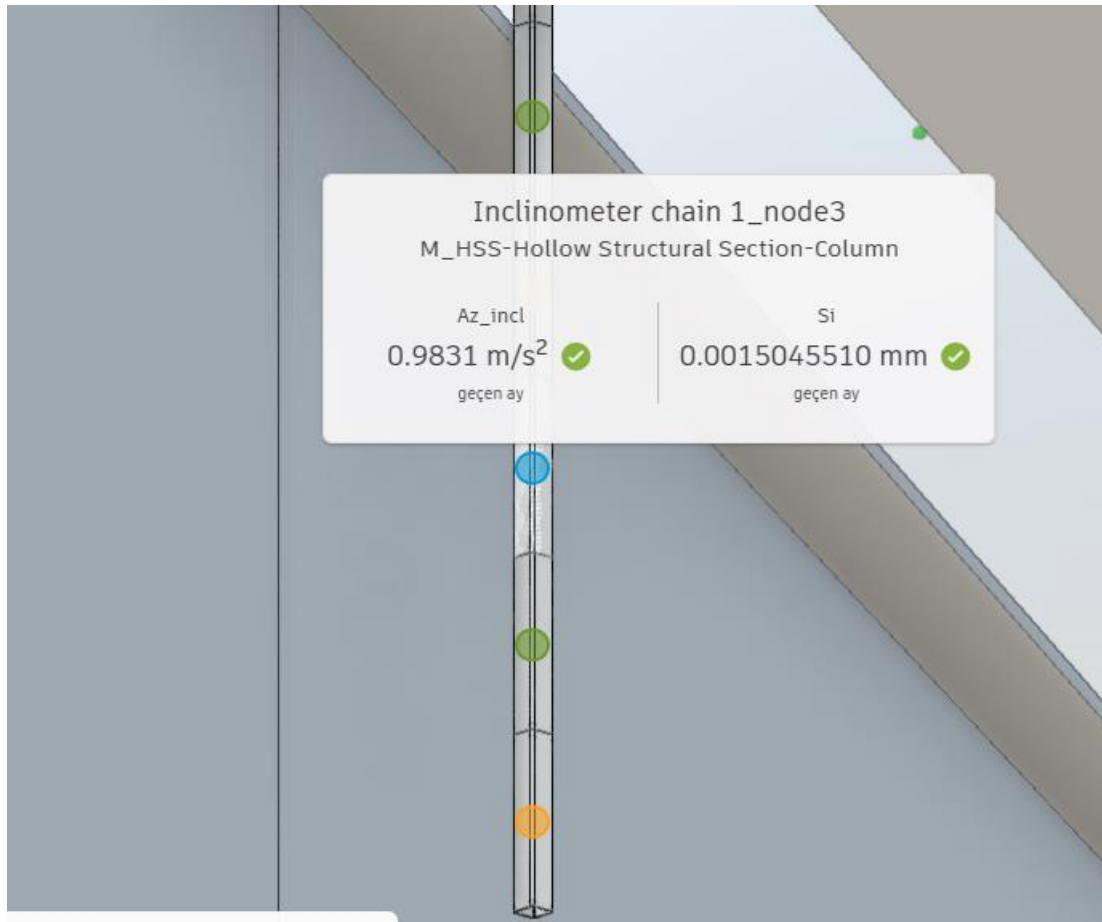


Figure 56 - Inclinometer Chain1 nodes

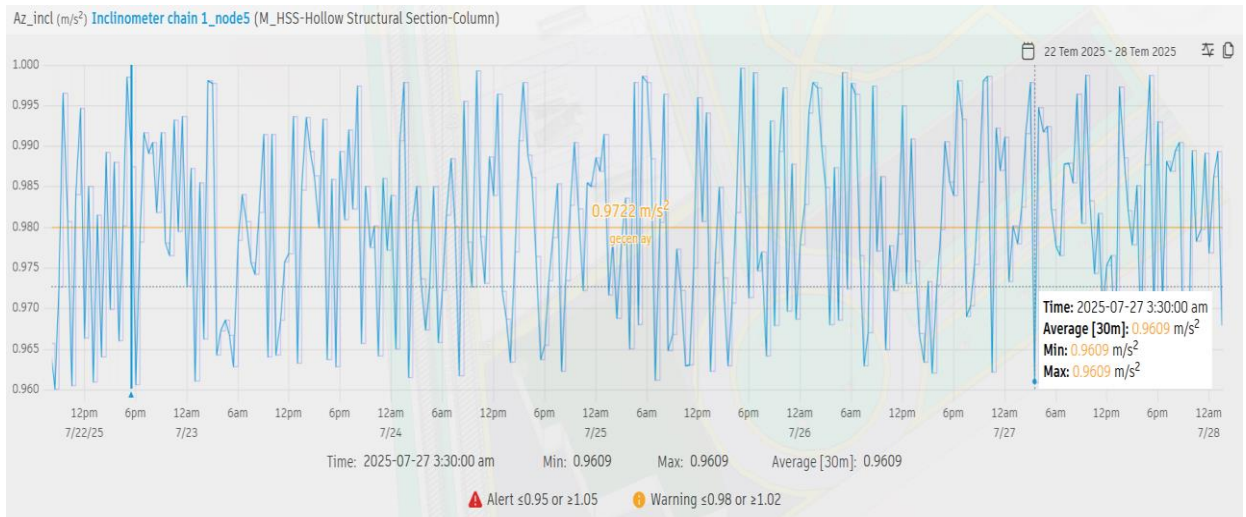


Figure 57 - Inclinometer Chain1 node-5 Az Chart

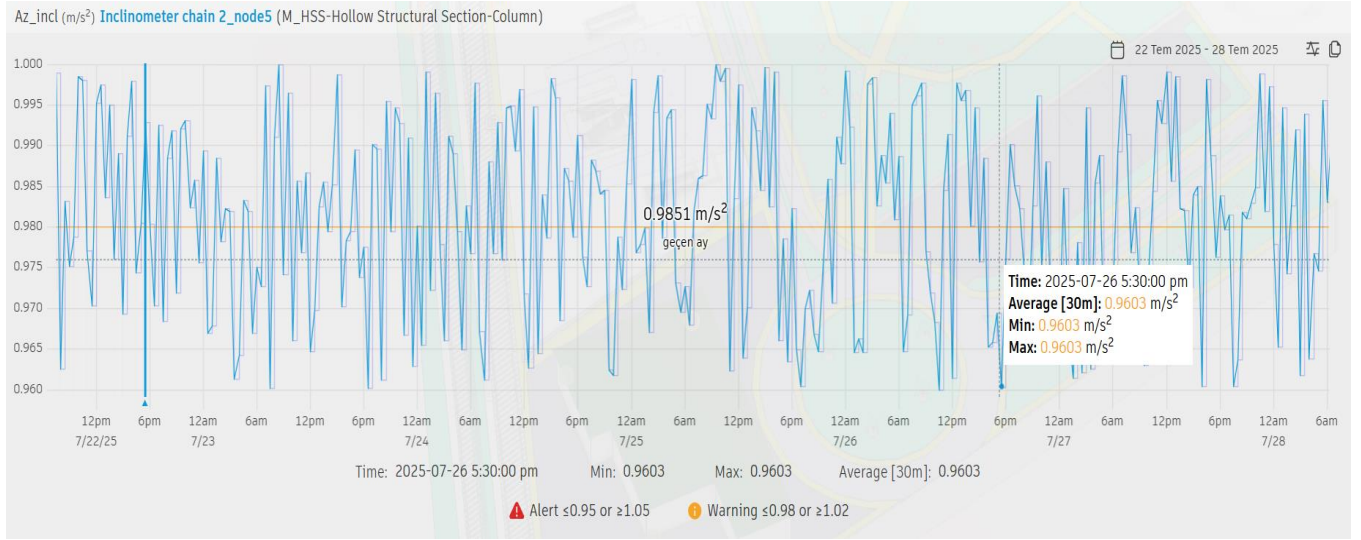


Figure 58 - Inclinator Chain 2 node-5 Az Chart

- **Surface Nodes (Node 5):** Slightly higher variability was observed, with episodic peaks approaching 0.985 m/s². These fluctuations are consistent with external influences such as minor traffic-induced vibrations, surface weathering effects, or sensor noise. They do not persist or trend upward, which suggests they are not indicative of progressive deformation.

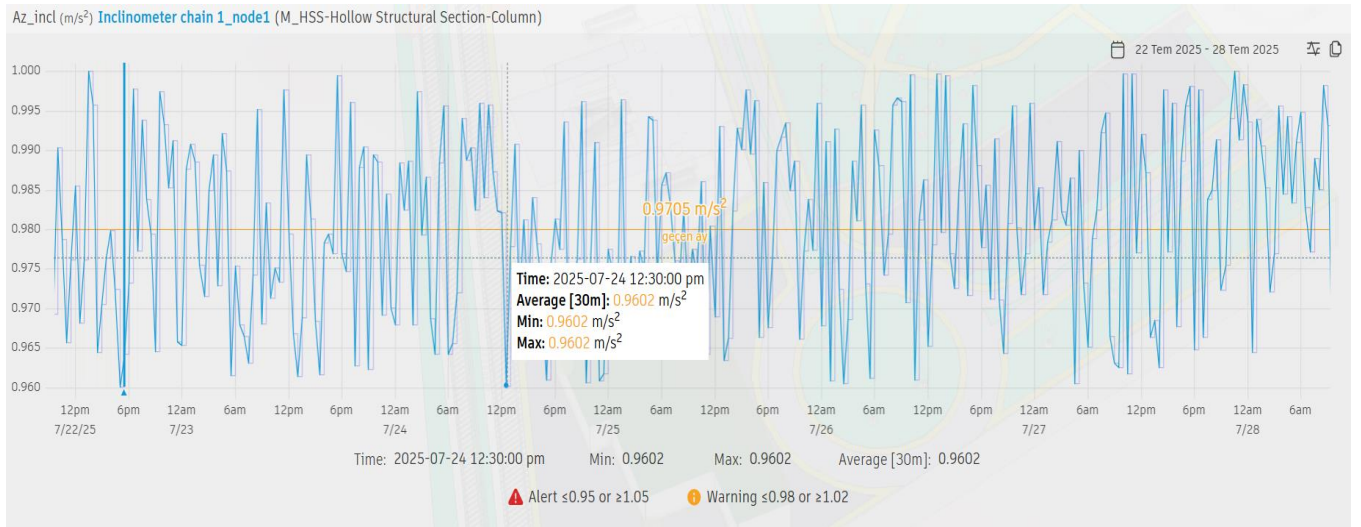


Figure 59 - Inclinator Chain 1 Node-1 Az Chart

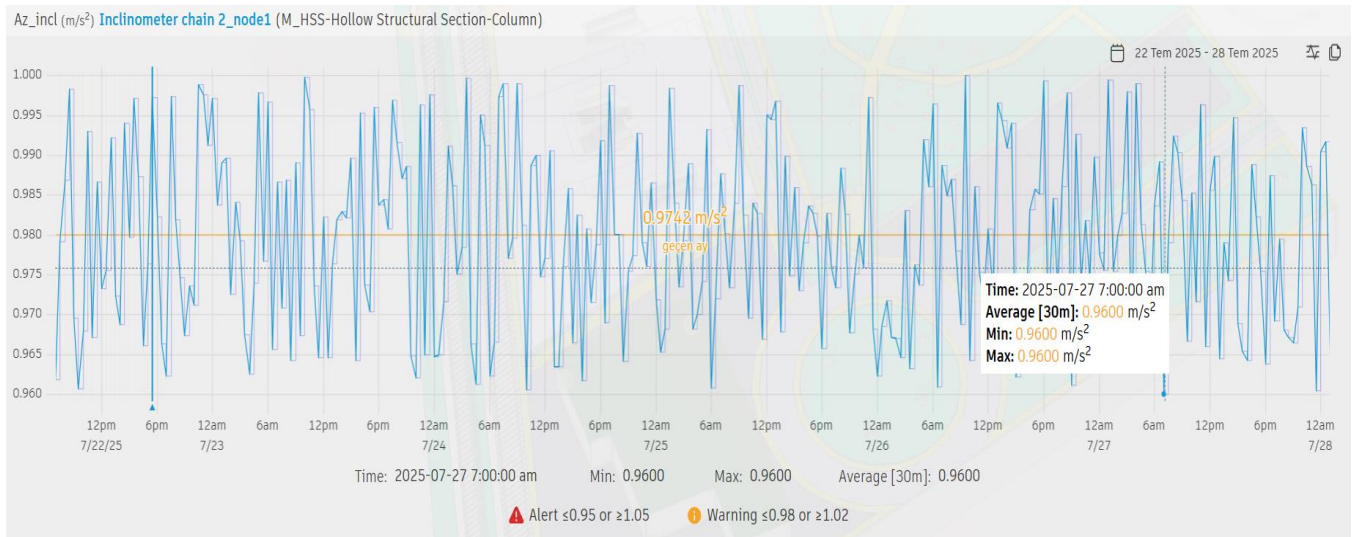


Figure 60 - Inclinator Chain 2 Node-1 Az Chart

- **Deep Nodes (Node 1):** The deepest readings remained remarkably stable, rarely deviating from 0.960–0.970 m/s^2 . These points act as fixed references anchored in undisturbed soil layers, confirming that the underlying strata are not experiencing significant displacement.

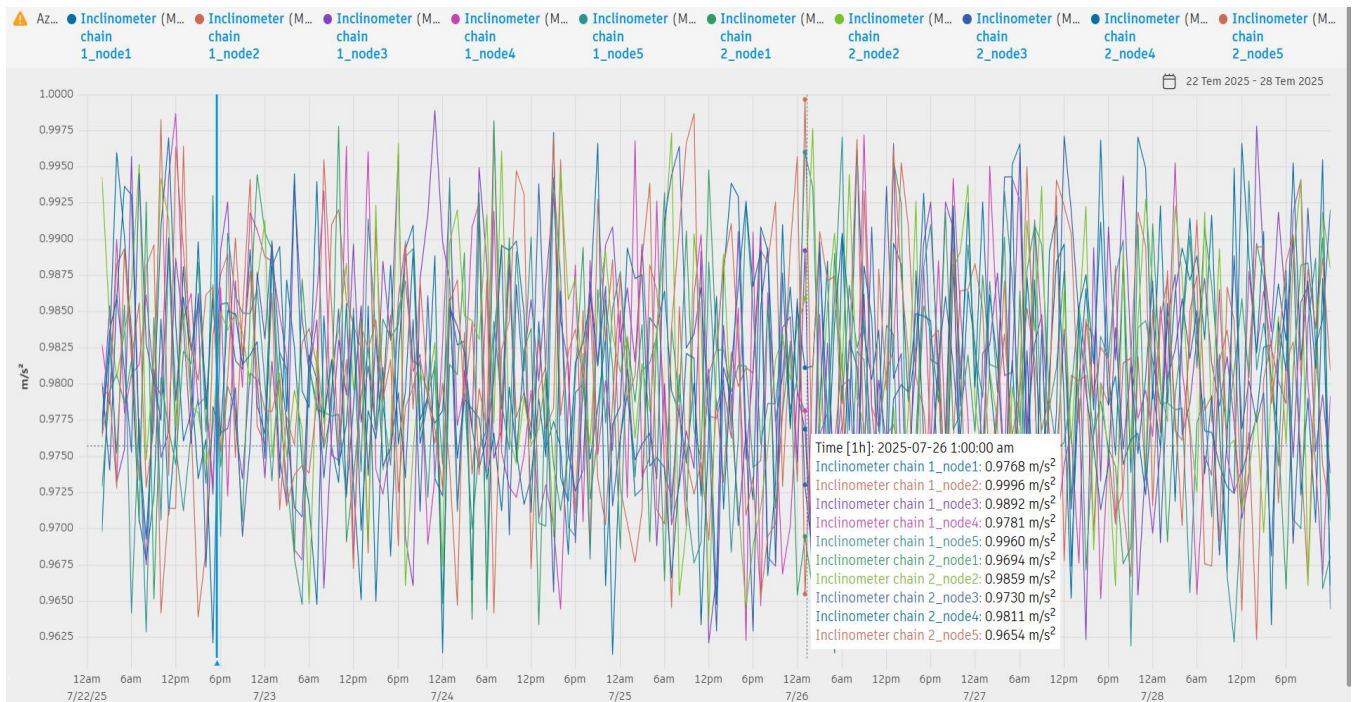


Figure 61 - Combined Chart of Inclinator Chains Az Data

The combined Az charts for all nodes across both chains support this conclusion: no sudden spikes or sustained drifts were detected. The similarity between the two chains—despite being placed on opposite sides of the railway—indicates symmetrical ground behavior and rules out differential settlement or lateral movement near the tunnel alignment.

3.5.3.2 Settlement (Si) Measurements

Settlement values (Si) for the selected nodes demonstrate similarly stable behavior. Across Chain 1 and Chain 2, Node 1 and Node 5 values range from 0.00148 mm to 0.00153 mm, which is several orders of magnitude below the predefined warning (± 3 mm) and alert (± 5 mm) thresholds.

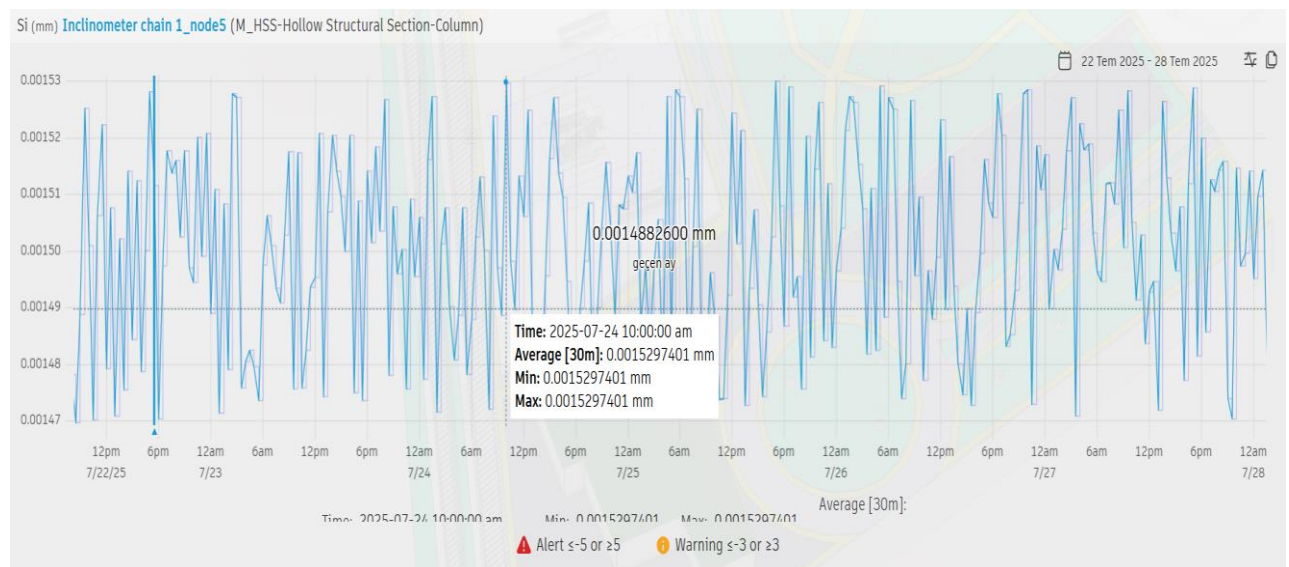


Figure 62 - Inclinometer Chain 1 Node-5 Si Chart

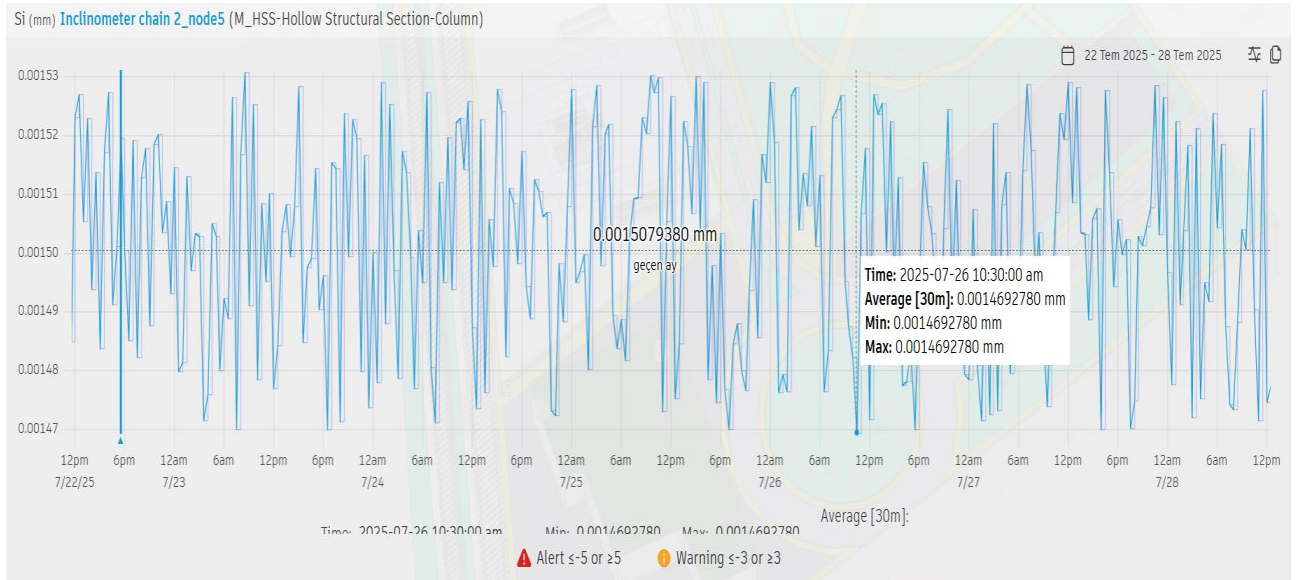


Figure 63 - Inclinometer Chain 2 Node-5 Si Chart

- **Surface Settlement (Node 5):** Minor scatter is present, again likely reflecting environmental noise or surface-level activities rather than actual ground movement.

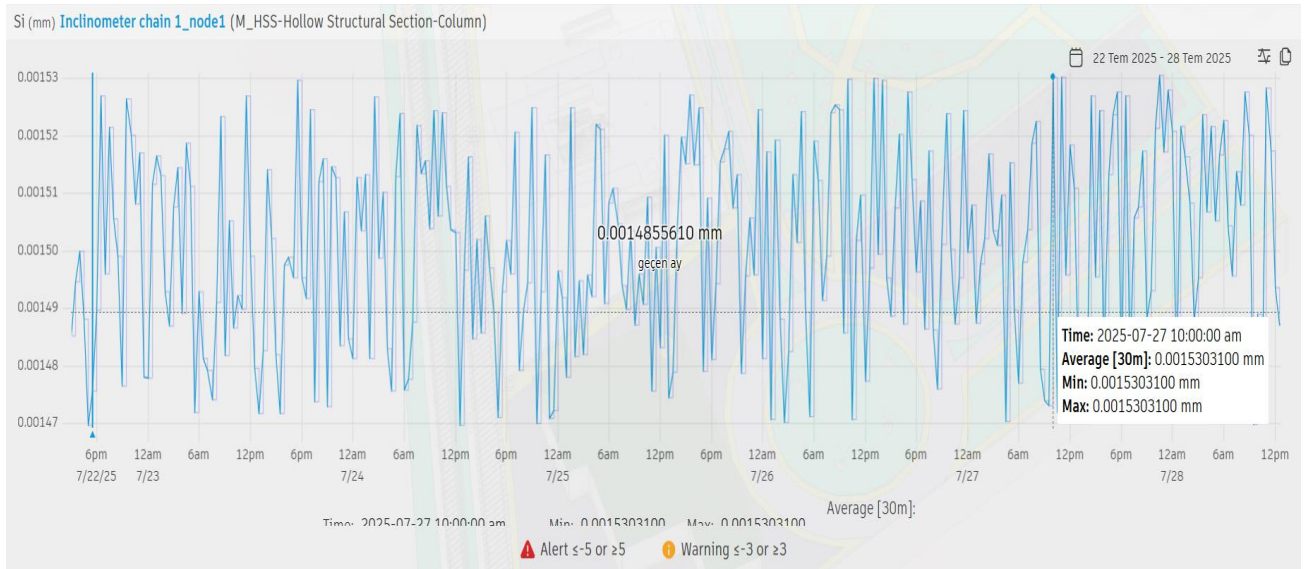


Figure 64 - Inclinometer Chain 1 Node-1 Si Chart

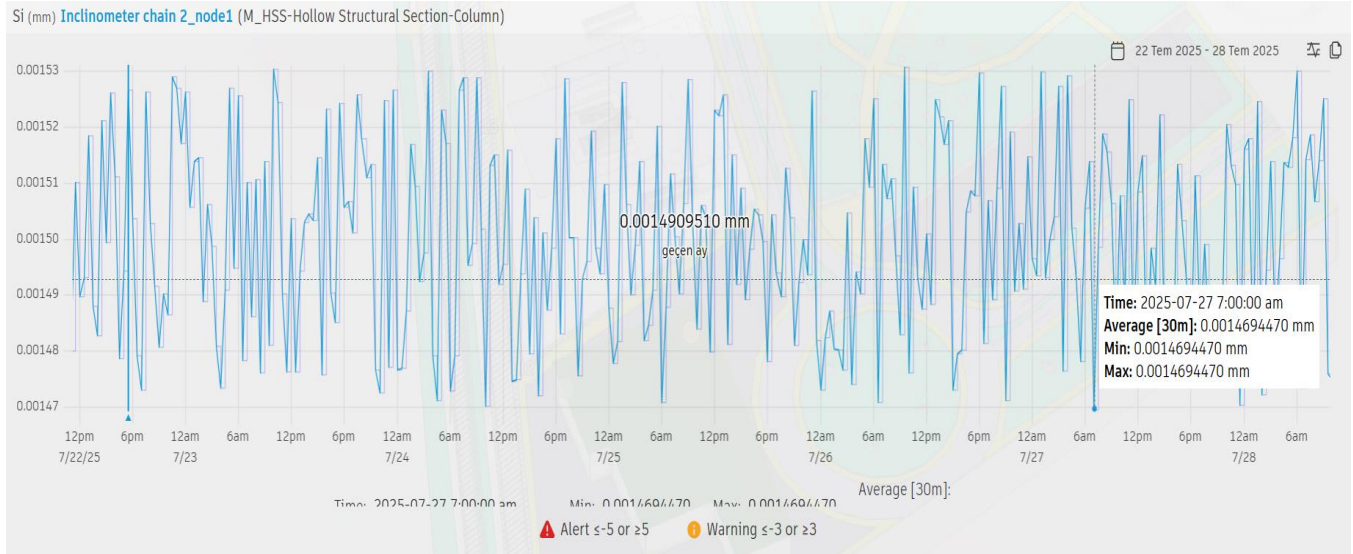


Figure 65 - Inclinator Chain 2 Node-1 Si Chart

- **Deep Settlement (Node 1):** The deepest points show even tighter clustering, suggesting the deeper soil layers remain unaffected by tunneling or surface loads.

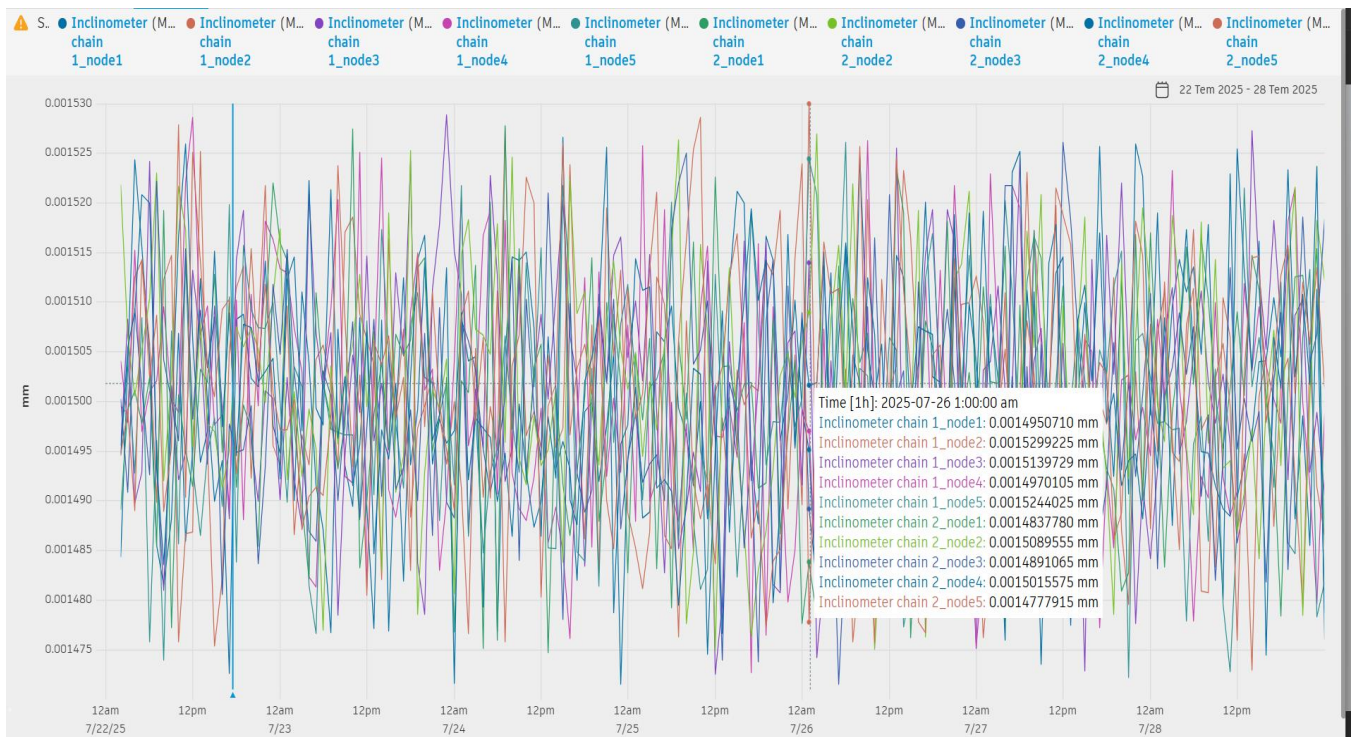


Figure 66 - Combined Inclinator Chain Chart of Si Values

The combined Si chart reinforces these findings: all nodes across both inclinometer chains exhibit nearly overlapping trends with no sign of differential settlement or progressive deformation.

3.5.3.3 Risk Assessment

Taken together, the Az and Si measurements demonstrate that no significant ground deformation occurred during the two-week monitoring window. The observed fluctuations are small, random, and transient rather than directional or cumulative. Importantly, the lack of divergence between the two chains confirms that both sides of the railway behave similarly under current conditions, which minimizes the likelihood of uneven ground displacement that could jeopardize structural stability.

While the data indicate a low risk environment, continuous monitoring remains essential, particularly during active excavation or when external factors such as heavy rainfall or construction traffic could influence soil conditions. Early detection of deviation from baseline values—especially persistent acceleration spikes at surface nodes or gradual settlement increases at deep nodes—would be critical for implementing timely mitigation measures such as adjusting construction sequences, adding ground support, or reinforcing nearby structures.

From a critical perspective, the measurable parameters in the inclinometer chains are the depth-dependent inclination values (Az) and the derived settlement profiles (Si). The critical points are defined both by absolute thresholds (e.g., ± 3 mm settlement for warning and ± 5 mm for alert) and by the shape of displacement with depth, since localized curvature between nodes can reveal developing shear zones that cumulative values alone might overlook. The chains therefore provide a unique ability to distinguish between surface settlement and deep-seated soil deformation.

The trade-off is that inclinometer chains deliver the most diagnostic geotechnical insight, but they are also invasive, costly, and lower in sampling frequency compared to surface sensors. This makes them less suited for capturing rapid, transient effects, but highly effective for identifying progressive, potentially irreversible movements in the ground. In the Certosa case, they serve as the ground-truth layer that validates whether surface rotations and vibrations detected by accelerometers and tiltmeters are accompanied by subsurface shifts. Their continued use is essential for ensuring that apparently minor changes at the surface are not early signs of deeper instability.

3.5.4 Topographic Benchmark Analysis

Topographic benchmark measurements were recorded every 5 minutes for a continuous 2-week period and organized in Excel for analysis. Five benchmark sections were installed at 10 m intervals along a line perpendicular to the tunnel alignment, located in the park adjacent to the metro line. For clarity and to avoid redundancy, only the representative benchmarks from the first, third (middle), and fifth (last) sections are discussed here, since none of the five locations showed warning-level or alert-level values.

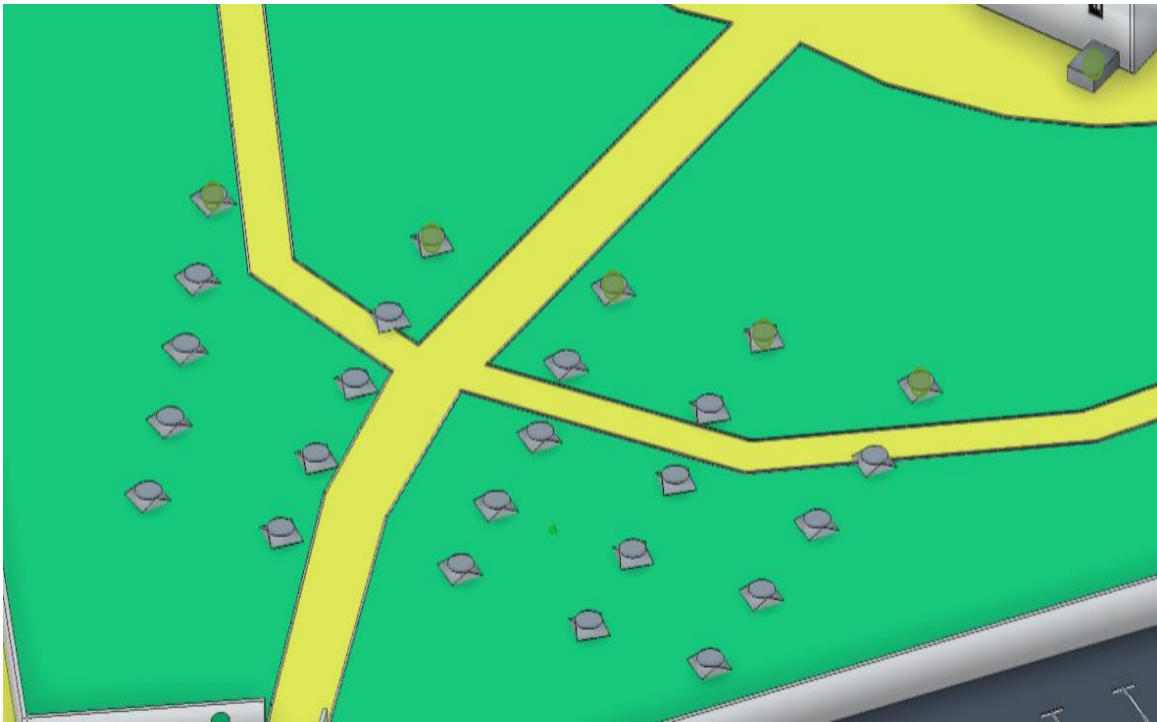


Figure 67 - Topographic Benchmarks in Park Area

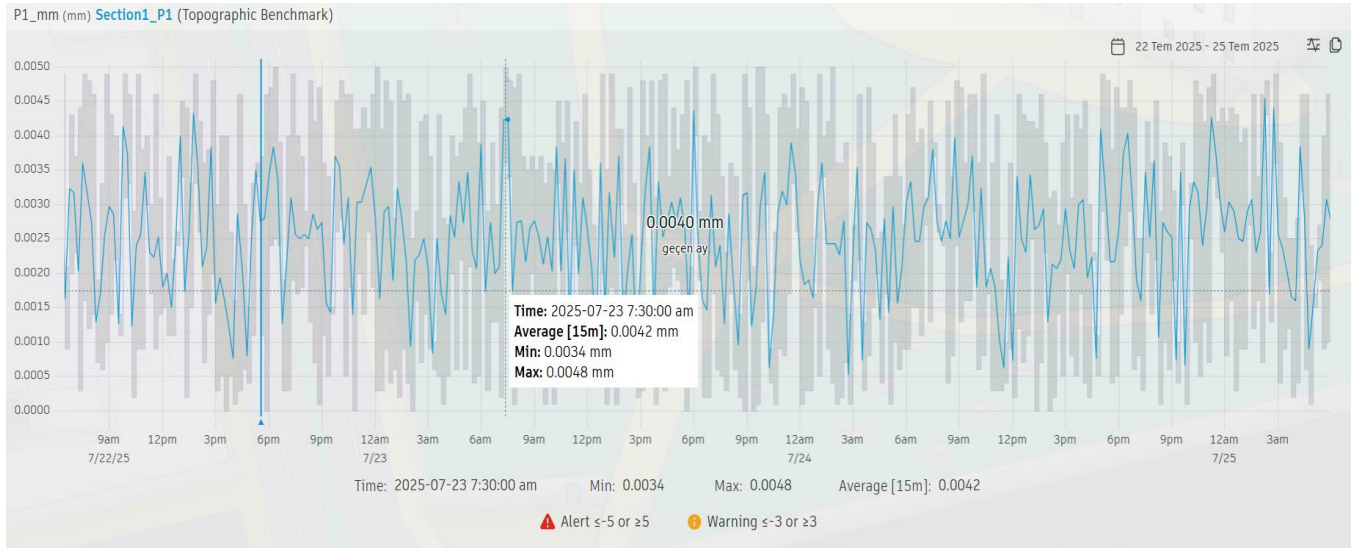


Figure 68 - Topographic Benchmark Section 1 Chart

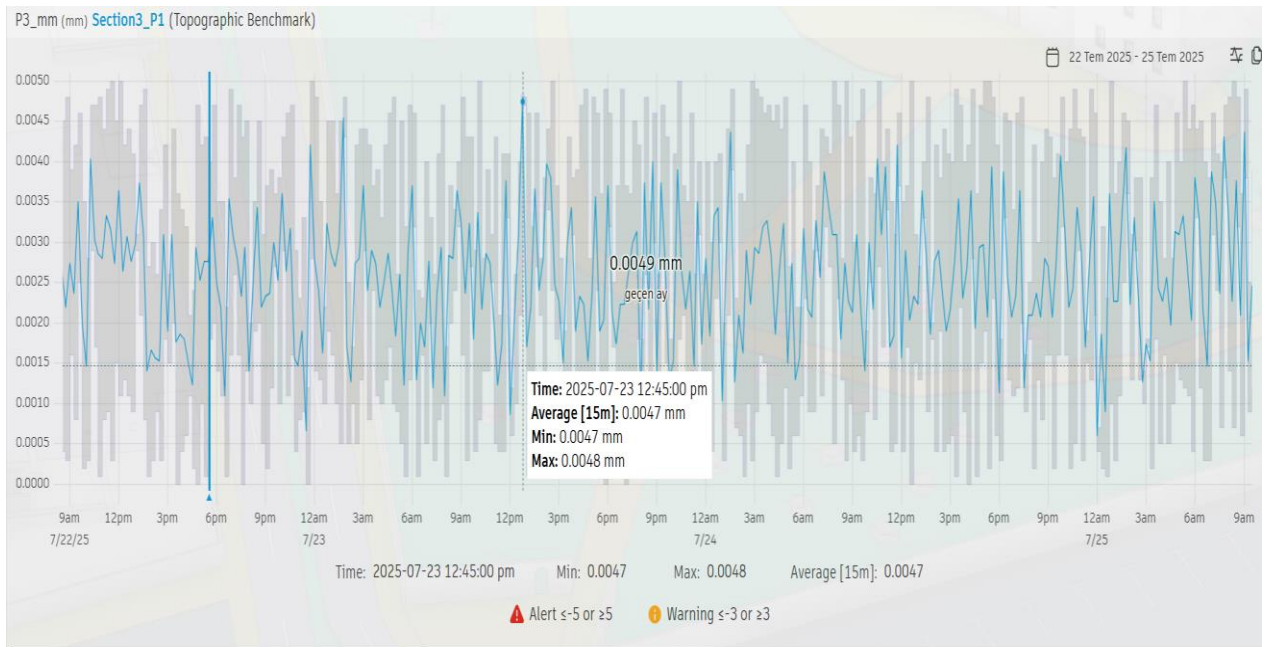


Figure 69 - Topographic Benchmark Section 3 Chart

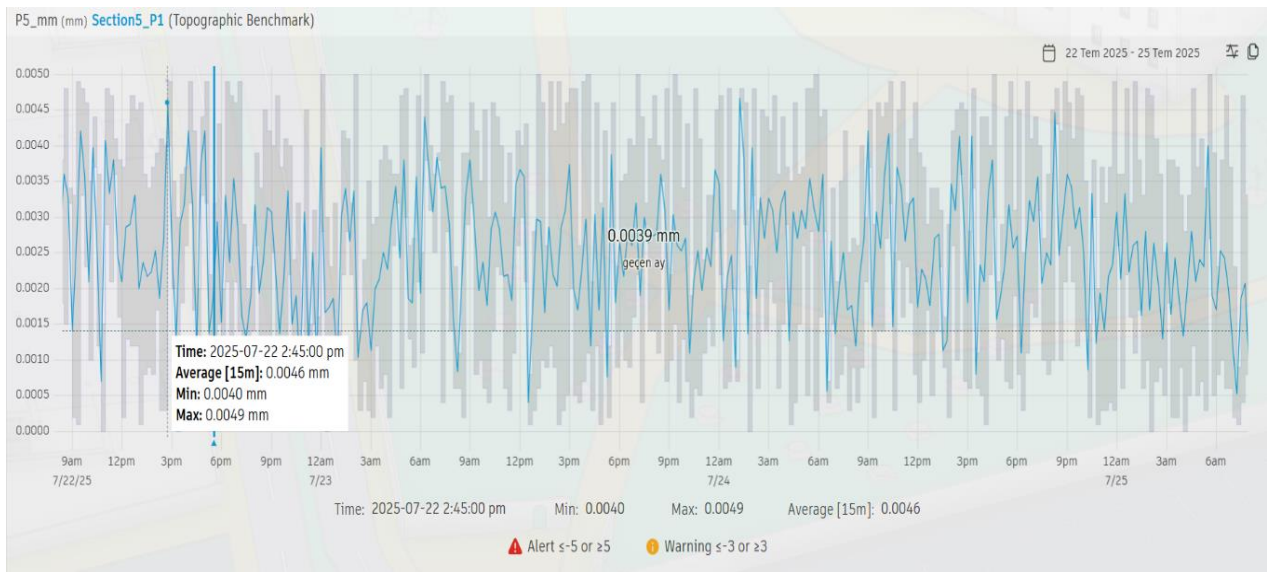


Figure 70 - Topographic Benchmark Section 5 Chart

Across all three selected benchmarks (P1, P3, and P5), displacements remained extremely small, between 0.0034 mm and 0.0049 mm, which is well below the warning thresholds (± 3 mm) and far from the alert limits (± 5 mm). The time-series plots reveal minor short-term fluctuations, likely attributable to environmental noise, ground surface temperature changes, or instrument precision, but no persistent upward or downward trends that would indicate progressive settlement or uplift. The average values for each benchmark were consistent: approximately 0.0042 mm for Section 1_P1, 0.0047 mm for Section 3_P1, and 0.0046 mm for Section 5_P1.

The uniformity of the readings across sections positioned at different distances from the tunnel alignment suggests that tunneling activities or nearby structural loads did not generate measurable ground deformation in this period. Because the benchmarks were placed orthogonally to the tunnel axis, they provide a reliable cross-sectional perspective of surface stability over the metro alignment. The absence of spatial variation or anomalous peaks confirms that both the excavation zone and surrounding park terrain remain stable, with no evidence of localized settlement or heave.

These results indicate that the benchmark network is functioning as expected and provides an effective early-warning system, even though no interventions are presently required.

In the case of the benchmarks, what is directly measured is the change in elevation of surface points positioned orthogonally to the tunnel axis. Their value lies not only in detecting absolute settlement magnitudes but also in revealing spatial patterns, for example, whether adjacent sections begin to diverge or develop a gradient that could indicate uneven ground behavior. A shift of just a few millimeters between neighboring points can be more critical than a uniform movement across the entire section.

The critical aspect of this technique is therefore its ability to serve as a surface-level reference frame for the entire monitoring system. Benchmarks do not provide information at depth and cannot capture transient vibrations, but they anchor the interpretation of inclinometer data and help confirm whether tiltmeter rotations or accelerometer peaks correspond to actual ground settlement.

From a practical standpoint, the advantage of benchmarks is their simplicity, low cost, and reliability; the drawback is the dependence on periodic surveys rather than automated, high-frequency readings. In the Certosa project, their stability during the monitoring window reinforces the conclusion that tunneling activity had no measurable surface impact. Nevertheless, by maintaining this reference grid over time, engineers can quickly detect the onset of progressive settlement, even if other sensors produce ambiguous results.

4. Discussion

The monitoring campaign around the Certosa Metro Station produced a comprehensive dataset that illustrates both the structural and geotechnical responses of the surrounding environment during the observation period. Results from accelerometers, tiltmeters, inclinometer chains, and topographic benchmarks consistently demonstrated stable conditions, with no measurements surpassing alert thresholds. Nevertheless, small transient variations observed across several instruments merit closer interpretation through a critical approach, where the focus is not only on absolute values but also on what can be measured, what constitutes a critical point, and what trade-offs exist between sensor types.

From a structural perspective, the two monitored buildings, Gruppo CIDIU (B1) and the abandoned structure (B2), showed only minor tilting fluctuations. Maximum tiltmeter readings remained within warning ranges, with occasional peaks approaching caution levels but never exceeding the alert thresholds. Here, the measurable is angular rotation, and the critical point is not just the 0.10° alert threshold but also the persistence of small but repeated warnings. This trade-off highlights that tiltmeters are highly effective in capturing slow rotational trends but may be sensitive to environmental drift. Their role is therefore less about detecting single events and more about identifying progressive inclinations that could accumulate over time.

The accelerometer data confirmed dynamic vibrations well below harmful limits. Peaks slightly exceeding warning thresholds were short-lived and associated with simulated train activity. In this case, the measurable is façade-level acceleration, while the critical point lies in repeated clusters of warning-level vibrations, especially in the closer B1 building. The trade-off is that accelerometers provide high-frequency, low-cost insights into dynamic conditions but cannot directly indicate structural damage. Their true value is as an early-warning tool, which, when combined with tiltmeters and benchmarks, helps determine whether vibrations are

translating into cumulative effects.

Regarding soil deformation, inclinometer chain data revealed consistent acceleration trends across both railway flanks. Surface nodes displayed slightly higher variability than deeper reference nodes, a pattern also described in the literature, indicating that upper soil layers are more sensitive to surface disturbances and environmental factors. Here, the critical points are not only settlement values exceeding ± 3 mm (warning) or ± 5 mm (alert) but also changes in displacement profiles with depth, which can indicate shear zones. The trade-off is that inclinometer chains deliver the most diagnostic geotechnical information but at higher cost and complexity. Their reliability makes them essential for confirming whether surface-level anomalies are underpinned by deeper instability.

The topographic benchmarks, positioned orthogonally to the tunnel axis at 10 m intervals within the park, provided an independent confirmation of surface stability. All benchmark readings fluctuated only within a narrow band (<0.005 mm) and showed no progressive trends. The measurable is vertical displacement, and the critical point lies in relative differences between sections, rather than uniform movements. Benchmarks are inexpensive and precise but limited to periodic readings and surface-level information. Their role is therefore complementary: they validate inclinometer findings and provide a cross-sectional reference frame for settlement analysis.

From a sensor network performance standpoint, the integration of virtual sensors in Autodesk Revit and their linkage to Autodesk Tandem proved highly reliable. Continuous data streams, accurate mapping of IDs, and real-time visualization allowed immediate detection of threshold exceedances, replicating the benefits of BIM-SHM integration highlighted in previous works. However, limitations must also be acknowledged: environmental noise (e.g., temperature fluctuations, rainfall, human activity) likely caused short-term spikes, and the two-week monitoring window does not capture possible long-term cumulative effects.

Additionally, as Tandem is still an emerging platform, data loss and minor bugs occasionally occurred, underlining the trade-off between adopting cutting-edge tools and relying on their current level of maturity. Another important limitation relates to data visualization within Autodesk Tandem. In this study, heatmaps were not produced because Tandem requires the definition of “rooms” to generate spatial heat distributions. While this functionality is useful for building interiors, it is not always appropriate for civil engineering applications such as metro stations, tunnels, or open infrastructure, where monitoring focuses on localized sensors rather than enclosed spaces. This constraint reflects a misalignment between Tandem’s current visualization tools and the broader needs of digital twin applications in infrastructure. Highlighting this gap is important, as it suggests that future developments should provide more flexible visualization methods that can adapt to linear assets and open environments.

Another limitation to highlight is related to the nature of civil engineering sensors themselves. In practice, most monitoring devices used on construction sites are wired systems that log data locally to a datalogger for later manual retrieval. The integration of IoT principles, such as wireless communication, cloud storage, and real-time data streaming, is only beginning to emerge in the civil engineering field. Even when sensors are equipped with IoT capabilities, they are often designed to work within proprietary dashboards that display data to the operator but are not open to transmit measurements to external platforms such as Autodesk Tandem. This constraint illustrates a key trade-off: while IoT-enabled digital twins promise interoperability and centralized monitoring, the reality of current sensor technologies still limits seamless integration. The Certosa case study, therefore, can be seen as a forward-looking prototype, testing workflows that anticipate a future in which sensors and digital platforms will be more natively connected.

In comparison with published work, this study confirms that combining BIM-based modeling with IoT-enabled monitoring provides a robust framework for risk management in underground infrastructure projects. The Certosa case study demonstrates that distributing sensors across structures, subsurface layers, and surface benchmarks yields a multi-scale understanding of soil–structure interaction and offers a replicable approach for future metro or tunneling projects.

Finally, the implications for design and maintenance strategies are significant. The findings suggest that the construction methods and support systems for the Certosa Metro line are effective in minimizing environmental impacts. Yet the critical question remains: which parameters should be prioritized in future monitoring campaigns? If cost and simplicity are most important, benchmarks and tiltmeters may be sufficient. If diagnostic accuracy is the priority, inclinometer chains become indispensable. If real-time vibration awareness is valued, accelerometers are essential. This balance mirrors the broader trade-off between speed, cost, and accuracy in infrastructure monitoring. Continued monitoring during full metro operation, combined with careful evaluation of these priorities, will ensure that risk is minimized while resources are used efficiently.

5. Recommendations and Future Work

The findings of this thesis confirmed that a BIM–SHM workflow can support the creation of a functional digital twin for underground infrastructure. Building this validated prototype, the next phase should consolidate the system with real sensor measurements, longer campaigns, and stronger data governance. The recommendations below are grouped into a roadmap that addresses monitoring strategy, system architecture, operational integration, and research directions.

The current two-week simulation should be expanded into a three-stage program: (1) a baseline phase before construction, (2) an intensive monitoring phase during excavation and commissioning, and (3) long-term operation. Sampling frequencies should be adaptive, with higher resolution during train passages or excavation works and lower resolution during routine conditions. This phased approach ensures both efficiency and early-warning capability.

The existing sensor configuration proved effective, but adding redundancy will strengthen reliability. For buildings, tiltmeters on upper floors and corners could capture differential rotations more accurately. Along the track, an additional inclinometer chain near soil transition zones would increase coverage. In the park, denser benchmark spacing and external reference points would improve settlement detection. Supplementary environmental sensors (temperature, rainfall, humidity) will also help distinguish structural changes from environmental noise.

Replacing synthetic data with live sensor feeds requires a robust IoT architecture. Standardized protocols (e.g., HTTPS) should feed time-series databases, with buffering to prevent data loss and clear latency targets for alarms. Automated QA/QC routines, such as range checks, unit consistency, and drift detection, will be necessary to maintain data quality. A formal calibration plan and uncertainty documentation will ensure that sensor readings remain credible and traceable over time.

Beyond data collection, the system must translate alerts into actionable steps. Standard operating procedures (SOPs) should define responsibilities, response times, and inspection protocols when warnings or alarms are triggered. Linking Tandem dashboards to asset management systems would allow alarms to generate automatic work orders and track follow-up actions, improving accountability and responsiveness.

Future work should move beyond simple threshold monitoring. Frequency-domain analysis of accelerometers (e.g., FFT, OMA) can identify resonances close to natural building frequencies. For inclinometer and benchmark data, trend detection and change-point analysis can provide early signs of cumulative deformation. Replacing static thresholds with multi-sensor, duration-aware rules will reduce false positives and highlight events of real significance.

The workflow should be evaluated not only from a technical but also from an organizational perspective. Infra.To and municipal authorities could benefit from dashboards that simplify decision-making, reduce uncertainty, and support transparent reporting to the public. Generalizing the workflow into reusable scripts and training materials would enable replication at other metro sites, maximizing the return on investment in digital twin technology.

Finally, coupling monitoring with numerical models and machine-learning approaches could enhance predictive capacity. Controlled trials after metro commissioning (e.g., trains at defined speeds and loads) will provide valuable ground truth for calibrating models and refining thresholds. At the same time, future research should address the current limitations of emerging platforms like Autodesk Tandem, where bugs or temporary data losses highlight the need for greater robustness before widespread adoption.

In short, the path forward involves transitioning from a validated prototype to a fully operational system: extending monitoring windows, densifying sensor networks, introducing robust IoT data pipelines, embedding analytics, and ensuring organizational readiness. Together, these steps will transform the Certosa Metro digital twin into a practical decision-support tool for safe, efficient, and resilient urban infrastructure.

6. Conclusion

This thesis set out to integrate Building Information Modeling (BIM) technologies with Structural Health Monitoring (SHM) strategies to develop a functional digital twin for the Certosa Metro Station area in Turin. Using a BIM model provided by Infra.To and expanded with surrounding buildings, terrain, and virtual sensors, a georeferenced digital environment was created in Autodesk Revit, InfraWorks, and Tandem. Synthetic datasets, generated in Excel according to manufacturer specifications and validated through Jupyter Notebook, were used to simulate accelerometer, tiltmeter, inclinometer chain, and topographic benchmark measurements. These streams were successfully mapped into Autodesk Tandem, ensuring real-time visualization and cross-referencing within the twin environment.

The Validation and Testing phase confirmed that all sensors performed within expected ranges: accelerometer data revealed transient peaks but no alert-level vibrations; tiltmeters recorded minor, short-term angular variations, particularly on the Gruppo CIDIU building closest to the metro line; inclinometer chains detected no significant subsurface deformation; and topographic benchmarks remained stable with no progressive settlement. The consistency of results across different sensor types demonstrates the reliability of the monitoring framework and its capacity to detect even subtle changes.

These findings are significant for the Certosa Metro project, confirming that current excavation and support methods are effective in minimizing ground movement and structural impacts. More broadly, they illustrate the potential of BIM-based SHM systems for urban infrastructure projects, where combining surface, structural, and subsurface monitoring within a digital twin environment enhances risk management and decision-making.

At the same time, this study highlights some limitations and challenges. During testing, Autodesk Tandem occasionally experienced bugs or temporary data losses, a reminder that digital twin platforms in construction are still evolving. These

interruptions did not compromise overall validation but underscored the importance of robustness testing when adopting new technologies. In fact, part of the thesis's objective was to evaluate Tandem's reliability as an emerging digital twin solution, making the observed imperfections an essential part of the research findings.

From a critical approach, this research also addressed the question of what is measurable, what is critical, and what trade-offs exist. Accelerometers measure vibrations with high temporal precision, but their critical point lies not in single peaks, but in clusters of repeated warnings. Tiltmeters directly capture structural rotation, where even small but persistent changes can become significant over time. Inclinator chains provide the most diagnostic geotechnical profiles, but at higher cost and complexity, while benchmarks supply inexpensive and accurate surface references albeit without depth resolution. Together, these instruments reveal that the choice of sensor depends on the monitoring priority: if rapid vibration awareness is needed, accelerometers are most effective; if long-term settlement detection is critical, benchmarks and inclinometer chains are indispensable; if direct building response is the focus, tiltmeters provide the clearest evidence.

Scientifically, this work contributes a replicable workflow for integrating IoT sensor data with BIM platforms, highlighting best practices for parameter mapping, metadata structuring, and threshold configuration. Practically, it demonstrates how real-time, multi-sensor data, when visualized within a digital twin, can transform static engineering models into dynamic decision-support tools. By bridging design documentation and live monitoring, the Certosa Metro case study shows how digital twins can support safer, more efficient, and better-informed infrastructure development in complex urban settings, while also pointing to areas where these tools must mature before achieving widespread, dependable adoption.

References

- [1] X. Hu, G. Olgun, and R. H. Assaad, "An intelligent BIM-enabled digital twin framework for real-time structural health monitoring using wireless IoT sensing, digital signal processing, and structural analysis," *Expert Systems with Applications*, vol. 252, Part A, Oct. 2024, Art. no. 124204. Available: <https://www.sciencedirect.com/science/article/abs/pii/S0957417424010704>
- [2] A. Armijo and D. Zamora-Sánchez, "Integration of railway bridge structural health monitoring into the Internet of Things with a digital twin: A case study," *Sensors*, vol. 24, no. 7, 2024. Available: <https://www.mdpi.com/1424-8220/24/7/2115>
- [3] L. Doni, *BIM as a Tool for Structural Health Monitoring*, Master's thesis, Politecnico di Torino, Turin, Italy, 2021. Available: <https://webthesis.biblio.polito.it/19448/>
- [4] H.-N. Li, L. Ren, Z.-G. Jia, T.-H. Yi, and D.-S. Li, "State-of-the-art in structural health monitoring of large and complex civil infrastructures," *J. Civ. Struct. Health Monit.*, vol. 6, pp. 3–16, 2016. Available: <https://link.springer.com/article/10.1007/s13349-015-0108-9>
- [5] Z.-Q. Li, J.-H. Zhang, and J. Dong, "Retraction notice to 'Subway structure health monitoring system based on Internet of Things' [Structures, 61 (2024) 106112]," *Structures*, vol. 61, 2024. Available: <https://www.sciencedirect.com/science/article/pii/S2352012424011007>

- [6] M. A. Mahmud, K. Bates, T. Wood, A. Abdelgawad, and K. Yelamarthi, "A complete Internet of Things (IoT) platform for structural health monitoring (SHM)," in *Proc. IEEE Int. Conf. Commun.*, 2018. Available: <https://ieeexplore.ieee.org/abstract/document/8355094/authors#authors>
- [7] A. Abdelgawad and K. Yelamarthi, "Structural health monitoring: Internet of Things application," in *Proc. IEEE Int. Conf. Commun.*, 2017. Available: <https://ieeexplore.ieee.org/document/7870118>
- [8] C. Harshitha, M. Alapati, and N. K. Chikkakrishna, "Damage detection of structural members using Internet of Things paradigm," *Procedia Struct. Integr.*, vol. 34, pp. 432–439, 2021. Available: <https://www.sciencedirect.com/science/article/abs/pii/S2214785321007768>
- [9] F. Lamonaca, P. F. Sciammarella, C. Scuro, D. L. Carnì, and R. S. Olivito, "Internet of Things for structural health monitoring," in *Proc. IEEE Int. Instrum. Meas. Technol. Conf.*, 2018. Available: <https://ieeexplore.ieee.org/abstract/document/8439038>
- [10] M. Valinejadshoubi, A. Bagchi, and O. Moselhi, "Development of a BIM-based data management system for structural health monitoring with application to modular buildings: Case Study," *J. Comput. Civ. Eng.*, vol. 33, no. 4, 2019, Art. no. 04019026. Available: [https://doi.org/10.1061/\(ASCE\)CP.1943-5487.0000826](https://doi.org/10.1061/(ASCE)CP.1943-5487.0000826)

- [11] R. S. Panah and M. Kioumars, "Application of building information modelling in the health monitoring and maintenance process: A systematic review," *Sensors*, vol. 21, no. 3, 2021, Art. no. 837. Available: <https://www.mdpi.com/1424-8220/21/3/837>
- [12] X. Liu, H. Liu, and C. Serratella, "Application of structural health monitoring for structural digital twin," in *Proc. Offshore Technol. Conf. Asia*, 2020. Available: <https://onepetro.org/OTCASIA/proceedings-abstract/200TCA/450897>
- [13] D. Wu, A. Zheng, W. Yu, H. Cao, Q. Ling, J. Liu, and D. Zhou, "Digital twin technology in transportation infrastructure: A comprehensive survey of current applications, challenges, and future directions," *Appl. Sci.*, vol. 15, no. 4, 2025, Art. no. 1911. Available: <https://www.mdpi.com/2076-3417/15/4/1911>
- [14] R. Al-Sehrawy, B. Kumar, and R. Watson, "A digital twin uses classification system for urban planning & city infrastructure management," *Proc. Inst. Civ. Eng. – Smart Infrastruct. Constr.*, 2021. Available: <https://pureportal.strath.ac.uk/en/publications/a-digital-twin-uses-classification-system-for-urban-planning-amp->
- [15] Y. Zhao, Y. Liu, and E. Mu, "A review of intelligent subway tunnels based on digital twin technology," *Buildings*, vol. 14, no. 8, 2024, Art. no. 2452. Available: <https://www.mdpi.com/2075-5309/14/8/2452>

- [16] X. Cheng, C. Wang, F. Liang, H. Wang, and X. B. Yu, "A preliminary investigation on enabling digital twin technology for operations and maintenance of urban underground infrastructure," *Discover Infrastructure*, vol. 4, 2024, Art. no. 21. Available: <https://link.springer.com/article/10.1007/s43503-024-00021-x>
- [17] B. Yan et al., "Digital twin in transportation infrastructure management: a systematic review," *Infrastructure Intelligence*, 2023. Available: <https://academic.oup.com/iti/article/doi/10.1093/iti/liad024/7370943>
- [18] F. Faraji and S. R. Samaei, "Flood risk management in urban subway systems using digital twins: A case study of the New York City subway," 2025. Available: https://www.researchgate.net/publication/388177685_Flood_Risk_Management_in_Urban_Subway_Systems_Using_Digital_Twins_A_Case_Study_of_the_New_York_City_Subway.pdf
- [19] M. Jafari, A. Kavousi-Fard, T. Chen, and M. Karimi, "A review on digital twin technology in smart grid, transportation system and smart city: Challenges and future," *IEEE Access*, 2023. Available: <https://ieeexplore.ieee.org/abstract/document/10034656>
- [20] A. Segalini, L. Chiapponi, M. Drusa, and B. Pastarini, "New inclinometer device for monitoring of underground displacements and landslide activity," *Communications – Scientific Letters of the University of Zilina*, vol. 16, no. 4, pp. 58–62, 2014. Available: <https://doi.org/10.26552/com.C.2014.4.58-62>

[21] I. Gkountis and T. Zayed, "Subway infrastructure condition assessment," *J. Constr. Eng. Manage.*, vol. 141, no. 3, 2015. Available: [https://doi.org/10.1061/\(ASCE\)CO.1943-7862.0001014](https://doi.org/10.1061/(ASCE)CO.1943-7862.0001014)

[22] X. Zhang, P. Garcia, and D. Martínez, "Integrated IoT-BIM workflows for real-time tunnel deformation monitoring," *J. Constr. Eng. Manage.*, vol. 146, no. 12, 2020. Available: [https://doi.org/10.1061/\(ASCE\)CO.1943-7862.0001936](https://doi.org/10.1061/(ASCE)CO.1943-7862.0001936)